NASA Technical Paper 1020

Theoretical Parametric Study of the Relative Advantages of Winglets and Wing-Tip Extensions

Harry H. Heyson, Gregory D. Riebe,
and Cynthia L. Fulton

SEPTEMBER 1977

NASA

NASA Technical Paper 1020

Theoretical Parametric Study of the Relative Advantages of Winglets and Wing-Tip Extensions

Harry H. Heyson, Gregory D. Riebe,
and Cynthia L. Fulton

Langley Research Center
Hampton, Virginia

National Aeronautics
and Space Administration

**Scientific and Technical
Information Office**

1977

SUMMARY

This study provides confirmation, for a wide range of wings, of the recommendations of Richard T. Whitcomb in NASA Technical Note D-8260. For identical increases in bending moment, a winglet provides a greater gain in induced efficiency than a tip extension. Winglet toe-in angle allows design trades between efficiency and root moment. A winglet shows the greatest benefit when the wing loads are heavy near the tip. Washout diminishes the benefit of either tip modification, and the gain in induced efficiency becomes a function of lift coefficient; thus, heavy wing loadings obtain the greatest benefit from a winglet, and low-speed performance is enhanced even more than cruise performance. Both induced efficiency and bending moment increase with winglet length and outward cant. The benefit of a winglet relative to a tip extension is greatest for a nearly vertical winglet. Root bending moment is proportional to the minimum weight of bending material required in the wing; thus, it is a valid index of the impact of tip modifications on a new wing design.

INTRODUCTION

The current high cost and, at times, limited availability of fuel have led to an extensive examination of possible ways to conserve aircraft fuel by increasing aircraft efficiency. The most obvious means of increasing efficiency, or lift-drag ratio, is to reduce induced drag by an increase in aspect ratio. On the other hand, any of several types of tip modification, generically referred to as end plates, could be appended to the tip of the wing.

End plates have been recognized for years (for example, ref. 1) as a means of increasing the effective aspect ratio of a wing. Numerous experimental investigations of end-plate effects are summarized in references 2 and 3. These studies concentrated on the simplest form of end plate, large-chord flat surfaces, where the associated increases in parasite drag largely offset the reduction in induced drag.

Examination of the basis for end-plate induced efficiency (ref. 1) reveals that the only requirement is to produce a suitable distribution of vorticity in the far wake. A simple flat plate is not an efficient means of producing the appropriate vorticity distribution. A highly optimized narrow-chord surface can produce the same, or greater, gain in induced efficiency at a far smaller cost in weight, parasite drag, and compressibility drag. This concept has been pioneered by Richard T. Whitcomb (refs. 4 and 5).

The improvement in overall performance over a simple end plate is so great that these modern surfaces are referred to as winglets to distinguish them from the older concepts.

Recent experimental tests (refs. 4 to 9) demonstrate that winglets could significantly improve the efficiency of transport aircraft, and reference 4, in particular, presents general rules for the design of such winglets. For other designs, such as the span-loaded aircraft of references 10 to 12, the application of winglets is envisioned on aircraft which differ radically from current transport aircraft. As yet, no sufficiently general study is available to provide guidance in the design of winglets for such aircraft.

Aerodynamic efficiency cannot be isolated from its impact on the overall aircraft configuration. Aerodynamic gains from either span extensions or winglets are accompanied by increased loads and increased wing weight. Since similar aerodynamic improvements can be obtained in either manner, the final choice will be largely determined by loads and weight.

This study examines a broad range of wings and explores the effects caused by varying aspect ratio, taper ratio, and washout. The relative gain in induced efficiency is presented as a function of the relative penalty in wing-root bending moment, which, in turn, is shown to be proportional to the minimum weight of material required to resist the aerodynamic bending moments imposed on the wing. The results of this study are intended to illustrate trends and not to provide design charts; thus, in order to reduce the number of variables to a manageable level, certain obvious features of practical wings are omitted. The wing and winglet have no camber; thus, all angles should be measured from zero lift. The wing has 30° leading-edge sweep. The winglet has a length which is a constant percentage of the wing span, is untwisted and of constant chord, and is canted outward 15°. The tip extensions are assumed to be simple linear continuations of the wing. The flow is assumed to be incompressible. A brief examination of the effect of varying these values is made for one set of wings with a taper ratio of 0.5 and 5° washout.

No attempt is made to examine theoretically optimum span-load distributions. The entire approach is based upon calculating the efficiencies and root moments of an arbitrarily selected set of wings with and without winglets and wing-tip extensions.

SYMBOLS

A aspect ratio of unmodified wing, b^2/S

b span of unmodified wing

c local wing chord

$C_{D,i}$	induced drag coefficient, D_i/qS
C_L	lift coefficient, L/qS
c_n	local normal-force coefficient, F_N/qc
c_r	root chord
c_t	tip chord of unmodified wing
D_i	induced drag
e	potential-flow induced efficiency factor, $C_L^2/\pi AC_{D,i}$
F_N	local normal force per unit span
g	acceleration due to gravity
h	local mean vertical distance between cover plates of wing box
i	winglet toe-in angle, measured normal to plane of winglet, positive with leading edge inward, deg
k	constant of proportionality
L	lift
ℓ	length, normal to span, of wing-box cover plates
M_ℓ	local bending moment
M_r	bending moment at root (or center) of wing
q	dynamic pressure
S	area of unmodified wing
$\bar{t}$	effective thickness of wing-box cover plates

W	minimum weight of wing bending material
y	distance along span measured from center line
y_c	lateral location of center of lift of wing panel
y_t	value of y at wing tip
Γ	circulation
γ	winglet cant angle, measured positive outward from vertical, deg
Δb	percentage increase in wing span
Λ	leading-edge sweep angle, positive rearward, deg
λ	taper ratio of unmodified wing, c_t/c_r
ρ	density
σ	local stress
σ_d	design stress

Subscripts:

w	winglet
with	with tip extension or winglet
without	without tip extension or winglet

BASIC CONSIDERATIONS

Computer Program

The computer program used for this study is a modified form of the North American Rockwell unified vortex lattice (NARUVL) program (ref. 13). The modifications consisted of a faster matrix solution routine and a substantially improved routine for far-wake

calculation of the induced drag. In addition, routines were added to calculate root bending moment, bending-moment distribution, and a factor proportional to the minimum weight of bending material. This program was chosen because it is relatively rapid and sufficiently accurate for parametric studies.

The NARUVL program satisfies the linearized boundary conditions with the local airfoil slopes. Airfoil thickness and out-of-plane displacements due to camber are ignored. Displacements due to dihedral are retained. No viscous effects are included; that is, there are no friction drag and no separation or stall. Induced drag is calculated in the Trefftz plane. Subsonic compressibility is treated as a Prandtl-Glauert stretching of ordinates; thus, supercritical regions are not represented accurately.

In the present study, the unmodified wing is always represented by 200 singularities, 10 chordwise and 20 spanwise. When the wing tip is extended, the total number of singularities is increased by a proportionately larger number of spanwise stations. Winglets are represented by an additional 50 singularities on the winglet, 5 chordwise and 10 spanwise. Both wings and winglets have no camber. As a rough approximation to the effect of camber, angles of attack and toe-in angles can be considered to be measured from zero lift. The flow is assumed to be incompressible, that is, at zero Mach number.

The input variable in the NARUVL program is angle of attack rather than lift coefficient. The present results for constant lift coefficient were obtained by two program executions: once to obtain lift coefficient as a function of angle of attack and then, using these results, to obtain values for the desired lift coefficients.

The effects of tip extensions and winglets are presented in the form of dimensionless ratios to the corresponding values for the unmodified wing at the same lift coefficient and Mach number. All coefficients are computed by using the aspect ratio and area of the unmodified wings; thus, the change in efficiency factor represents the total reduction in induced drag. This form of presentation yields an immediate rough estimate of the overall effect of modifying a given wing.

Standard Wings

Typical standard wing planforms considered in this study are illustrated in figure 1. Leading-edge sweep is fixed at 30°, and three taper ratios (1.0, 0.5, and 0.25) are considered. Five aspect ratios (4, 6, 8, 10, and 12) and three linear washouts (0°, 5°, and 10°) are considered. The ranges of taper ratio, aspect ratio, and washout are significantly greater than the ranges encountered in current design practice. Certain of these variables are altered subsequently to examine the relative magnitude of their effects.

Tip Extensions

Figure 1 also illustrates the tip extensions (5, 10, and 15 percent) that are considered herein. In each case, the tip extension is a simple linear extrapolation of the geometric characteristics of the basic wing. In this manner, taper ratio decreases, and washout increases, as the wing is extended. Despite these changes in the resulting wing, the extended wings are described herein in terms of the taper and washout of the original unmodified wing.

Standard Winglets

The typical standard winglet configuration studied in this paper is shown in figure 2. The winglet has no geometric twist since, as noted in reference 4, the basic wing flow field already introduces a significant aerodynamic twist. For simplicity, the winglet has no taper. The winglet chord is always one-half of the wing tip chord and its trailing edge is coincident with the trailing edge of the wing. The winglet leading-edge sweep is chosen to be 45°. In its own plane, the length of the winglet is chosen to be 15 percent of the wing semispan and it is canted outward 15°. These values are fairly representative of the winglets used in references 4 to 9. The angle of incidence, or toe-in, with which the winglet is attached to the wing is varied from -4° to 4° in increments of 2°.

Variation of Standard Parameters

The simple winglet design used herein is merely intended to illustrate trends. It is not intended to represent a practical design. A briefer study, using only wings with a taper ratio of 0.5 and 5° washout, was made in which a number of parameters were varied independently. These cases include: a Mach number of 0.8; wing leading-edge sweep of 0° with both swept and unswept winglets; winglet length of 0.3 wing semispan; winglet cant angles from -15° to 90°; winglet sweep angles of 0° and -45°; and a winglet with taper ratio of 0.5 and an area reduction of 25 percent. These results are presented after the results for the standard wing-winglet combinations.

RESULTS AND DISCUSSION

In the current study, winglets and tip extensions of arbitrary configuration are affixed to the standard wings. The interplay of the additional surfaces and the wing determines the load distribution, the induced efficiency, and the root moment. This procedure is in contrast to that of reference 14 where the wing and the modifications thereof are required to have an optimum load distribution. In that procedure, all the standard wing and winglet combinations would have identical induced efficiencies and root bending moments because they all have the same trace in the far wake (fig. 2(c)). The

present approach also differs from that of reference 15, where the wing was assumed to be fixed, but the winglet twist (which includes toe-in angle) was optimized in each case for minimum induced drag at one lift coefficient. Not only does the procedure of reference 15 tend to obscure the full effect of changes in winglet design, but it also negates the possibility of examining the offloaded winglets recommended by reference 4.

Standard Wings

Efficiency and lateral centroid of pressure. - The efficiency factors of the standard wings are shown as a function of the nondimensional lateral centroid of pressure in figures 3 to 5. It is helpful to examine these results in terms of basic and additional load distributions (ref. 16). The basic load distribution is the distribution at zero lift, is caused by twist, and is a function of both twist and taper. The additional load distribution is that caused by angle of attack. It is a function of taper and is unaffected by twist. The complete load distribution is a linear superposition, at any angle of attack, of the basic and additional load distributions.

With no washout, the basic load distribution is zero; all the loading is caused by the additional load distribution. Therefore, the nondimensional load distribution, the efficiency factor, and the centroid of load (fig. 3) are independent of lift coefficient. It has been shown by Glauert (ref. 17) that a taper ratio of about 0.5 results in the best efficiency factor (approximately 0.99) for untwisted unswept wings. The increased tip loading associated with sweep alters this result. Indeed, figure 3 indicates that a taper ratio of 0.25 is still too great to achieve peak efficiency. This result is confirmed by the centroid of pressure which is always located farther out than the value of 0.42 associated with an elliptic load distribution.

Washout results in a basic load distribution which is positive over the inner portions of the wing and negative over the outer portions of the wing. Furthermore, the effect of washout is greatest at small lift coefficients where the basic load distribution is a proportionately larger part of the total load distribution. This effect is evident in figure 4, where, at $C_L = 0.4$, the best efficiency would be obtained with an inverse taper ($\lambda > 1.0$), and at $C_L = 1.0$, the best efficiency would be obtained with taper ratios on the order of 0.4. In the latter case, the centroid of load for best efficiency approximates the value of 0.42 associated with an elliptic load distribution. At cruising lift coefficients on the order of 0.4 (fig. 4(a)), the lateral centroid of pressure is generally more inboard than for elliptic loading with the result that the root moments are less than those in the ideal case.

With 10° washout, the wing tips are severely unloaded. This effect can result in large decrements in root moment at the expense of a large decrease in efficiency factor in cruise (fig. 5(a)). At greater lift coefficients, the additional load distribution increases

the tip loads with consequent increases in both efficiency factor and root moment (fig. 5(b)). This amount of washout is clearly excessive for $C_L = 0.4$, and it would not be incorporated into a practical design. It is included herein with the deliberate intent of obtaining information over a wider range of variables than would normally be encountered in practice.

Wing-Tip Extensions

No washout.- For an untapered, untwisted wing, a tip extension is merely a slight increase in span with no alteration in planform other than aspect ratio. The load distribution merely stretches outward in proportion to the increased span. Furthermore, since the basic load distribution is zero, the nondimensional ratios are independent of lift coefficient. Consequently, the calculated efficiency factor ratios are all the same linear function of the root bending-moment ratio and the results for all aspect ratios collapse to a single line in figure 6.

When the wing planform is tapered, the linear extrapolation used in extending the wing tip results in a decrease in taper ratio (fig. 1). The results become a function of aspect ratio as in figures 7 and 8. The decrease in taper ratio with tip extension is proportionately greatest for the lowest taper ratio so that the dependence on aspect ratio is greatest in this case. (Compare figs. 7 and 8.) Examination of figure 3 shows that decreasing the actual taper ratio should increase the efficiency factor and produce a significant reduction in root moment. Furthermore, these effects should increase as the aspect ratio increases. These trends are shown clearly in figures 7 and 8.

Moderate washout.- When washout is incorporated in the basic wing, linear extrapolation of the wing to a greater span results in increasing the total twist of the wing. Therefore, as shown in figures 9 to 11, the performance of the modified wings is always a function of aspect ratio. Furthermore, since the basic load distribution is nonzero, the load distribution, and thus the performance, becomes a function of lift coefficient.

When the wing has no taper and 5° washout, the unmodified wing operates near peak efficiency at $C_L = 0.4$; however, it operates at lesser efficiency at $C_L = 1.0$. Figure 4 shows that the centroid of pressure at $C_L = 1.0$ is further out than for an elliptic load distribution; thus, the decrease in efficiency is caused by excessive tip loading. As a result, figure 9 shows that induced efficiency is only a slight function of C_L as the wing span is increased. At either lift coefficient, the increased span results in an increased root bending moment. The loading in the outer regions of the wing increases disproportionately with C_L as the span increases because of the lesser role of the basic load distribution; thus, the root bending moments also suffer a disproportionate increase as the span is extended.

When taper is added to a wing with 5° washout, this situation is altered. Now the basic wing is too lightly loaded at the tips at $C_L = 0.4$; thus, the efficiency improves as the lift coefficient increases (fig. 4). The increased taper and twist associated with a linear tip extension accentuate this trend. Therefore, as shown in figures 10 and 11, the gain in induced efficiency at the lower lift coefficient is not as great as the square of the span, the deficiency increasing as the taper ratio decreases. Since increasing the lift coefficient increases the relative loading near the tip, this effect is less marked at the larger lift coefficient. Root bending moment is also somewhat less because of the decreased tip loading.

Severe washout.- Increasing the washout to 10°, as in figures 12 to 14, accentuates the trends noted in the preceding section. Indeed, when combined with taper (figs. 13 and 14), this amount of washout can result in a loss, rather than a gain, in induced efficiency at $C_L = 0.4$ when the span is extended. At the larger lift coefficient, even those wings which lost efficiency at $C_L = 0.4$ show increases in both efficiency and root bending moment.

The design of a wing generally involves obtaining good induced efficiency for cruise where the lift coefficient is on the order of 0.4. On the other hand, the structure must be designed for the higher stresses associated with upset conditions or gusts, generally speaking, at about 2.5g. This is the ratio between the two lift coefficients for which the current calculations have been made. Figure 14 shows that simple extensions of the span of highly twisted and tapered wings can result in cases where the extension leads to both losses in efficiency and penalties in structural design. Furthermore, it indicates that the structural penalties of increased span cannot be fully offset by significantly increased twist in the tip extension because the increased twist decreases the tip loads to the point where the gain in efficiency, if any, is marginal.

Winglets

No washout.- Figure 15 shows the efficiency and moment ratios which result from adding the basic winglet to an untapered, untwisted, swept wing. The relative gain increases with aspect ratio and is a function of the winglet toe-in angle. The only toe-in angle for which the basic load distribution is zero is 0°. For this angle, the performance is independent of lift coefficient; all other toe-in angles result in a nonzero basic load distribution and dependence on lift coefficient. In general, efficiency factor increases with lift coefficient. Root bending-moment ratio increases with lift coefficient if the winglet is unloaded (toed-out) and may decrease if the winglet is overloaded (toed-in).

The possible gain in induced efficiency is as great as 40 percent for the untapered, untwisted wing (fig. 15); however, at constant aspect ratio, this gain diminishes, and the

toe-in angle at which it occurs increases as the taper ratio decreases (figs. 16 and 17). Fortunately, the root bending moments decrease simultaneously. The benefits of the winglet, as observed in reference 4, are greatest for wings with large outboard loadings.

Offloading the winglet from the best toe-in angle (figs. 15 to 17) results in losing a small percentage of the possible gain, but the increment in root bending moment is reduced by a larger percentage. Thus, variation of toe-in angle allows the designer a certain degree of freedom in trading induced efficiency against the weight penalties associated with the increased moments. This effect has also been noted in reference 4.

With washout.- Figures 18 to 23 present similar information for the wings with washout. Increases in washout and decreases in taper ratio reduce the loading on the outer wing panels with a consequent reduction in the possible increases in induced efficiency. At the lower lift coefficient representative of cruising flight ($C_L = 0.4$), this effect is greatest for the wings of greatest aspect ratio; for an aspect ratio of 12, the maximum efficiency factor ratio decreases from 1.4 in figure 15 to less than 1.01 in figure 23; whereas, for an aspect ratio of 4, the equivalent decrease is from 1.28 to 1.08. When the washout is an excessive 10° (figs. 21 to 23), an incorrect toe-in angle can result in a loss of induced efficiency for cruise conditions as compared with the basic wing.

Because of the increased loading near the tip with increased lift coefficient, the penalties in efficiency factor ratio are less at $C_L = 1.0$ (figs. 18 to 23). Thus, the benefits of winglets are a function of wing loading; for identical planform and twist, greater benefits result if the wing loading is larger.

First-generation jet transports such as the Boeing B-707 and the Douglas DC-8 tended to have wings designed for an essentially elliptic load distribution in cruise so as to minimize induced drag. More recent, or second-generation transports, typified by the Douglas DC-10, use a different design philosophy. Such aircraft have wings with additional taper and twist, offloading the wing tips, to reduce the bending moments and structural weight at the expense of some additional induced drag. Since the tip loading is less for the second-generation jet transports than the first-generation jet transports, it is obvious that the benefit of retrofitting winglets would also be somewhat smaller.

It is clear that the maximum benefit of winglets will be obtained if they are fitted to a wing specifically designed to operate with winglets. Such a wing would be designed to operate with tip loadings significantly heavier than those of even the first-generation jet transports.

Low-speed characteristics.- Low-speed flight is characterized by very large lift coefficients obtained through a combination of increased angle of attack and extensive use of flaps behind the inner portions of the wings. Although such cases are not specifically

included in the present calculations, the nature of the effect of these changes will be examined briefly in a qualitative manner.

The basic load distribution of the wing is increased over the flapped portion of the wing by the increased chord and camber of the flaps. These effects diminish rapidly for spanwise locations outboard of the flaps. The basic load distribution is defined as the load distribution at zero lift; thus, it is obtained at a lower angle of attack for the flapped wing than for the unflapped wing. Because of this decrease in angle of attack, the loads over the outer portion of the span become more negative; thus, the effect of flaps on the basic load distribution is qualitatively similar to that of increased washout.

The additional load distribution is modified slightly by chordwise extension of the flaps; however, the major effect is an overall increase (magnified further by the shift in zero-lift angle) caused by the increased angle of attack. This change in magnitude of the additional load distribution overpowers the effective increase in washout and leads to very heavy loading on the outer portions of the wing.

Since flight at low speeds increases the tip loading, it is evident from the preceding results that the winglet effectiveness at low speed is greater than at cruise conditions. This conclusion is confirmed by the experimental measurements of reference 9. Thus, even though the gain in induced efficiency may be small in cruise, the winglet may produce major reductions in induced drag at low speed. This reduced drag improves take-off performance and second-segment climb capability as well as reduces the power required on landing approach. The reduction in throttle settings and the more rapid climb can be used to reduce community noise exposure near the airport.

It is clear that even though $\partial\Gamma/\partial y$ may be discontinuous across the junction of wing and winglet, the circulation itself must be continuous. Circulation is proportional to the product of local chord and local normal-force coefficient. In order to avoid interference drag and to maximize the winglet efficiency, the root chord of the winglet must be significantly smaller than the tip chord of the wing (ref. 4). This essentially discontinuous decrease in chord must be accompanied by an equally discontinuous increase in local normal-force coefficient in order to maintain continuity of the circulation across the junction. This result is shown clearly in the theoretical normal-force distributions presented in reference 18. In the present case, where the winglet root chord is one-half the wing tip chord, the normal-force coefficient at the winglet root must be twice that at the wing tip.

The large local normal forces make it likely that the wing-winglet combination will stall initially at the winglet root adjacent to the wing tip. Tip stall is dangerous on conventional wings since any asymmetry can produce large moments at the same time that

the stall reduces the aileron effectiveness. This danger may not exist for the wing-winglet combination because the ailerons on the wing are not in a stalled region when stall starts on the winglet. Indeed, the phenomenon could be beneficial since it alleviates bending moments at the large lift coefficients which determine the structural design.

Significance of Root Bending Moment

It has been tacitly assumed to this point that root bending moment is a satisfactory index of the effect on wing structure. Addition of a tip extension or a winglet alters the moment diagram over the entire wing span; thus, root moment alone is not necessarily a good indication of the effect at all span locations. The structural significance of root bending moment will be examined briefly in this section of the paper.

The moment imposed on the structure at any spanwise station y is found by integrating the local moments between that station and the cantilevered tip; that is,

$$M_l(y) = \int_y^{y_t} (y_t - y)\, c_n(y)\, c(y)\, q\, dy \tag{1}$$

The bending moment $M_l(y)$ is resisted locally by the stresses in the cover plates of the wing box. These cover plates have an effective thickness $\bar{t}(y)$, a width $\ell(y)$, and an effective vertical separation $h(y)$, all of which are noted to be functions of spanwise location. Thus, the stress in the cover plates is given by

$$\sigma(y) = \frac{M_l(y)}{\bar{t}(y)\, \ell(y)\, h(y)} \tag{2}$$

where $M_l(y)$ is given by equation (1).

The allowable stress is fixed by the material chosen. If this material is the same throughout the span, the design stress is constant. Thus, the required variation in cover-plate cross-sectional area is obtained by rearranging equation (2) after setting $\sigma(y) = \sigma_d$; thus,

$$\bar{t}(y)\, \ell(y) = \frac{|M_l(y)|}{\sigma_d\, h(y)} \tag{3}$$

The absolute value of $M_l(y)$ is required in equation (3) since positive cover-plate area is required to resist the moment regardless of whether the moment is positive or negative. The local weight of the two cover plates required to counter the applied moment

is proportional to their area. The total minimum weight of bending material is obtained by integrating the local weight over the entire span; that is,

$$W = \int_0^{y_t} 2\rho\, \bar{t}(y)\, \ell(y)\, dy \tag{4}$$

Now substitute equation (3) into equation (4) to obtain

$$W = \frac{2\rho}{\sigma_d} \int_0^{y_t} \frac{|M_\ell(y)|}{h(y)}\, dy \tag{5}$$

If, for simplicity, it is assumed that the wing has a constant thickness ratio, the separation $h(y)$ between the cover plates is proportional to the local chord $c(y)$; equation (5) becomes

$$W = k \int_0^{y_t} \frac{|M_\ell(y)|}{c(y)}\, dy \tag{6}$$

The integrations required by equations (1) and (6) have been performed for many of the configurations of figures 6 to 23. The wings considered range from heavy tip loading to negative tip loading. The values computed from equation (6) were then nondimensionalized with respect to the corresponding values from the unmodified wings in order to form weight ratios. These weight ratios are compared with the corresponding root bending-moment ratios in figure 24.

Figure 24 shows that the wing weight ratios are essentially proportional to the root bending-moment ratios. Weight increases only slightly more rapidly than root bending moment, and this increase is primarily because of the added weight of the bending material within the tip extensions and winglets. The weight increase within the wing itself is almost exactly proportional to the root bending moment.

The total weight of bending material in the wing of a modern jet transport tends to represent only 5 to 7 percent of the maximum take-off gross weight, and perhaps 12 to 20 percent of the operating empty weight. An increase of 5 to 10 percent in the weight of the bending material has a relatively small effect on either gross weight or empty weight. In many cases, it will be found that the drag decrement associated with either a tip extension or a winglet reduces the fuel consumption to the point where the take-off gross weight for a given mission is decreased despite the increase in structural weight.

The preceding analysis would apply to the preliminary design of a new wing. The retrofitting of either a tip extension or a winglet to an existing aircraft would require a far more detailed study than this simple analysis. Since the retrofit alters the loads over the entire span of the wing (at the wing tip, for example, where the loads prior to the modification are obviously zero, the percentage increase in load approaches infinity), the entire structure must be examined in the light of available flight-test and laboratory proof-test data to determine where the stresses are most critical. For some wings, the critical stresses may be at the root; however, the critical stresses for other wings may be located well out on the span. The moment ratios presented herein give only a general indication of the order of magnitude of the problems involved.

Comparison of Tip Extensions and Winglets

Rationale.- The primary design objective for a commercial transport is to obtain the best possible cruise efficiency at the minimum cost in structural weight. In the present study, the cruising lift coefficient has been chosen arbitrarily to be 0.4. The structure must be designed to withstand loads such as those encountered in upset or gust conditions. These design loads are generally 2.5 times greater than the cruise loads. Thus, the structural design loads in the present study are represented by a lift coefficient of 1.0. The comparison of the effects of tip extensions and winglets, in order to be consistent with the actual requirements, must couple the induced efficiency factors at 1g $\left(C_L = 0.4\right)$ with the root bending moments at 2.5g $\left(C_L = 1.0\right)$. This comparison is presented in figures 25 to 33.

No washout.- When the wing is untwisted, figures 25 to 27 show clearly that it would be difficult to design a winglet so poorly that it would not obtain a greater gain in induced efficiency (at the same cost in root moment) than a tip extension. A properly designed winglet should develop an induced efficiency increment ranging from two to five times as great as that obtainable from a tip extension.

Moderate washout.- The possible gain in induced efficiency from a winglet has been shown to decrease as washout is introduced into the configuration. Both the absolute gain and the gain relative to a tip-extension decrease (figs. 28 to 30). At a constant penalty in root bending moment and with 5° washout, the peak gain in efficiency tends to be only 1.5 to 2 times the gain from a tip extension. The design of the winglet must be considered carefully for too much, or too little, toe-in can result in losing the gain relative to the tip extension.

Jet transports have wings roughly typified by the wing of figure 29. The induced drag decrement for a typical aspect ratio of 7 is about 15 percent which is twice the decrement possible for a tip extension having the same root bending moment. Second-generation wide-body transports tend to have greater twist and taper than the earlier

transports; thus, the gain relative to a tip extension is less, and very careful winglet design will be required to obtain the maximum gain.

Severe washout.- The tip extension and winglet are compared in figures 31 to 33 for wings with 10° washout. This severe washout is significantly greater than that used in current aircraft design. It has been included only to extend the trends noted earlier.

For the larger aspect ratios, figures 31 to 33 show that neither the tip extension nor the winglet results in a gain in induced efficiency commensurate with the increase in root bending moment. When the wing has a small taper ratio, as in figure 33, either modification may decrease induced efficiency even though the root bending moment has been increased. Under such conditions, only the lower aspect ratio wings are benefited by modification and, even then, the improvement in induced efficiency is achieved only with a disproportionate increase in root bending moment.

Variation of Configuration Parameters

The preceding portions of this paper have considered only a limited number of parameters in order to maintain reasonable bounds on the extent of the study. Variations in many of the previously fixed parameters can affect the results. A number of such variations are now considered for a single set of wings. The chosen wings have 5° washout and a taper ratio of 0.5. This is the central set of the foregoing portion of the study (figs. 19 and 29). As noted earlier, it is reasonably representative of jet transports. In all cases, the induced efficiency factors at $C_L = 0.4$ are coupled with the root bending moments at $C_L = 1.0$ in the remaining figures.

Free-stream Mach number.- Figure 34 compares the tip extension and winglet when the free-stream Mach number is 0.8. In preparing this figure, the efficiency factors and bending moments of the unmodified wing (the denominators of the ratios of fig. 34) were also computed at the higher Mach number. Thus, a comparison of figure 34 with figure 29 does not show the effect of Mach number as such; it shows only the relative effect of the tip modification when the basic wing is operating at a high subsonic speed rather than in incompressible flow.

Comparison of figure 34 with figure 29 shows that the induced efficiency gains of both tip extension and winglet are adversely affected by the choice of a greater Mach number, the greatest loss occurring at the largest aspect ratios. The root bending-moment ratios of the tip extensions are essentially unaffected. The root bending-moment ratios of the winglets increase; this effect decreases as the aspect ratio increases. The increase in root bending moment is greatest when the winglet is overloaded (that is, toed-in), and it is relatively small when the winglet is offloaded (toed-out).

Figures 29 and 34 do not include profile drag, nor has the finite thickness of wing or winglet been considered. It is obvious that there is more opportunity for Mach number to create adverse interference effects on profile and compressibility drag with the winglet than with the tip extension. Many of the rules for winglet design presented in reference 4 were developed with precisely this point in mind. The short chord and rearward location of the winglet are chosen to maximize the distance between the peak velocities in the fields of the wing tip and the winglet. The sweep of the winglet further minimizes the interference. In practice (refs. 4 to 9), the winglet is generally provided with large rearward camber to further reduce the coincidence of the peak velocities.

Wing leading-edge sweep.- Figure 35 presents a comparison of tip extensions and winglets when the leading-edge sweep of the wing is reduced to zero. Figure 36 presents a similar comparison when the sweep of both the wing and the winglet is zero. In both cases, the results have been nondimensionalized with respect to the corresponding values for an unmodified wing with zero leading-edge sweep.

Sweepback tends to increase outboard loading; thus, its removal decreases the loads near the wing tip. As a result of the reduction in outboard loading, tip extensions are less effective in increasing induced efficiency for the unswept wing (fig. 35) than for the swept wing (fig. 29). Because of the reduced loads near the tip, the winglet is also less effective on the unswept wing than on the swept wing.

Unsweeping the winglet increases its lift-curve slope and makes it more effective. A comparison of figures 35 and 36 shows that the unswept winglet has a greater impact than the swept winglet on both the efficiency factor and the root bending moment.

The effects shown in figures 35 and 36 appear to result primarily from the fact that the basic wing has a subelliptic loading near the tip (fig. 4). If the wing had a superelliptic loading near the tip (for example, an untapered untwisted wing), the results could be quite different.

Winglet length.- Figure 37 compares a tip extension with a winglet having a length of 30 percent of the wing semispan. This length is twice that of figure 29. The longer winglet, of course, is more effective (fig. 37) and, as a result, greater increases in both efficiency factor and root bending moment occur than for the shorter winglet (fig. 29). For a typical current aspect ratio of 7, the efficiency factor of the longer winglet is about 60 percent greater than that of the shorter winglet; the corresponding increase in root bending moment is about 90 percent greater. Neither effect increases as rapidly as the 100-percent increase in winglet length; however, the root bending moment increases at a significantly greater rate than the efficiency factor. The disparate rates at which these effects occur will limit the length of winglet which can be retrofitted to an existing wing.

Considerably more freedom in choosing winglet length is available in a new design where a totally new structure is created to carry the loads.

As observed in reference 4, no optimum value can be specified for winglet length without a detailed study of the relative structural cost of absorbing the increased loads created by the winglets. Operational constraints may further affect this choice. As an example, the choice of winglet length, or of winglet over wing-tip extension, could be significantly influenced by the need to restrict overall span to the space available at the loading docks of certain airports.

Winglet cant angle.- If the winglet was set vertically on the wing tip, it would behave purely in the manner of an end plate; that is, its own normal force would contribute nothing to lift except through its effects on the wing normal forces. On the other hand, if the winglet lay in the plane of the wing, its effect would be that of an irregular extension of the wing span. In practice, the winglet generally has some outward cant so that its influence is a mixture of both effects. The effect of winglet cant angle is shown and compared with the tip extension in figure 38. (Fig. 38(c) is identical to fig. 29, and it is included to provide continuity between the various parts of fig. 38.) Figure 39 summarizes figure 38 by collecting together the envelopes of the curves in figure 38.

Figure 38(a) shows that if the winglet is canted inward ($\gamma < 0$), it is possible to realize significant gains in induced efficiency at a very small penalty in root bending moment. Unfortunately, the acute angle between the wing tip and the winglet would probably increase the interference drag to the point where it would overshadow the gain in induced efficiency.

Both the peak induced efficiency ratio and the root bending-moment ratio increase continuously as the cant angle is increased. The difference in efficiency factor ratio between the tip extension and the winglet is relatively constant with aspect ratio at equal root bending moments. This difference is greatest for an essentially vertical winglet, and it suffers a modest decrease as cant angle increases. The difference in efficiency factor ratio between tip extension and winglet diminishes at $\gamma = 90^{\circ}$ to about half the value at $\gamma = 0^{\circ}$. Therefore, the relative advantage of the winglet over the tip extension is greatest for small cant angles. Thus, one justification for the modest cant angles generally employed in recent experiments (refs. 4 to 9) would appear to be the resulting decrease in mutual interference at the junction of the wing tip and the winglet.

The foregoing conclusions as to the effect of cant angle must be tempered by the recognition that the geometric characteristics of the winglet remain unaltered as the cant angle is varied. Its characteristics have been chosen largely as a reflection of current studies of winglets with small cant angles. Such a winglet is not necessarily an

appropriate design for a winglet with a large cant angle. This effect can be seen most clearly when the cant angle is 90° (fig. 38(h)). In this case, the winglet becomes an extension of the basic wing; however, it is an unusual extension in that there are gross discontinuities in sweep angle, chord, twist, and spanwise rate of twist at the junction.

For $\gamma = 90^{\circ}$, the efficiency of the winglet is greater than that of the tip extension only for large positive toe-in angles. At this cant angle, a positive toe-in angle is purely a local increase in airfoil incidence. The gain in efficiency occurs solely because the excessively light outboard loading of both the basic and the extended wings is modified. The resultant span-load distribution is very lumpy; thus, the winglet used herein is obviously not the most efficient way to increase the tip loads. It is equally obvious that a more efficient device than the present winglet could be designed to perform the same function. Determination of the best design for each cant angle is, however, beyond the scope of the present study.

Winglet leading-edge sweep.- Figure 40 compares tip extensions and winglets when the winglet sweep is changed to 0° and -45°. This figure, when compared with figure 29, shows that the improvement in induced efficiency is greater for either sweep angle than for the winglet of figure 29. The root moments increase simultaneously with the efficiency factor.

The rearward sweep of the basic winglet was chosen since, as observed in reference 4, it tends to minimize interference and compressibility drag in the junction by offsetting the velocity fields of the wing and winglet. Either zero sweep or forward sweep will increase the junction drag. Zero sweep tends further to be undesirable because it reduces the critical Mach number of the winglet. Forward sweep tends to introduce divergent aeroelastic problems. These factors, together with the indicated increases in root bending moment, tend to support the recommendation of reference 4 that the winglet sweep should be as great as the wing sweep.

Winglet taper and area.- The wing tip extension and winglet are compared in figure 41 for a winglet with a taper ratio of 0.5. Taper was obtained by removing the rearward half of the winglet tip chord while leaving the winglet root chord unaltered. Thus, in addition to the taper, the winglet of figure 41 has 25 percent less area than the winglet of figure 29.

Comparison of figures 29 and 41 indicates that the winglet toe-in angle for greatest induced efficiency is increased slightly; however, the peak induced efficiency and the root bending moment required for peak efficiency are essentially unaltered by the changes in winglet planform.

It is not surprising that the reduction in winglet area has little effect on the efficiency. In theoretical studies of optimum nonplanar surfaces, such as reference 14, the

only winglet variable of interest is the winglet length. Winglet area is required only to maintain stall-free levels of c_n for the desired span-load distribution. The fact that the area is less for the tapered winglet than for the untapered winglet accounts for the aforementioned result that the toe-in angle for peak efficiency is greater in figure 41 than in figure 29.

Although winglet taper is desirable structurally, it does not appear to be helpful in reducing induced drag (fig. 41). This result is in opposition to the recommendation in favor of taper in reference 4; however, the recommendation of reference 4 is based largely upon studies (such as ref. 14) of totally optimized span-load distributions on both wing and winglet. In the present analysis, the span-load distribution across the wing is not optimum for minimum drag irrespective of the presence or absence of the winglet. This fact may tend to obscure the apparently small effect of winglet planform taper.

CONCLUSIONS

This parametric study of the relative advantages of tip extensions and winglets provides, in general, a confirmation, for a wide range of wing designs, of the recommendations of Richard T. Whitcomb in NASA Technical Note D-8260; more specifically,

1. At an identical level of root bending moment, a winglet provides a greater induced efficiency increment than does a tip extension.

2. Winglet toe-in angle provides design freedom to trade small percentage reductions in induced efficiency increment for larger percentage reductions in the root bending-moment increment.

3. The gain in induced efficiency for a winglet is greatest, both in an absolute sense and relative to a tip extension, for a wing which has large loads near the tip. The greatest gain for a winglet will be obtained with a wing that is specifically designed to operate with a winglet.

4. Washout diminishes the favorable effect of both winglet and wing-tip extension. Washout significantly greater than that in current use can result in a decrease in induced efficiency when either a winglet or a tip extension is added.

5. For wings with washout, the gain from a winglet increases with lift coefficient because of the increased loads near the tip; thus, heavily loaded wings are most favorably influenced by a winglet. The size of the gains at large lift coefficients should improve performance in take-off, second-segment climb, and landing.

6. Both induced efficiency and root bending moment increase with winglet length. Although moment increases more rapidly than efficiency, neither effect increases in

proportion to the length. The best winglet length can be determined only by weighing the increased structural stresses against the improvement in induced efficiency.

7. Both induced efficiency and root bending moment increase continuously as the winglet is canted further outward. For the winglets studied herein, the greatest advantage relative to a tip extension is obtained for nearly vertical winglets. The best cant angle will be a compromise between induced efficiency and junction interference drag.

8. Root bending moment was found to be essentially proportional to the minimum weight of bending material required to resist the aerodynamic loads; thus, it is a valid index of the structural impact of tip modifications to a completely new wing design. The structural problems encountered in retrofitting a tip modification to an existing wing can only be determined by a detailed analysis of the existing structure.

Langley Research Center
National Aeronautics and Space Administration
Hampton, VA 23665
July 27, 1977

REFERENCES

1. Von Karman, Theodore; and Burgers, J. M.: General Aerodynamic Theory – Perfect Fluids. Vol. II of Aerodynamic Theory, div. E, ch. IV, sec. 19, W. F. Durand, ed., Dover Publ., Inc., 1963, pp. 211-212.

2. Hoerner, Sighard F.: Fluid-Dynamic Drag. Hoerner Fluid Dynamics (Brick Town, N.J.), c.1965.

3. Hoerner, Sighard F.; and Borst, Henry V.: Fluid-Dynamic Lift. Hoerner Fluid Dynamics (Brick Town, N.J.), c.1975.

4. Whitcomb, Richard T.: A Design Approach and Selected Wind-Tunnel Results at High Subsonic Speeds for Wing-Tip Mounted Winglets. NASA TN D-8260, 1976.

5. Flechner, Stuart G.; Jacobs, Peter F.; and Whitcomb, Richard T.: A High Subsonic Speed Wind-Tunnel Investigation of Winglets on a Representative Second-Generation Jet Transport Wing. NASA TN D-8264, 1976.

6. Jacobs, Peter F.; and Flechner, Stuart G.: The Effect of Winglets on the Static Aerodynamic Stability Characteristics of a Representative Second Generation Jet Transport Model. NASA TN D-8267, 1976.

7. Jacobs, Peter F.; Flechner, Stuart G.; and Montoya, Lawrence C.: Effect of Winglets on a First-Generation Jet Transport Wing. I – Longitudinal Aerodynamic Characteristics of a Semispan Model at Subsonic Speeds. NASA TN D-8473, 1977.

8. Montoya, Lawrence C.; Flechner, Stuart G.; and Jacobs, Peter F.: Effect of Winglets on a First-Generation Jet Transport Wing. II – Pressure and Spanwise Load Distributions for a Semispan Model at High Subsonic Speeds. NASA TN D-8474, 1977.

9. Montoya, Lawrence C.; Jacobs, Peter F.; and Flechner, Stuart G.: Effect of Winglets on a First-Generation Jet Transport Wing. III – Pressure and Spanwise Load Distributions for a Semispan Model at Mach 0.30. NASA TN D-8478, 1977.

10. Lange, R. H.: Design Concepts for Future Cargo Aircraft. J. Aircr., vol. 13, no. 6, June 1976, pp. 385-392.

11. Whitlow, David H.; and Whitener, P. C.: Technical and Economic Assessment of Span-Distributed Loading Cargo Aircraft Concepts. NASA CR-144963, 1976.

12. Technical and Economic Assessment of Span-Loaded Cargo Aircraft Concepts. NASA CR-144962, 1976.

13. Tulinius, J.: Unified Subsonic, Transonic, and Supersonic NAR Vortex Lattice. TFD-72-523, Los Angeles Div., North American Rockwell, Apr. 27, 1972.

14. Lundry, J. L.: A Numerical Solution for the Minimum Induced Drag, and the Corresponding Loading, of Nonplanar Wings. NASA CR-1218, 1968.

15. Ishimitsu, K. K.; VanDevender, N.; Dodson, R.; et al.: Design and Analysis of Winglets for Military Aircraft. AFFDL-TR-76-6, U.S. Air Force, Feb. 1976.

16. Anderson, Raymond F.: Determination of the Characteristics of Tapered Wings. NACA Rep. 572, 1936.

17. Glauert, H.: The Elements of Aerofoil and Airscrew Theory. Second ed., Cambridge Univ. Press, 1948.

18. Goldhammer, M. I.: A Lifting Surface Theory for the Analysis of Nonplanar Lifting Systems. AIAA Paper No. 76-16, Jan. 1976.

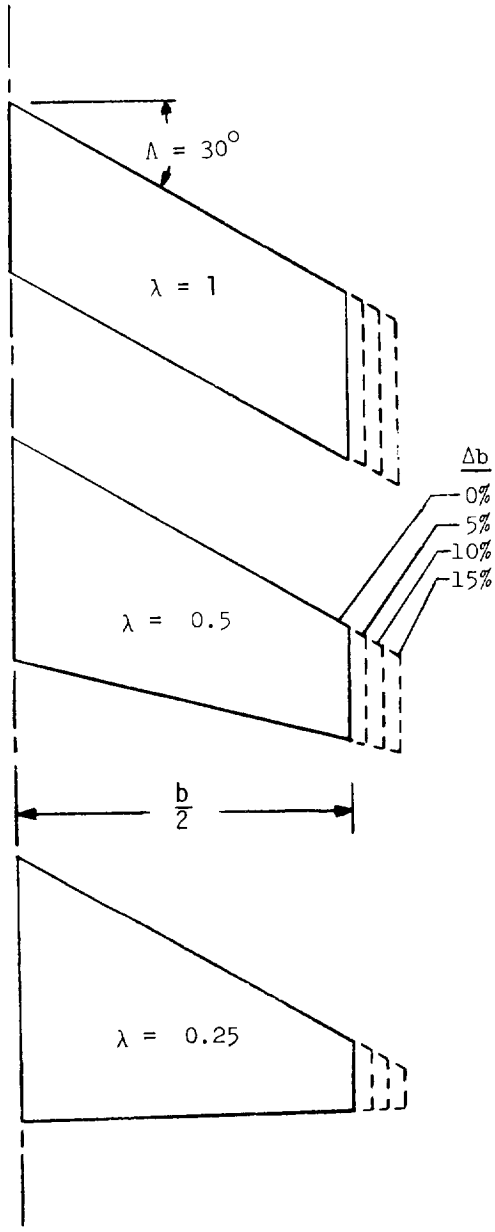

Figure 1.- Typical wing and wing-tip extensions (5, 10, and 15 percent) of parametric study.

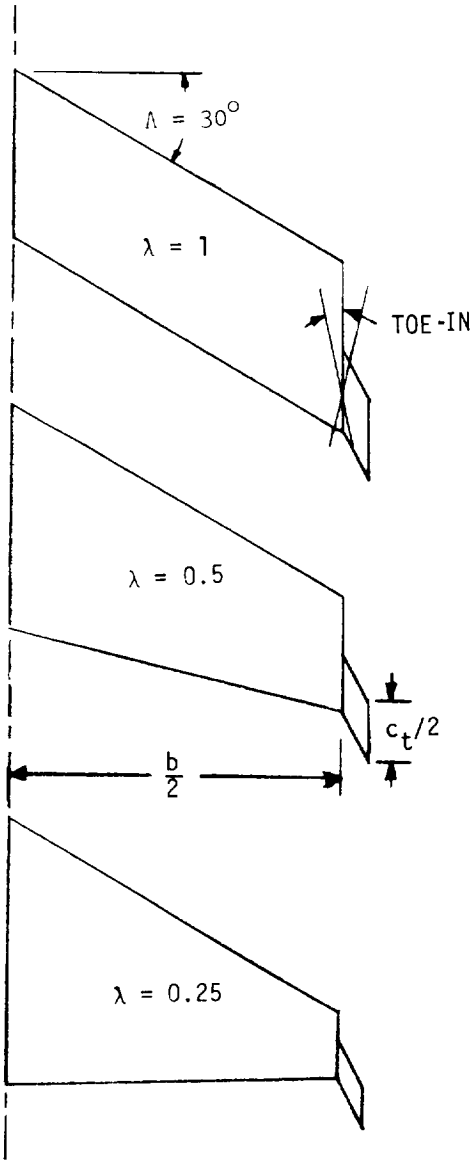

(a) Plan view of wing and winglet.

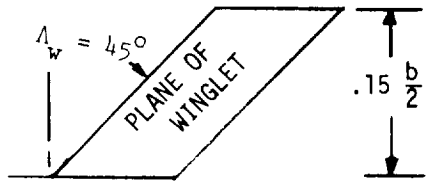

(b) Plan view of winglet.

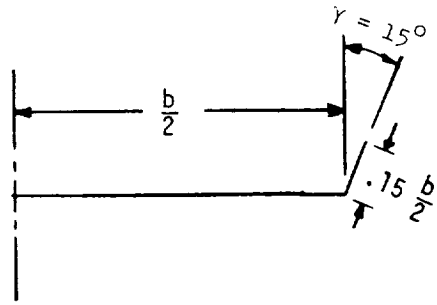

(c) Rear view of wing and winglet.

Figure 2.- Typical wing and winglet of parametric study.

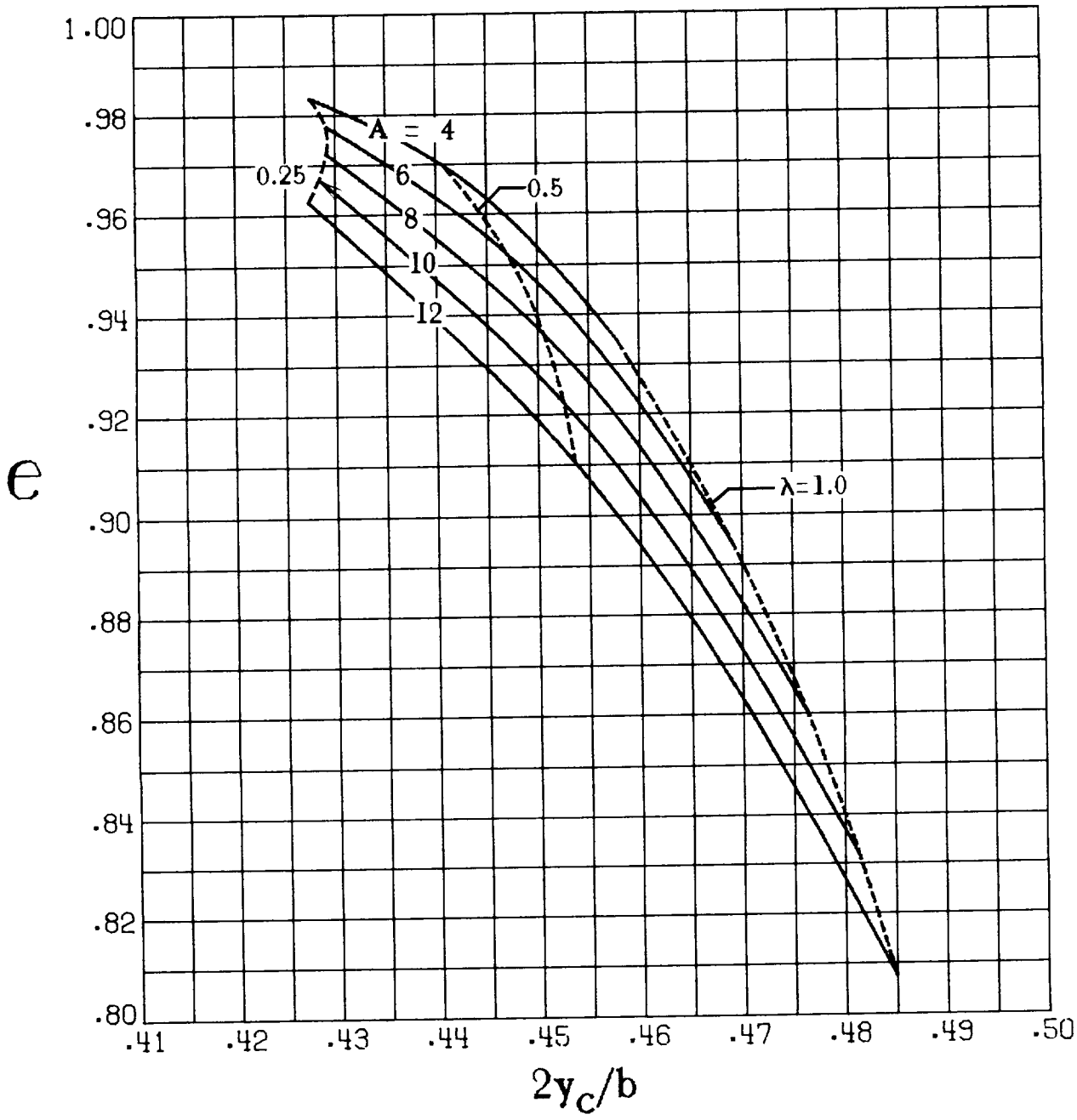

Figure 3.- Potential-flow efficiency factor and lateral centroid of pressure for the basic untwisted wings with 30° of leading-edge sweep. These results are independent of lift coefficient.

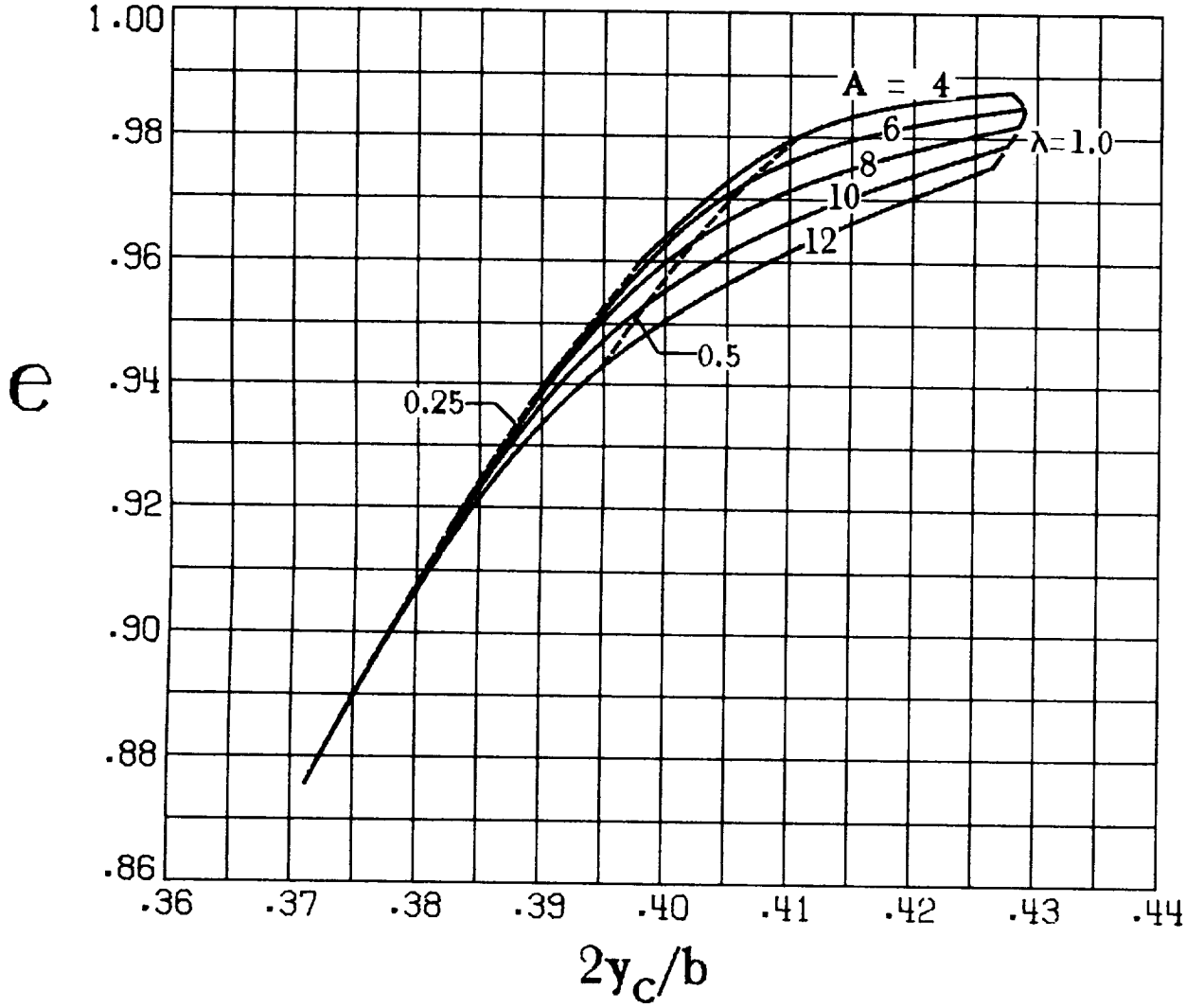

(a) $C_L = 0.4$.

Figure 4.- Potential-flow efficiency factor and lateral centroid of pressure for the basic wings with 5^o of washout and 30^o of leading-edge sweep.

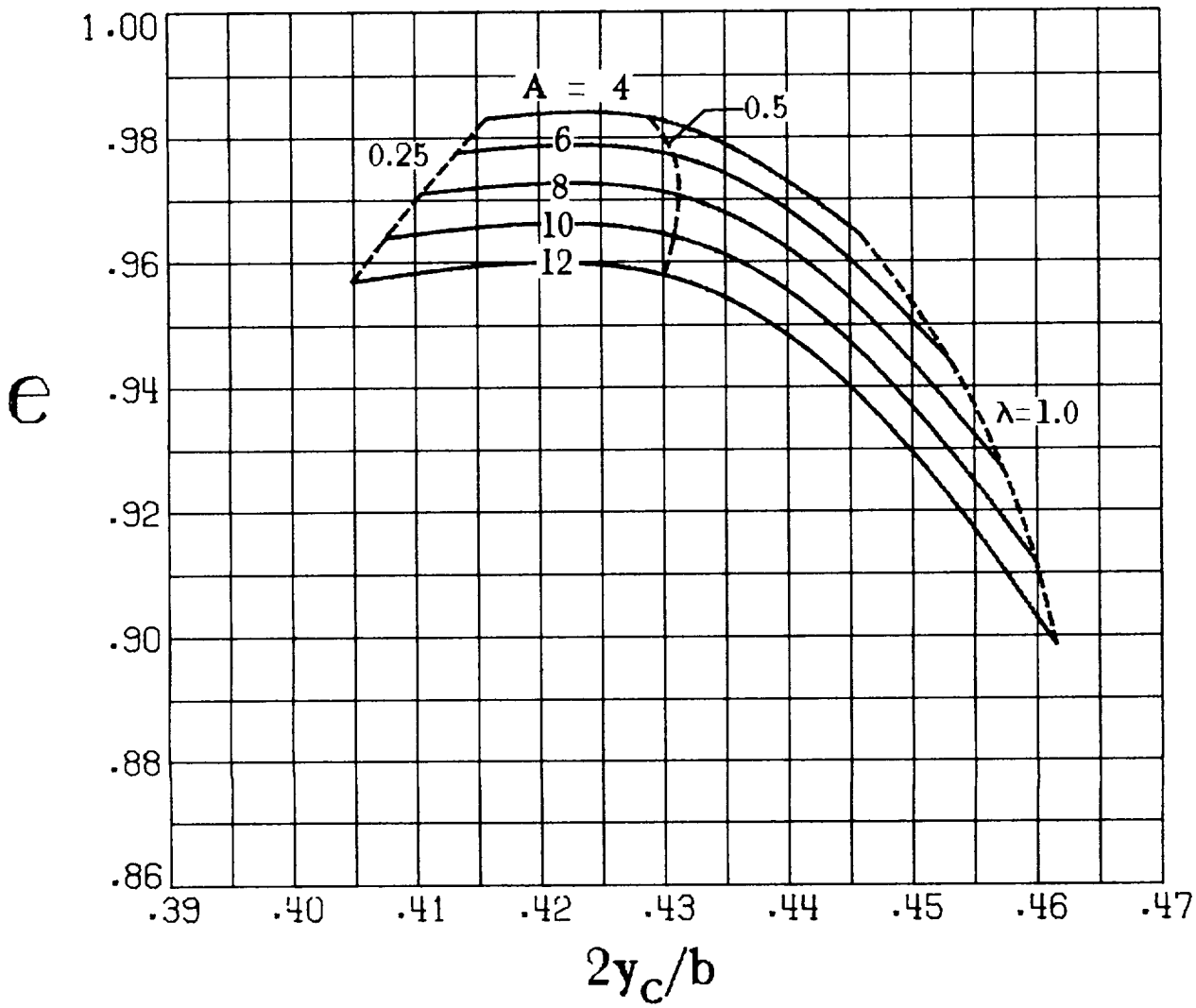

(b) $C_L = 1.0$.

Figure 4.- Concluded.

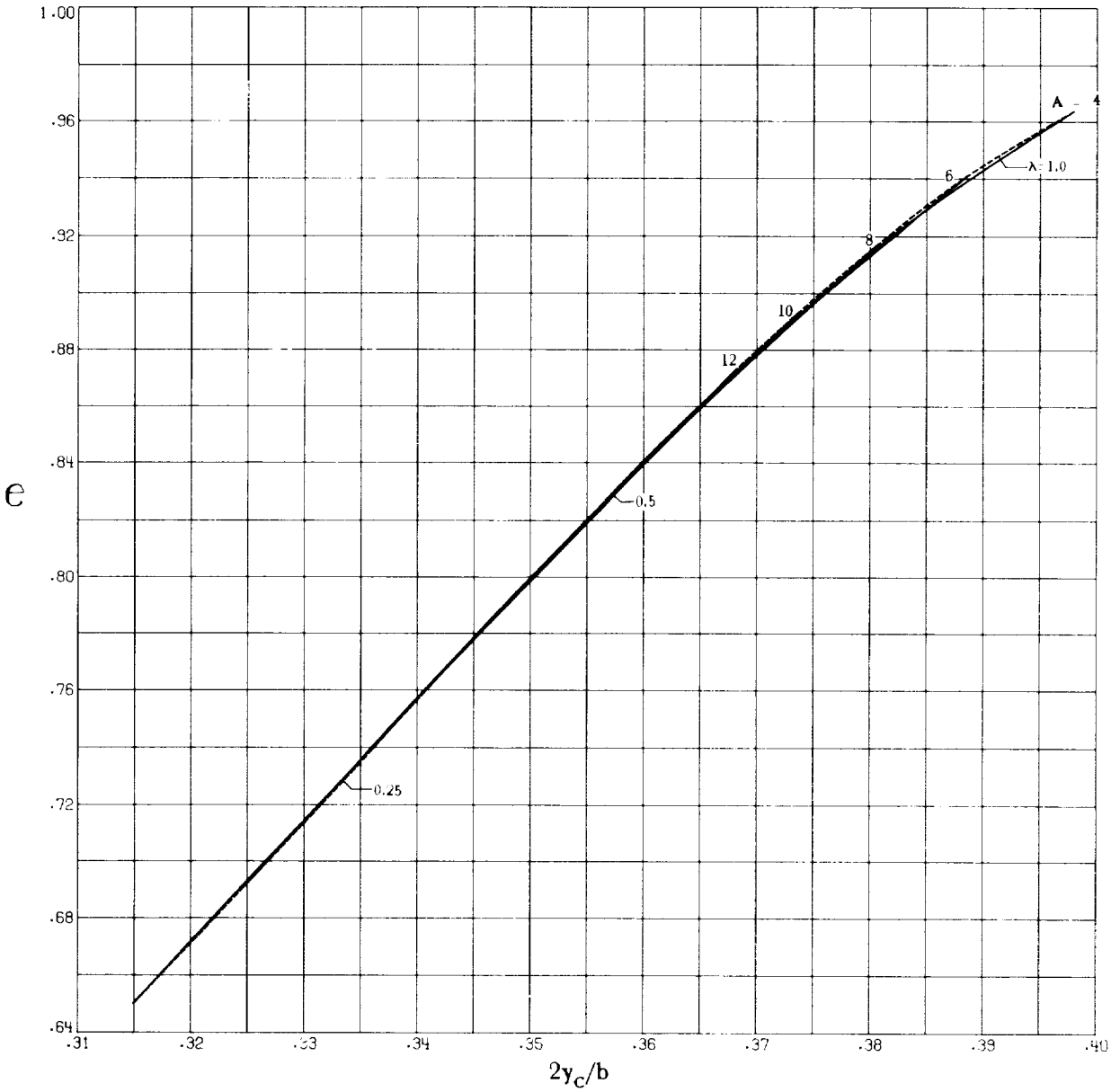

(a) $C_L = 0.4$.

Figure 5.- Potential-flow efficiency factor and lateral centroid of pressure for the basic wings with 10^o of washout and 30^o of leading-edge sweep.

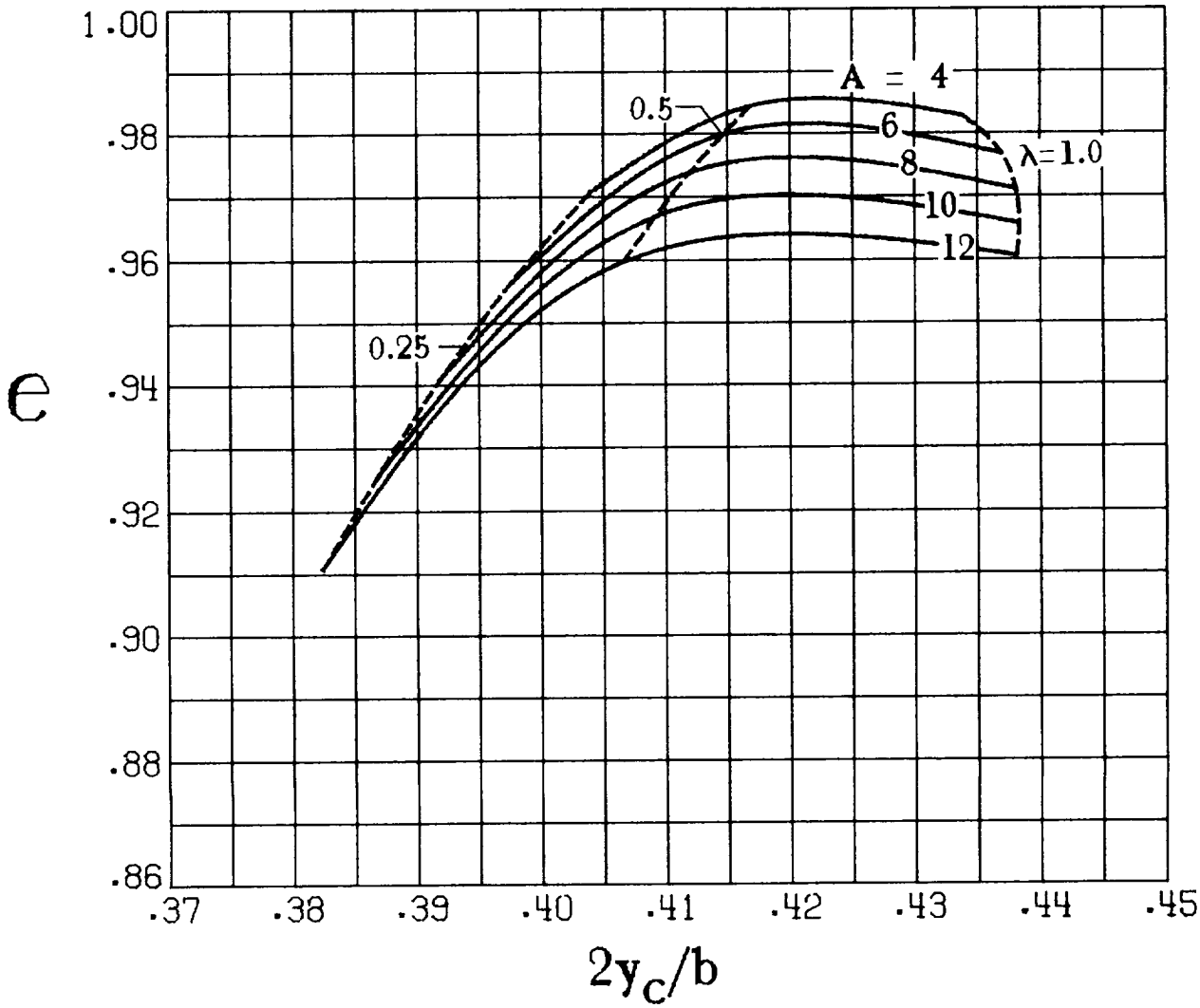

(b) $C_L = 1.0$.

Figure 5.- Concluded.

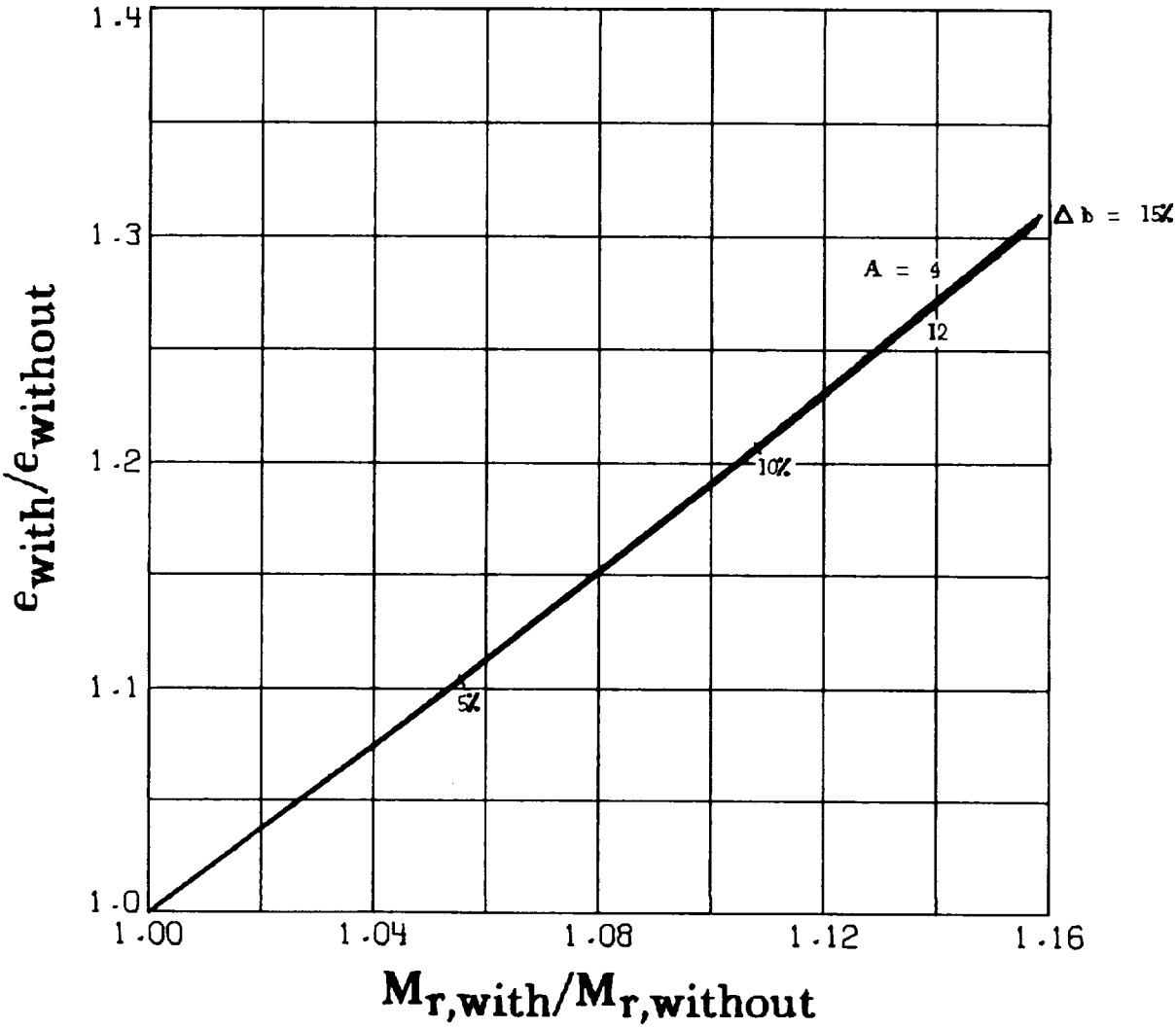

Figure 6.- Potential-flow efficiency factor ratio and root bending-moment ratio for tip extension on untwisted wings. $\lambda = 1.0$. These results are independent of lift coefficients.

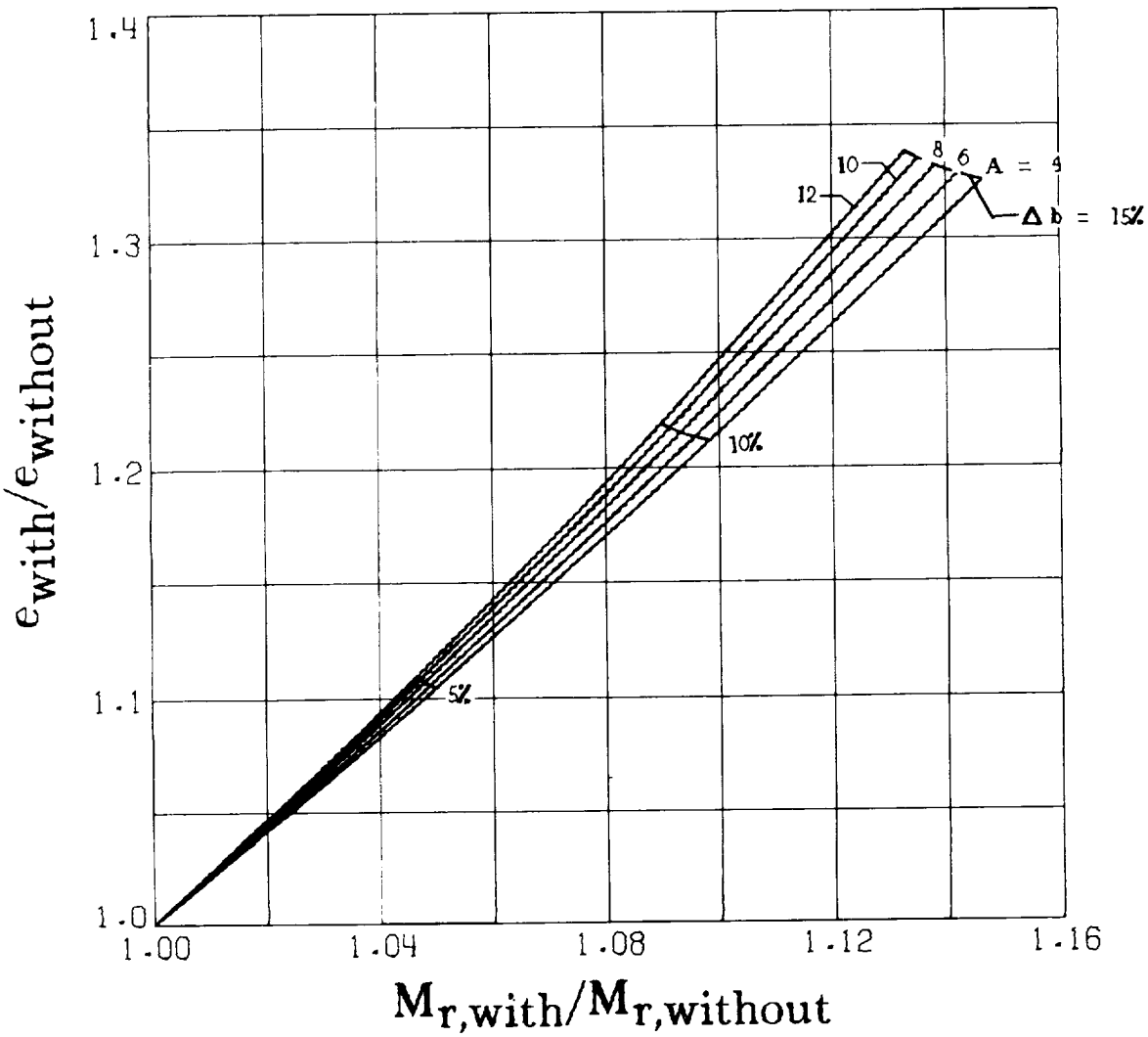

Figure 7.- Potential-flow efficiency factor ratio and root bending-moment ratio for tip extension on untwisted wings. $\lambda = 0.5$. These results are independent of lift coefficient.

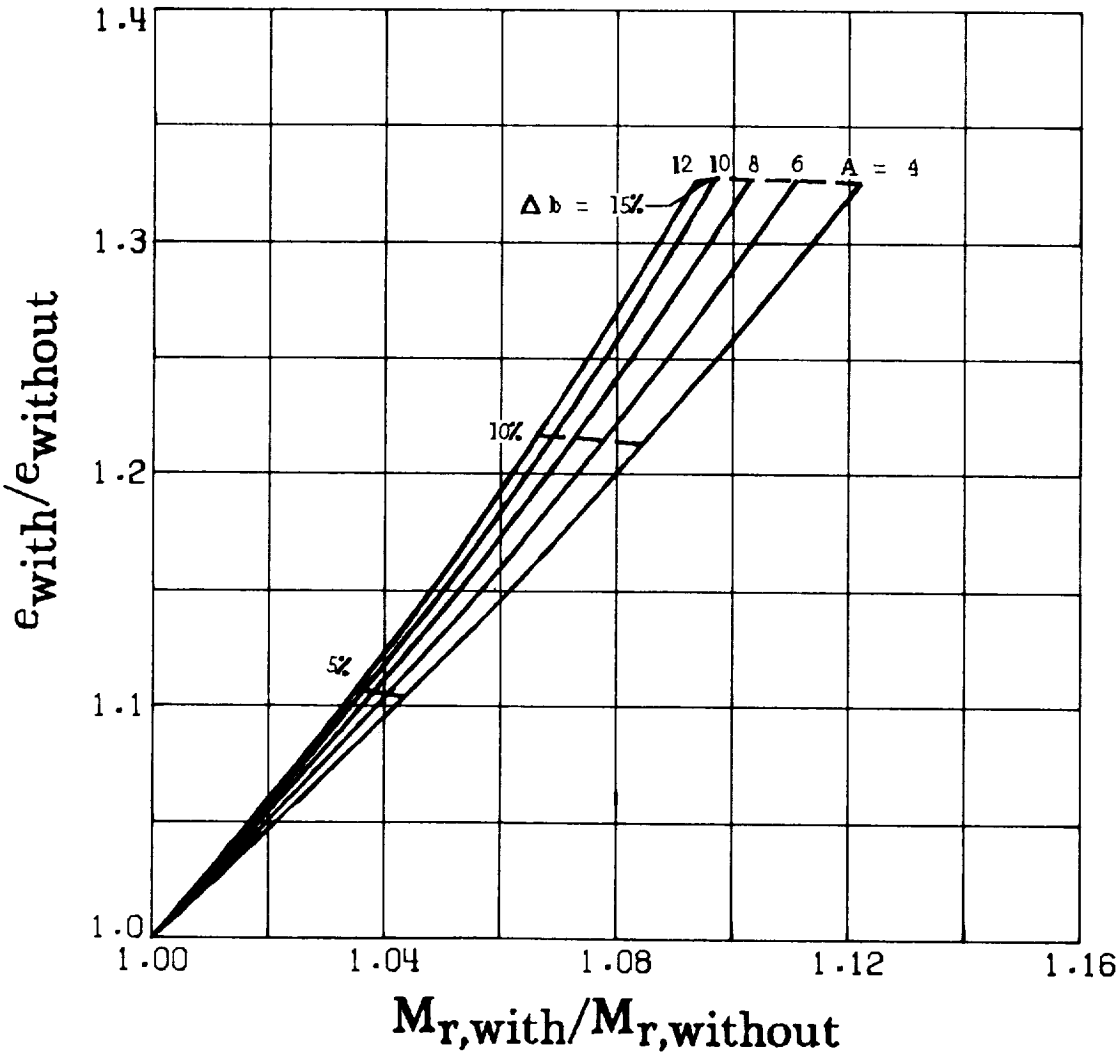

Figure 8.- Potential-flow efficiency factor ratio and root bending-moment ratio for tip extension on untwisted wings. $\lambda = 0.25$. These results are independent of lift coefficient.

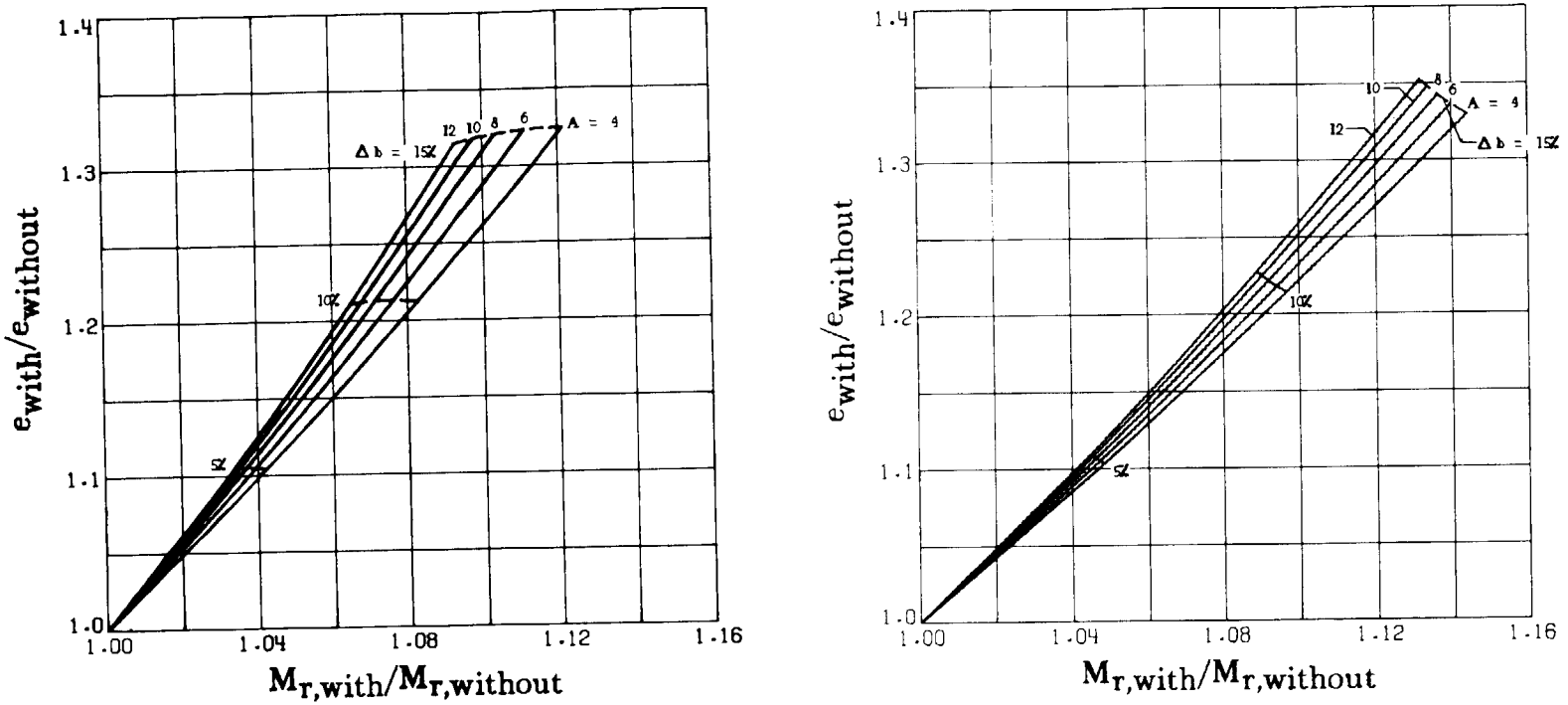

(a) $C_L = 0.4$.

(b) $C_L = 1.0$.

Figure 9.- Potential-flow efficiency factor ratio and root bending-moment ratio for tip extension on wings with 5^o washout. $\lambda = 1.0$.

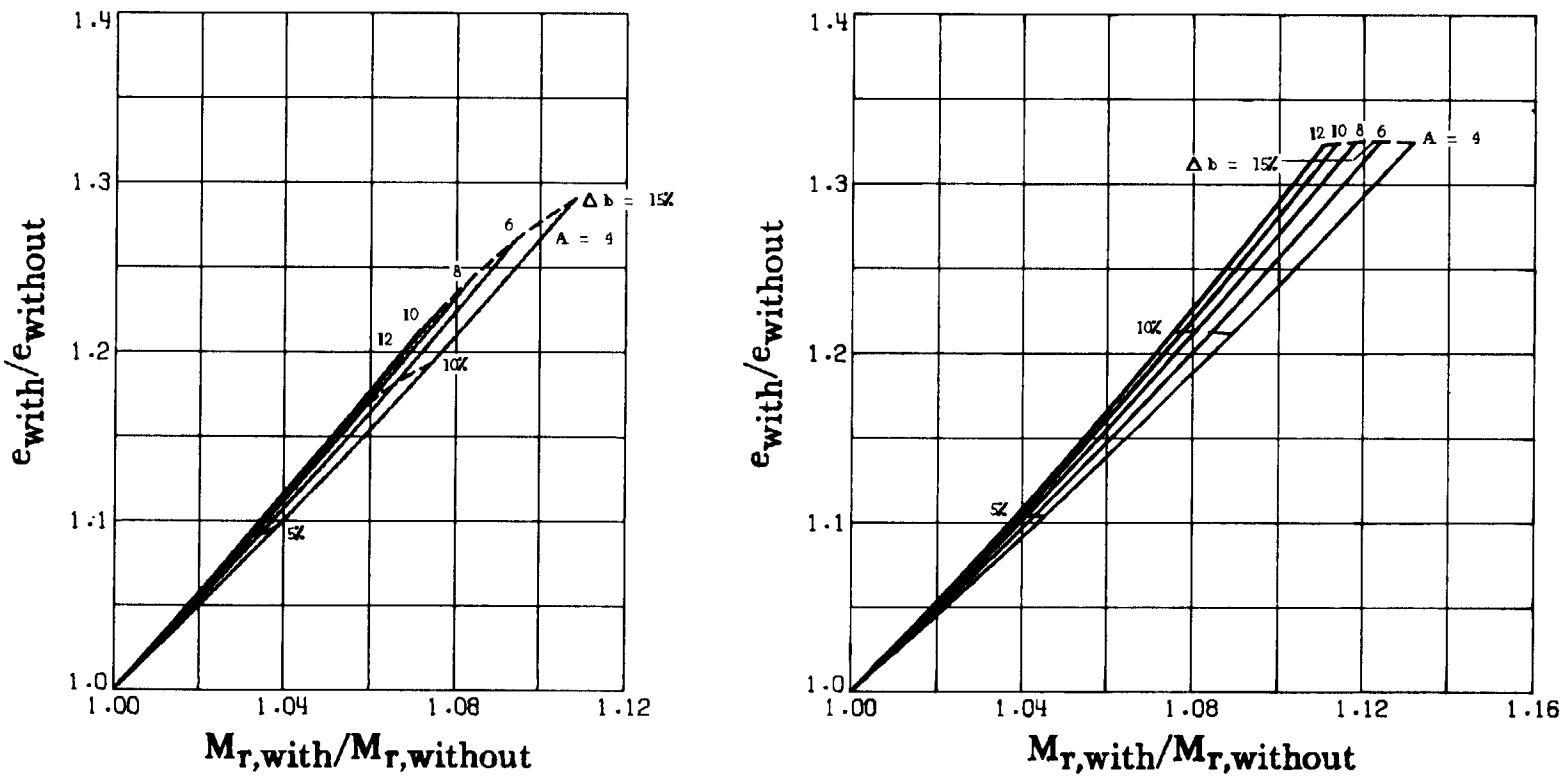

(a) $C_L = 0.4$.

(b) $C_L = 1.0$.

Figure 10.- Potential-flow efficiency factor ratio and root bending-moment ratio for tip extension on wings with 5^o washout. $\lambda = 0.5$.

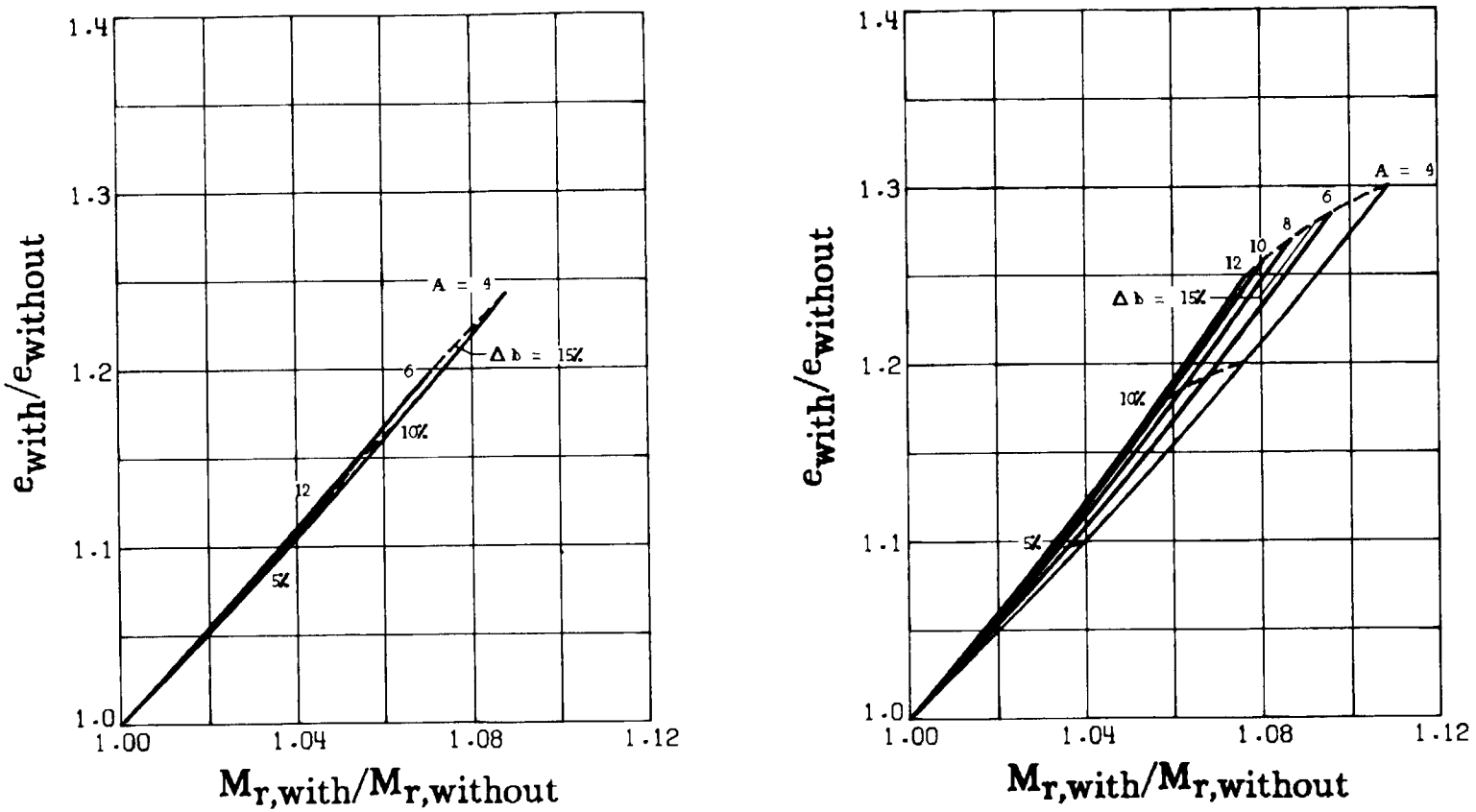

(a) $C_L = 0.4$.

(b) $C_L = 1.0$.

Figure 11.- Potential-flow efficiency factor ratio and root bending-moment ratio for tip extension on wings with 5^o washout. $\lambda = 0.25$.

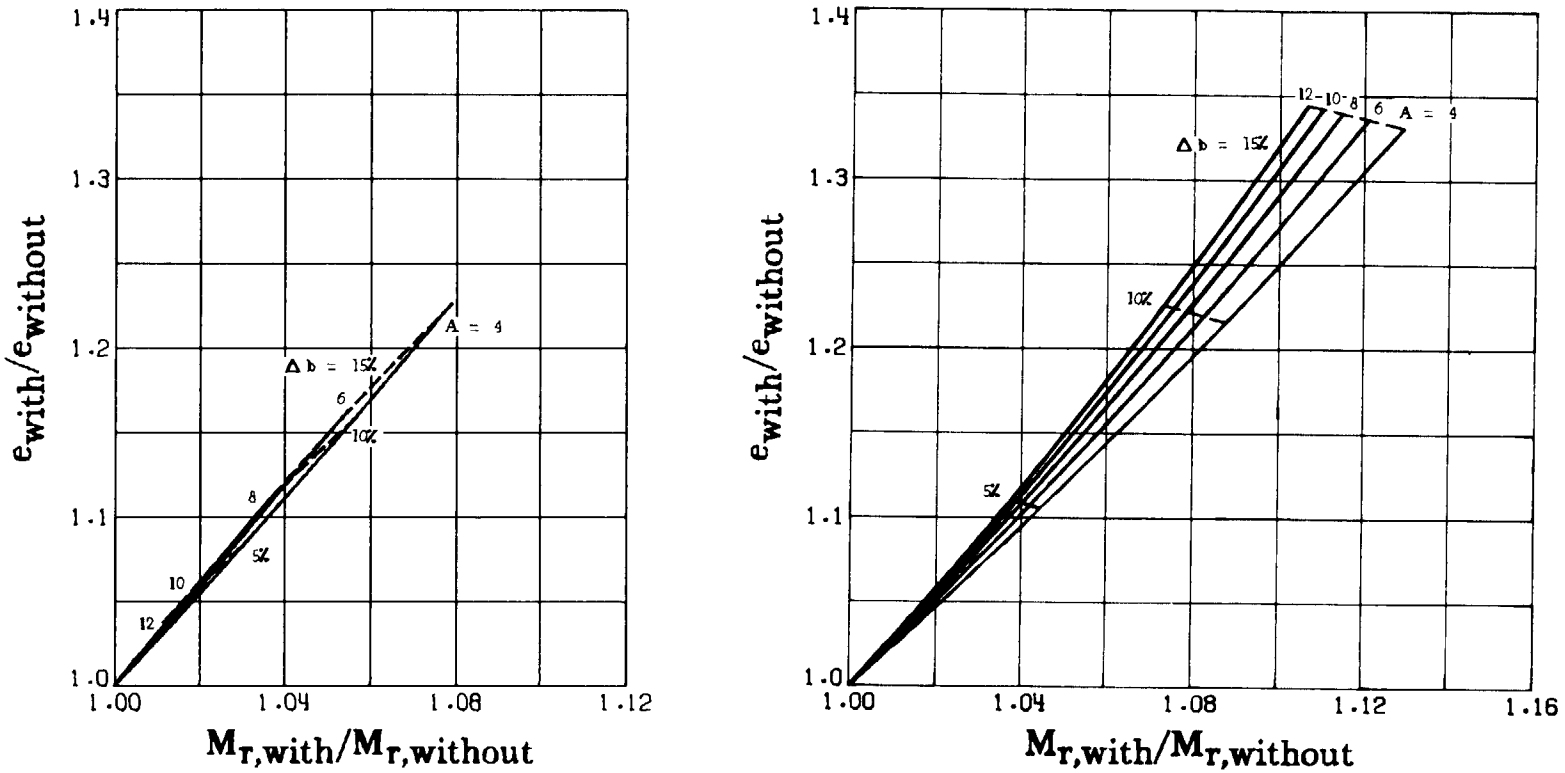

(a) $C_L = 0.4$.

(b) $C_L = 1.0$.

Figure 12.- Potential-flow efficiency factor ratio and root bending-moment ratio for tip extension on wings with 10° washout. $\lambda = 1.0$.

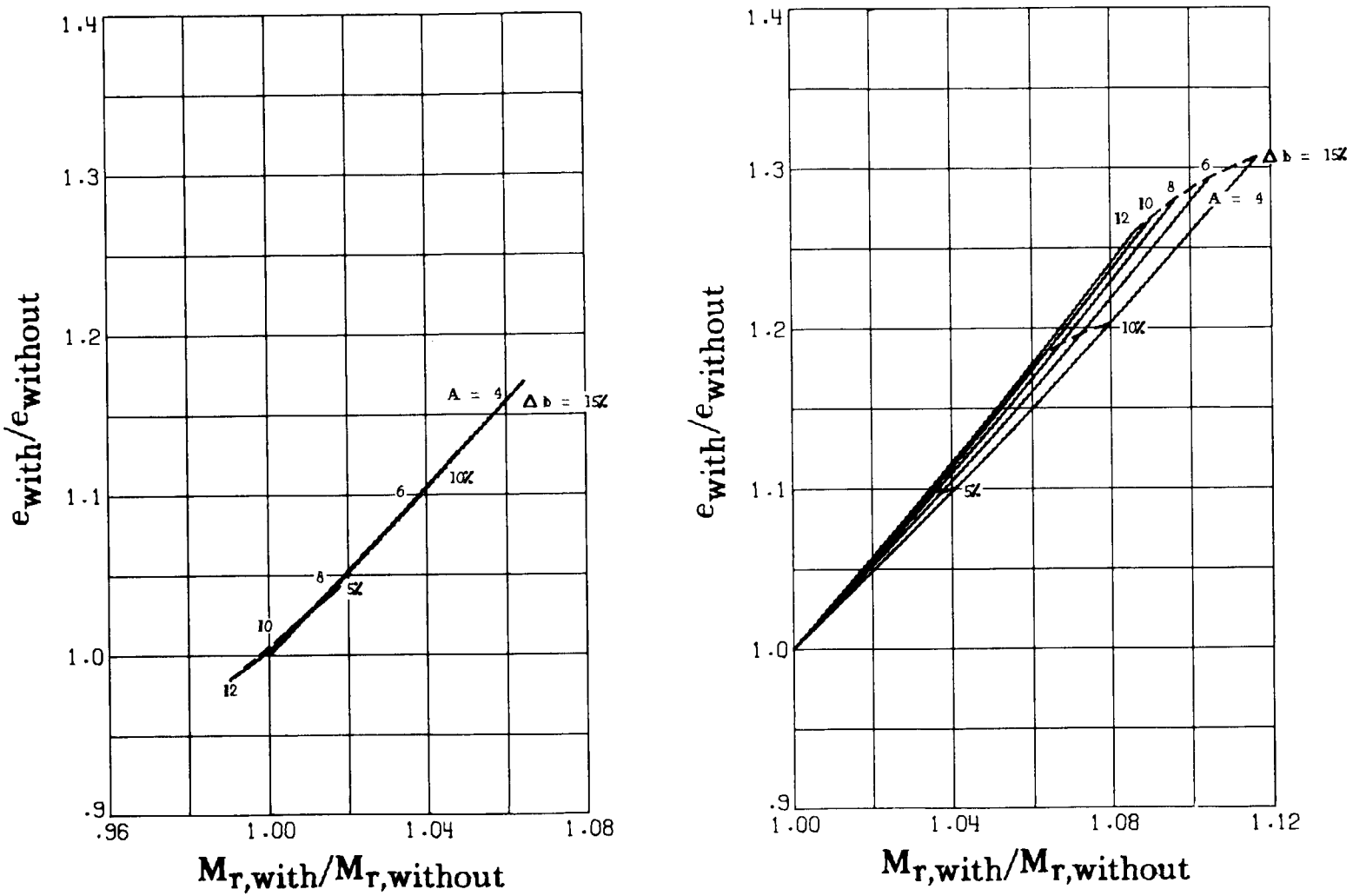

(a) $C_L = 0.4$.

(b) $C_L = 1.0$.

Figure 13.- Potential-flow efficiency factor ratio and root bending-moment ratio for tip extension on wings with 10^o washout. $\lambda = 0.5$.

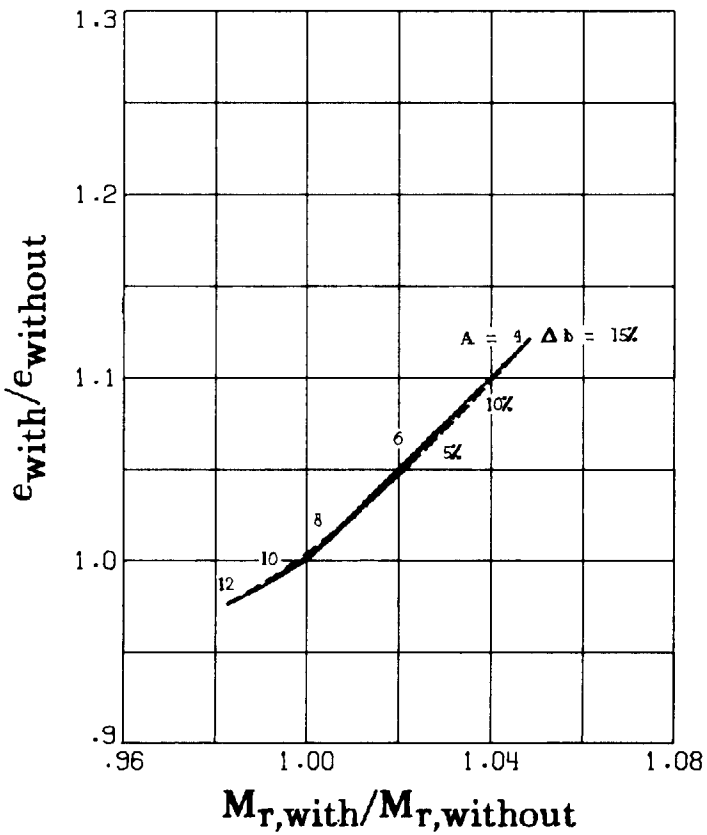

(a) $C_L = 0.4$.

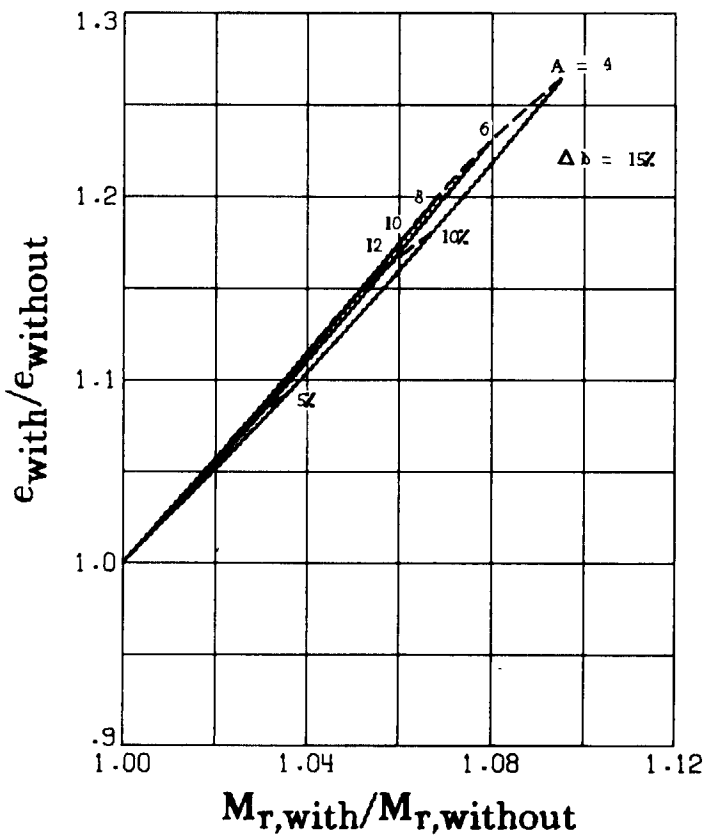

(b) $C_L = 1.0$.

Figure 14.- Potential-flow efficiency factor ratio and root bending-moment ratio for tip extension on wings with 10^o washout. $\lambda = 0.25$.

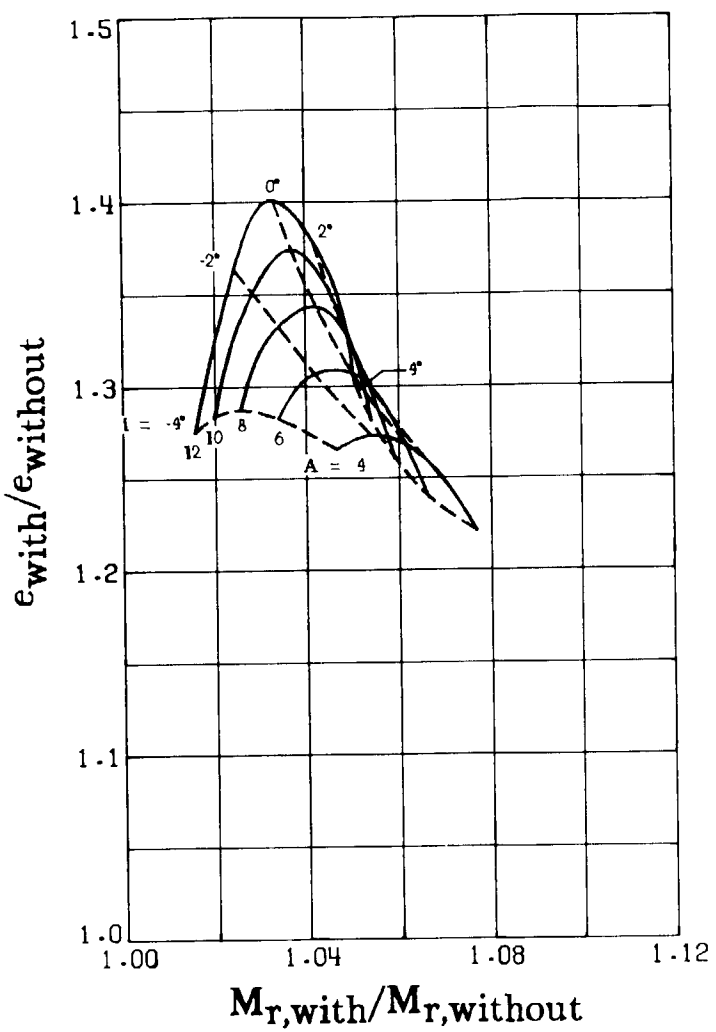

(a) $C_L = 0.4$.

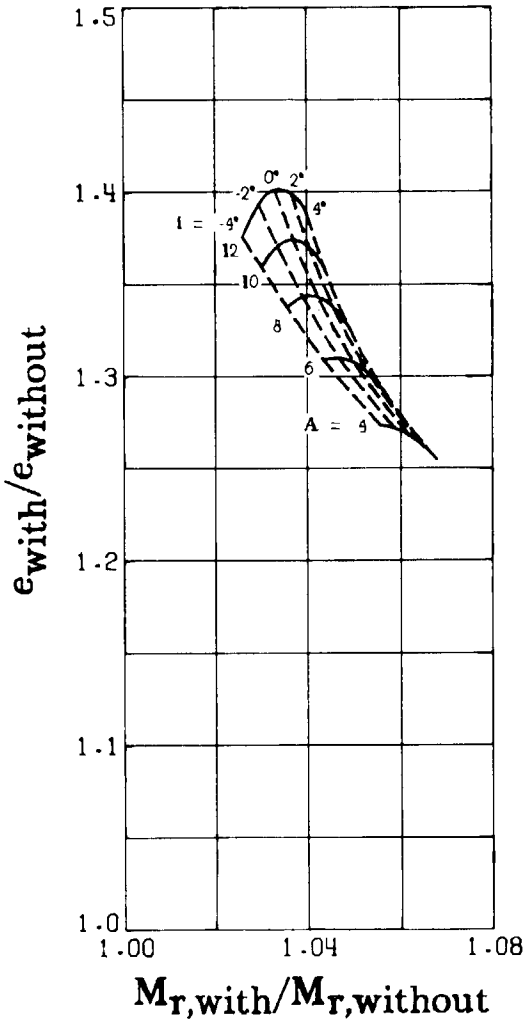

(b) $C_L = 1.0$.

Figure 15.- Potential-flow efficiency factor ratio and root bending-moment ratio for winglet on untwisted wings. $\lambda = 1.0$.

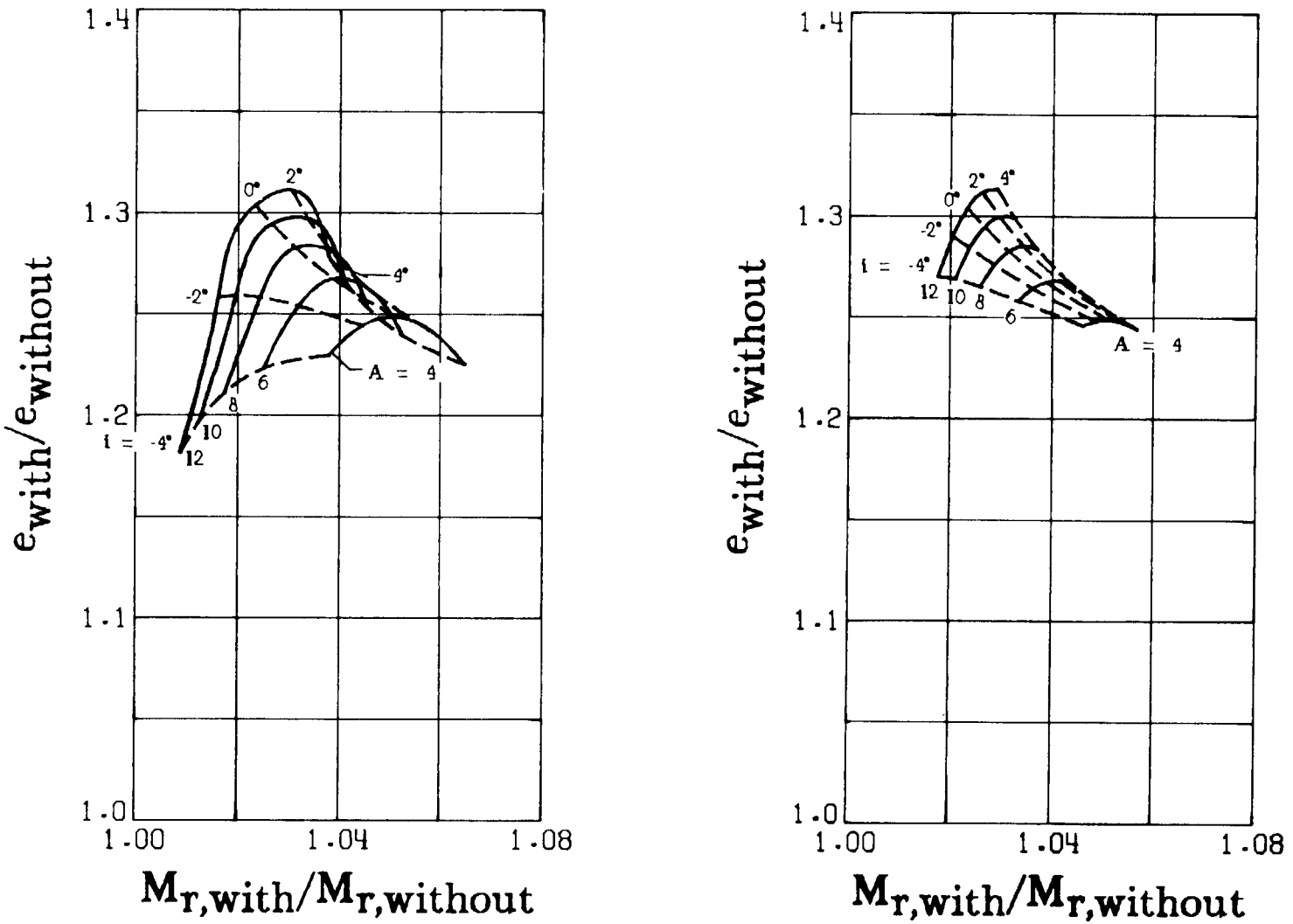

(a) $C_L = 0.4$.

(b) $C_L = 1.0$.

Figure 16.- Potential-flow efficiency factor ratio and root bending-moment ratio for winglet on untwisted wings. $\lambda = 0.5$.

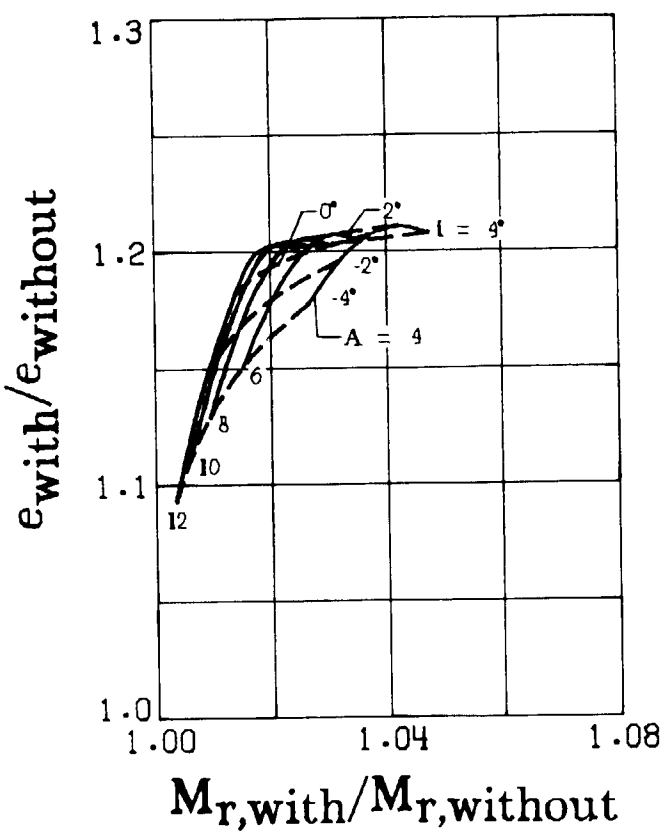

(a) $C_L = 0.4$.

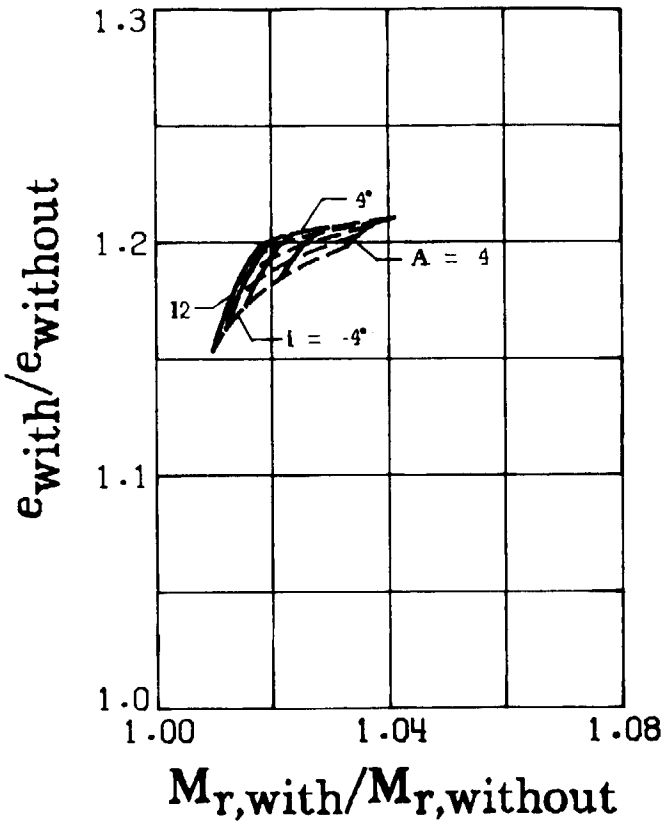

(b) $C_L = 1.0$.

Figure 17.- Potential-flow efficiency factor ratio and root bending-moment ratio for winglet on untwisted wings. $\lambda = 0.25$.

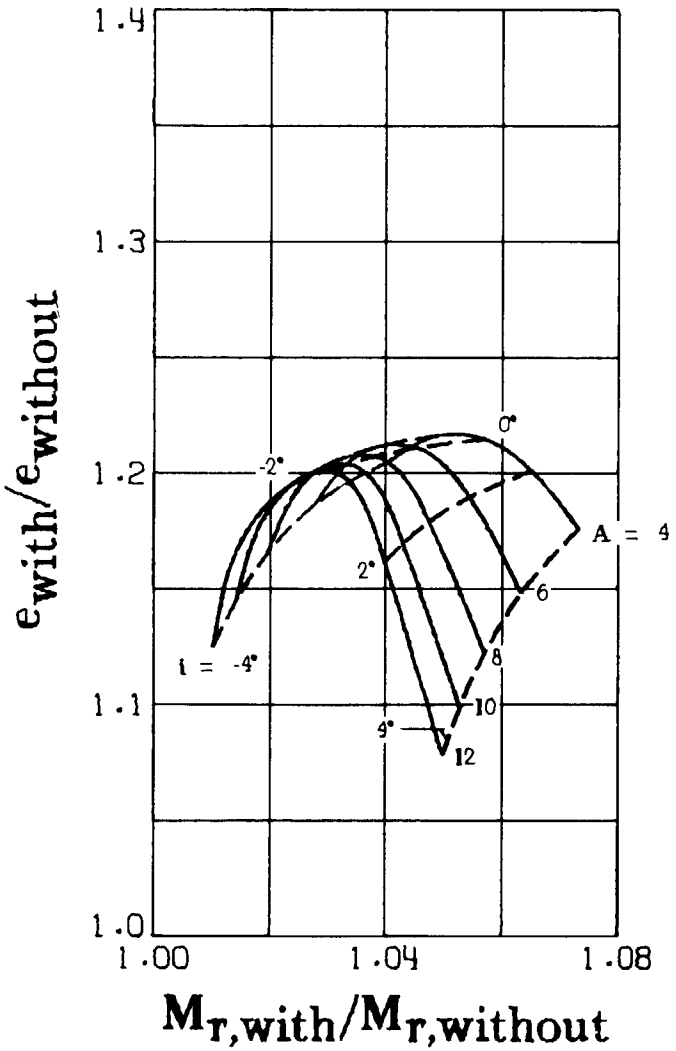

(a) $C_L = 0.4$.

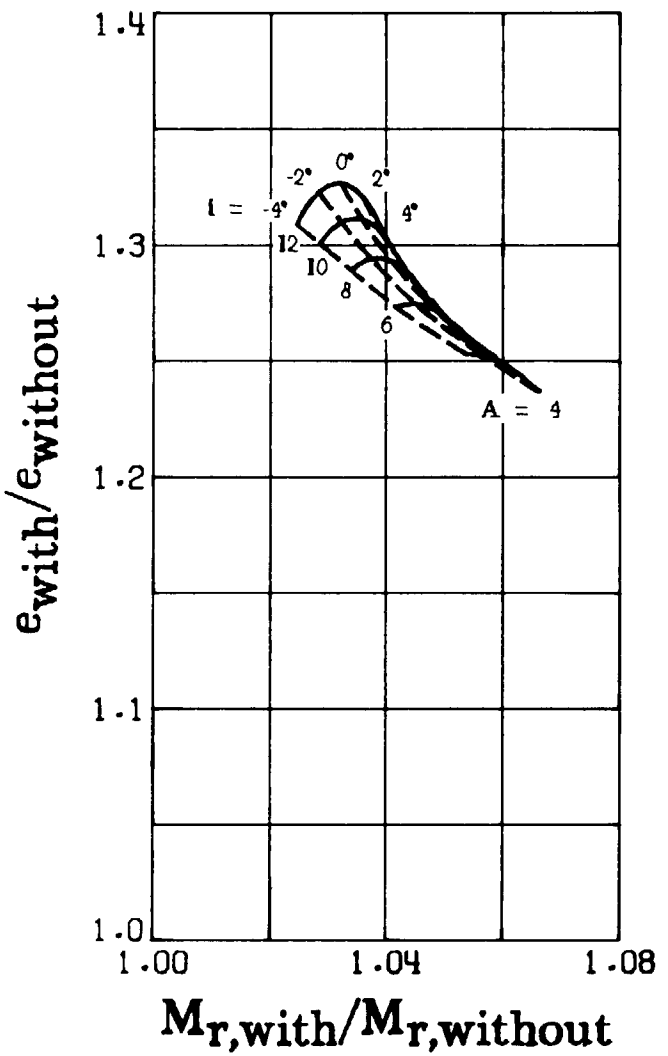

(b) $C_L = 1.0$.

Figure 18.- Potential-flow efficiency factor ratio and root bending-moment ratio for winglet on wings with 5^o washout. $\lambda = 1.0$.

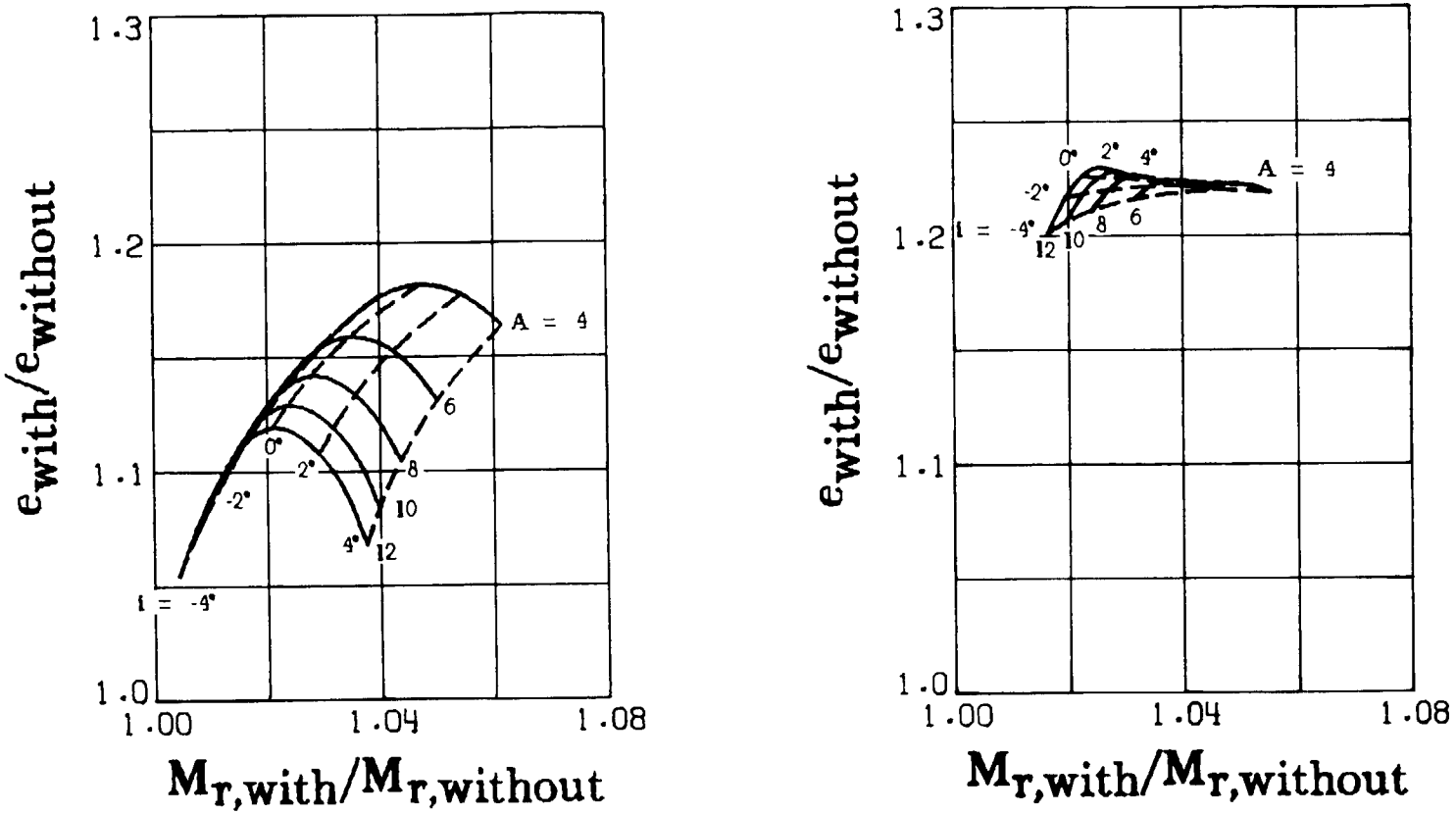

(a) $C_L = 0.4$.

(b) $C_L = 1.0$.

Figure 19.- Potential-flow efficiency factor ratio and root bending-moment ratio for winglet on wings with 5^o washout. $\lambda = 0.5$.

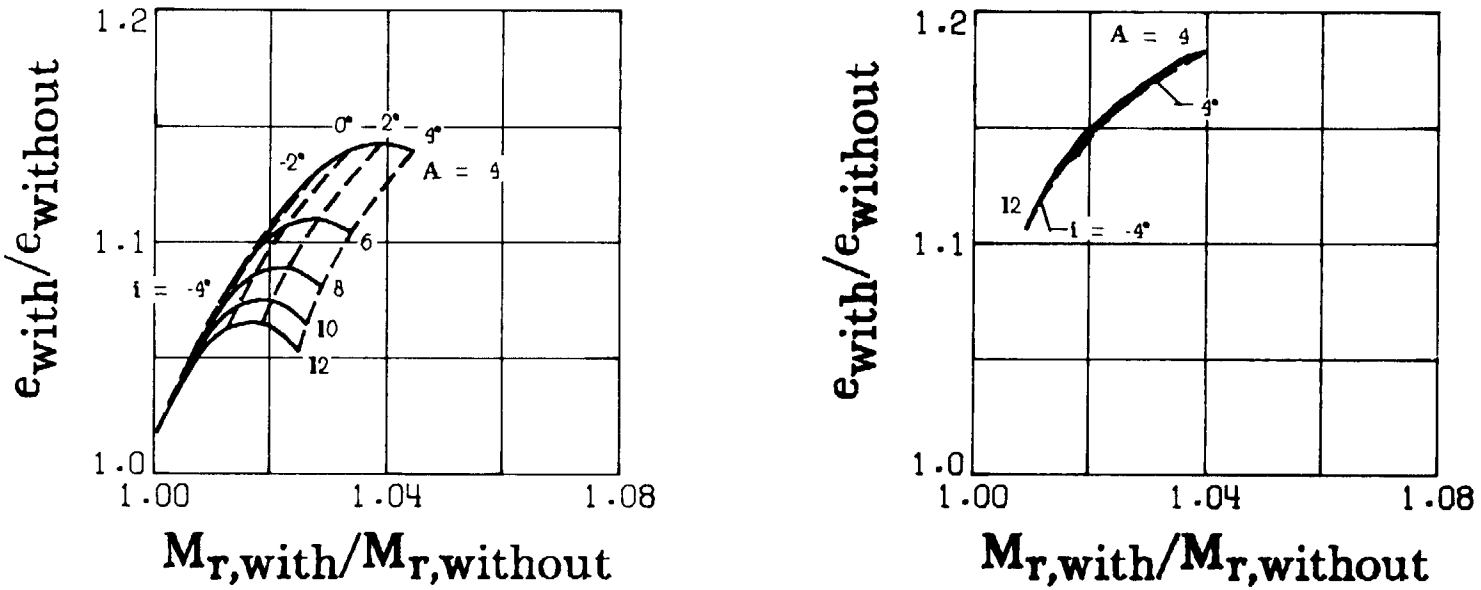

(a) $C_L = 0.4$.

(b) $C_L = 1.0$.

Figure 20.- Potential-flow efficiency factor ratio and root bending-moment ratio for winglet on wings with 5^o washout. $\lambda = 0.25$.

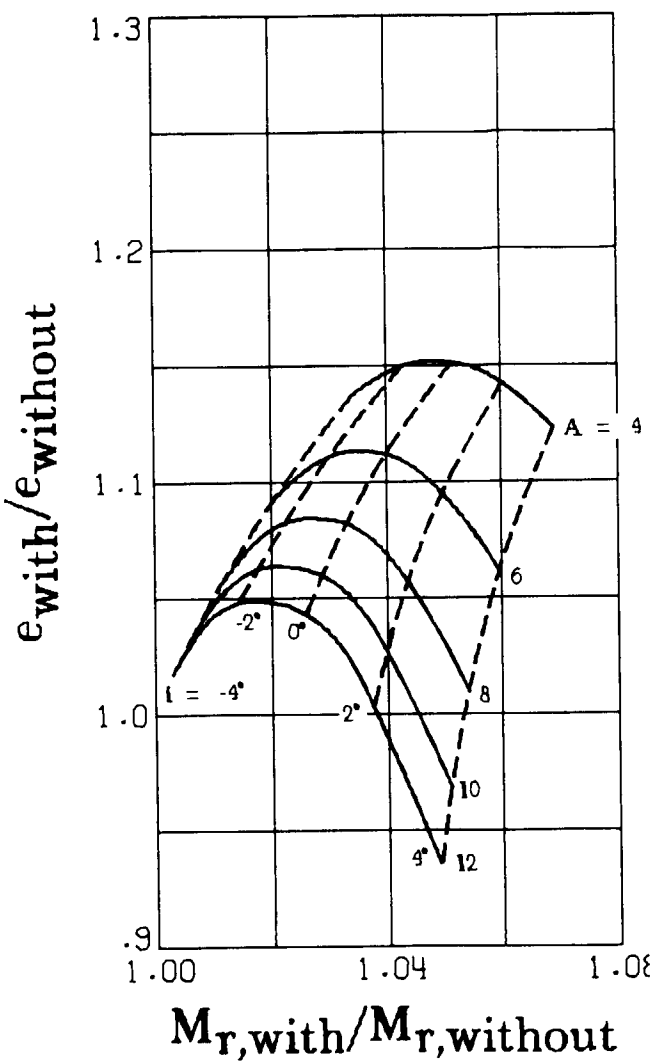

(a) $C_L = 0.4$.

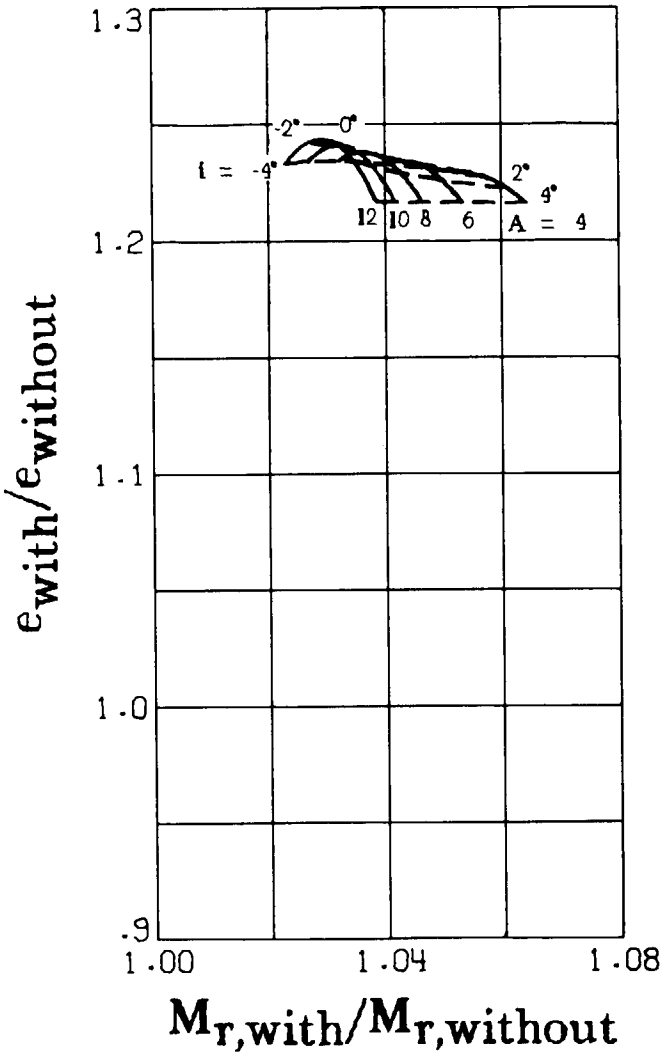

(b) $C_L = 1.0$.

Figure 21.- Potential-flow efficiency factor ratio and root bending-moment ratio for winglet on wings with 10° washout. $\lambda = 1.0$.

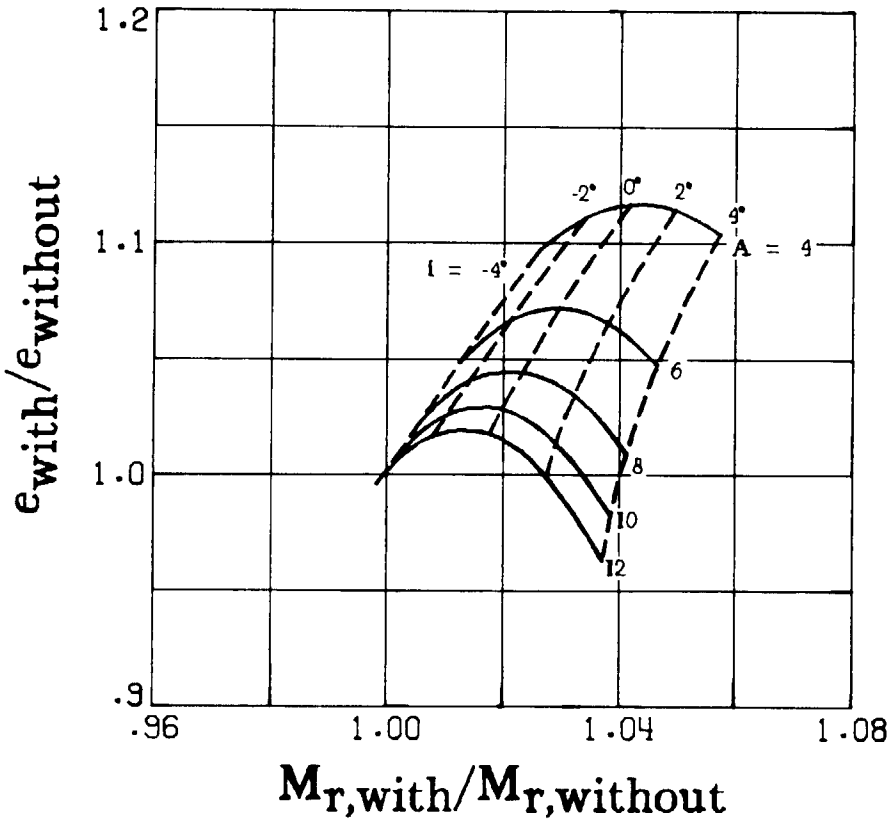

(a) $C_L = 0.4$.

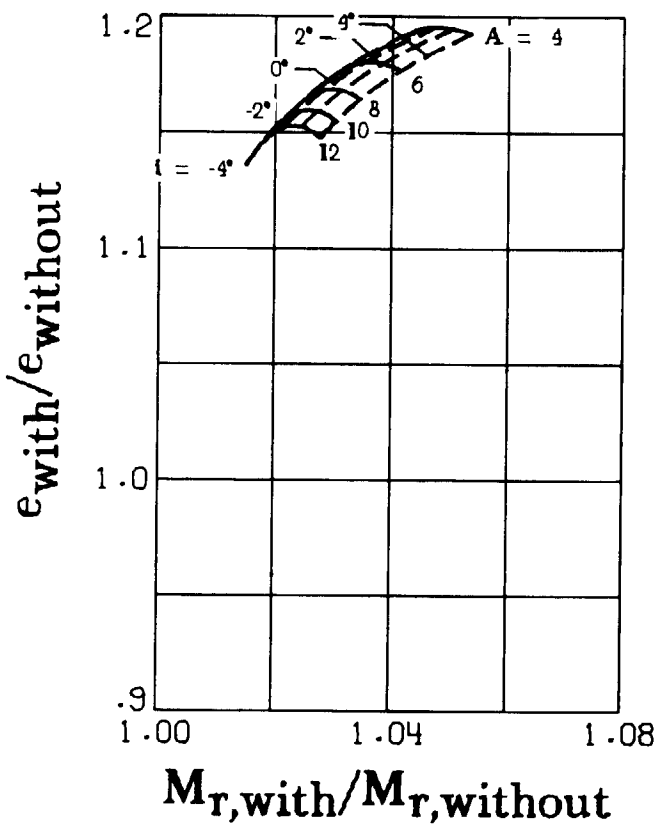

(b) $C_L = 1.0$.

Figure 22.- Potential-flow efficiency factor ratio and root bending-moment ratio for winglet on wings with 10^o washout. $\lambda = 0.5$.

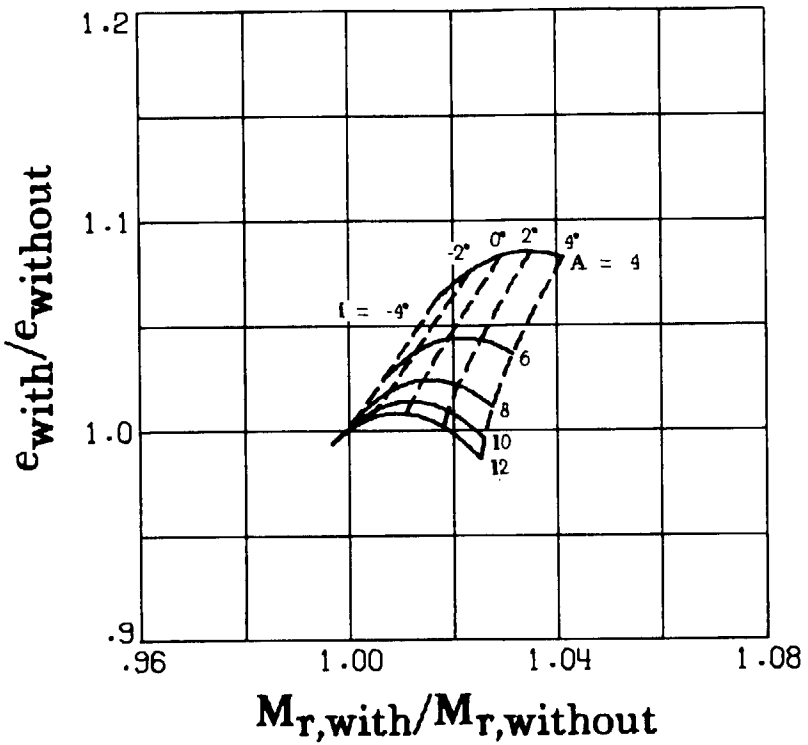

(a) $C_L = 0.4$.

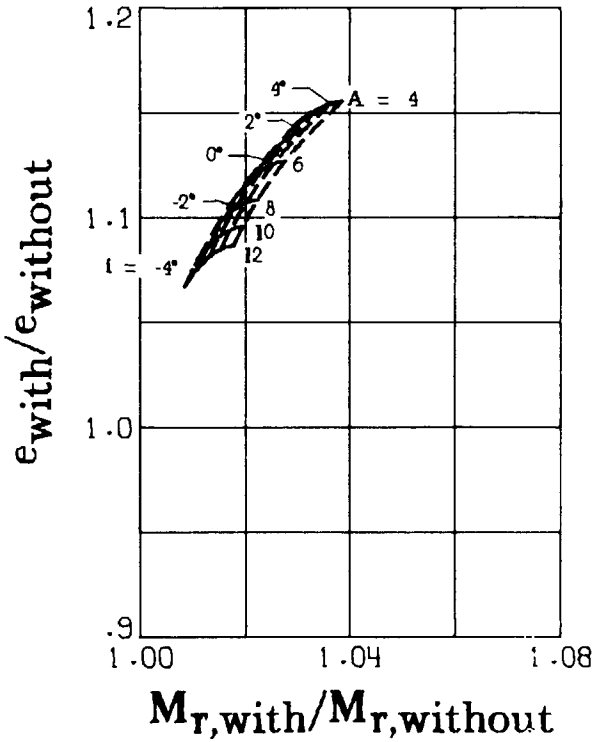

(b) $C_L = 1.0$.

Figure 23.- Potential-flow efficiency factor ratio and root bending-moment ratio for winglet on wings with 10^o washout. $\lambda = 0.25$.

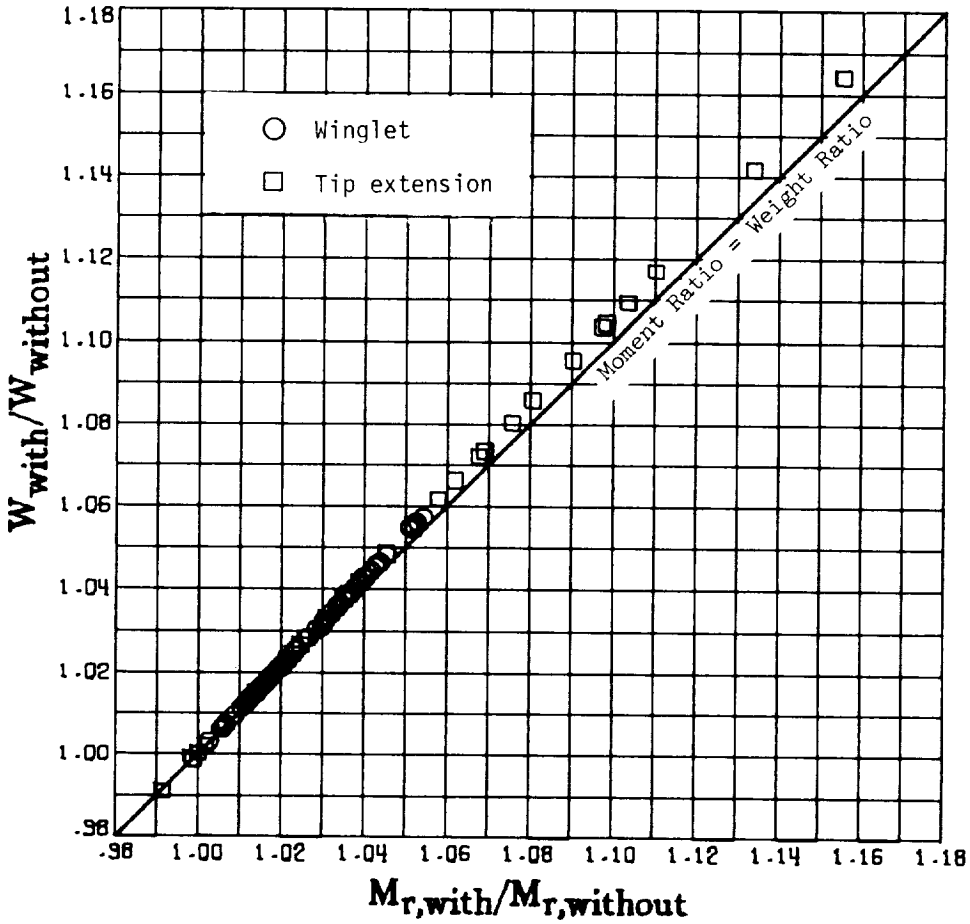

Figure 24.- Correlation of ratio of minimum weight of bending material with the ratio of root bending moment.

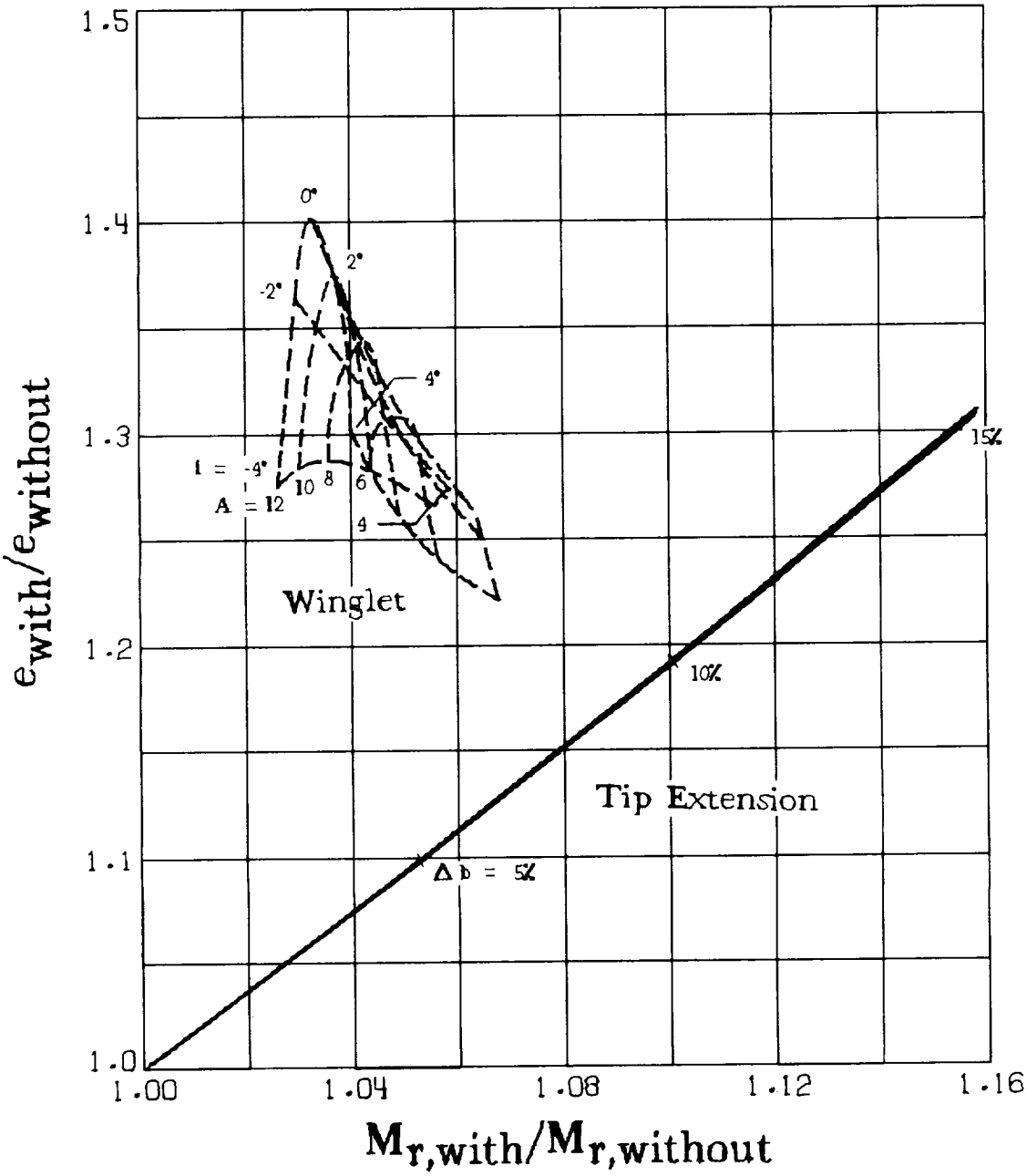

Figure 25.- Comparison of tip extension and winglet when added to an untwisted wing. $\lambda = 1.0$. Efficiency factor ratios are calculated for $C_L = 0.4$; moment ratios are calculated for $C_L = 1.0$.

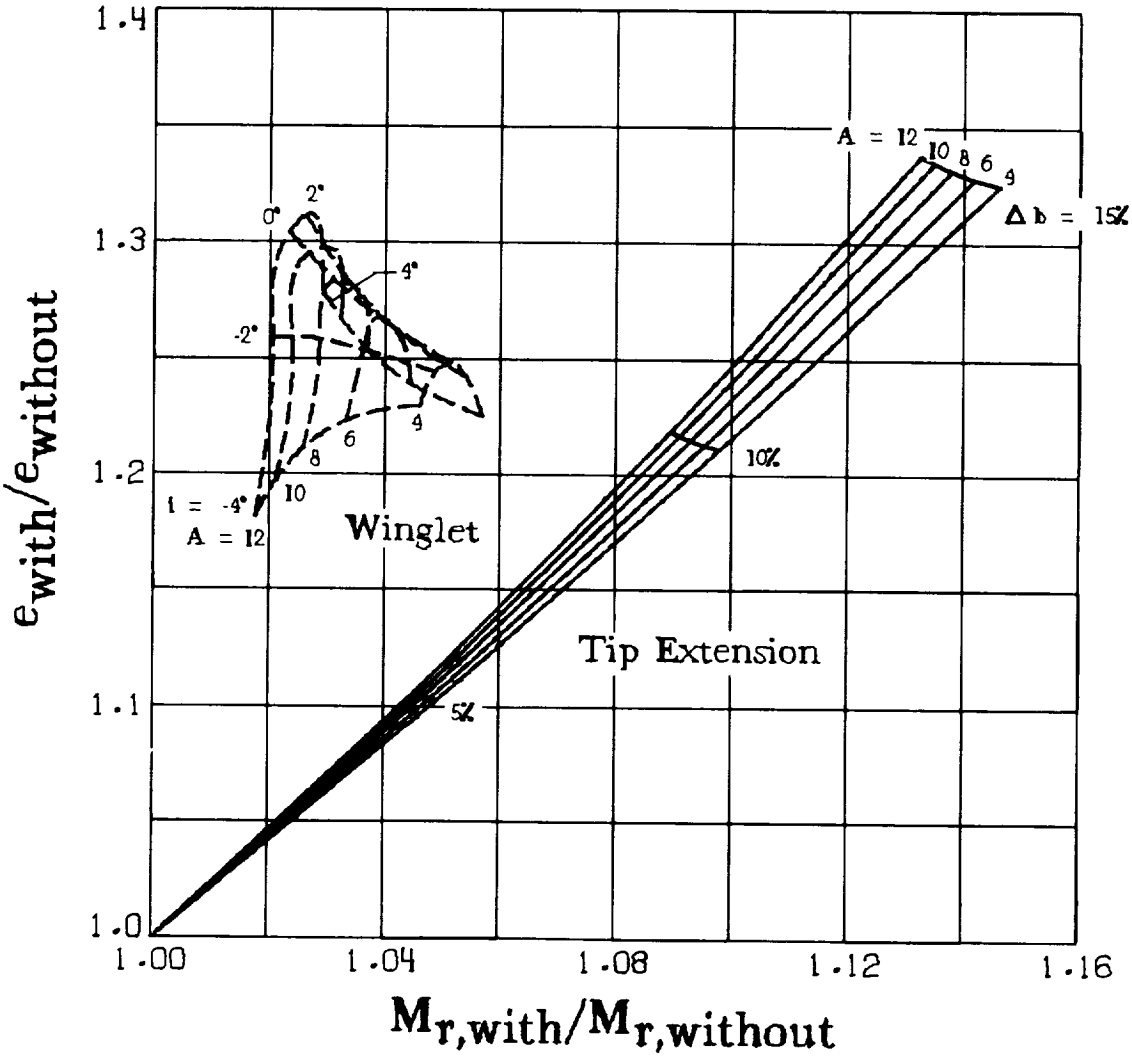

Figure 26.- Comparison of tip extension and winglet when added to an untwisted wing. $\lambda = 0.5$. Efficiency factor ratios are calculated for $C_L = 0.4$; moment ratios are calculated for $C_L = 1.0$.

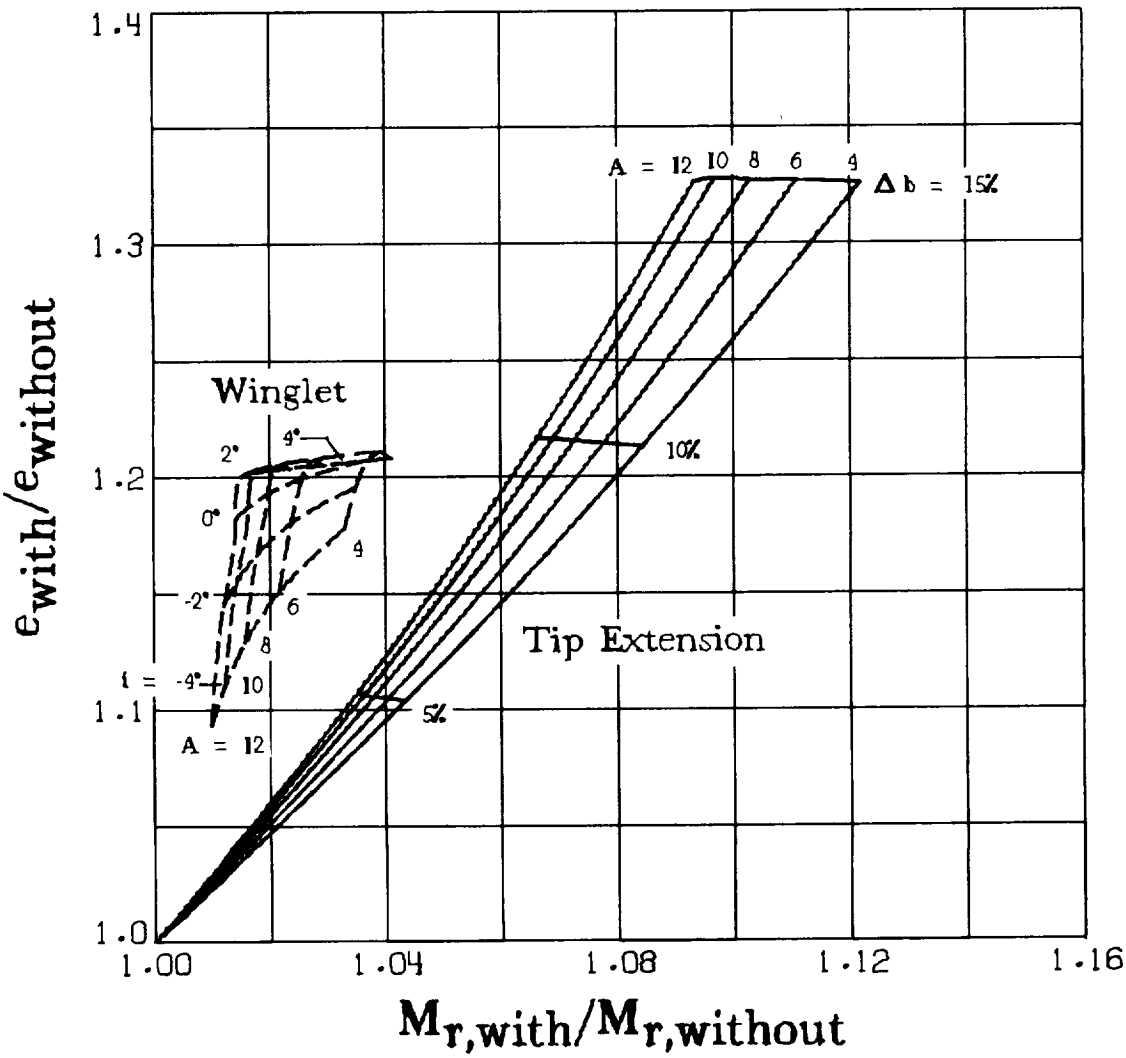

Figure 27.- Comparison of tip extension and winglet when added to an untwisted wing. $\lambda = 0.25$. Efficiency factor ratios are calculated for $C_L = 0.4$; moment ratios are calculated for $C_L = 1.0$.

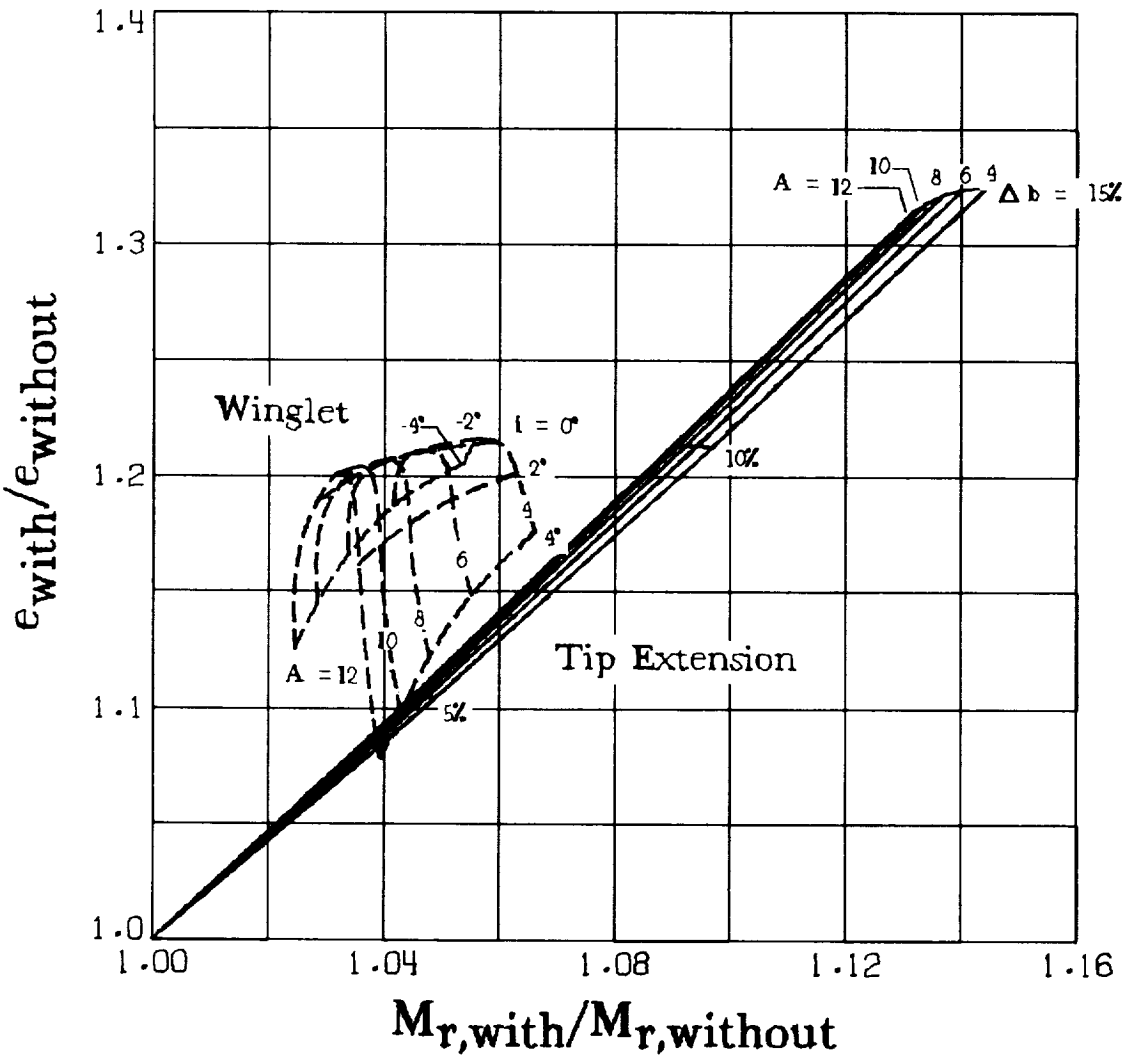

Figure 28.- Comparison of tip extension and winglet when added to a wing with 5^{o} washout. $\lambda = 1.0$. Efficiency factor ratios are calculated for $C_L = 0.4$; moment ratios are calculated for $C_L = 1.0$.

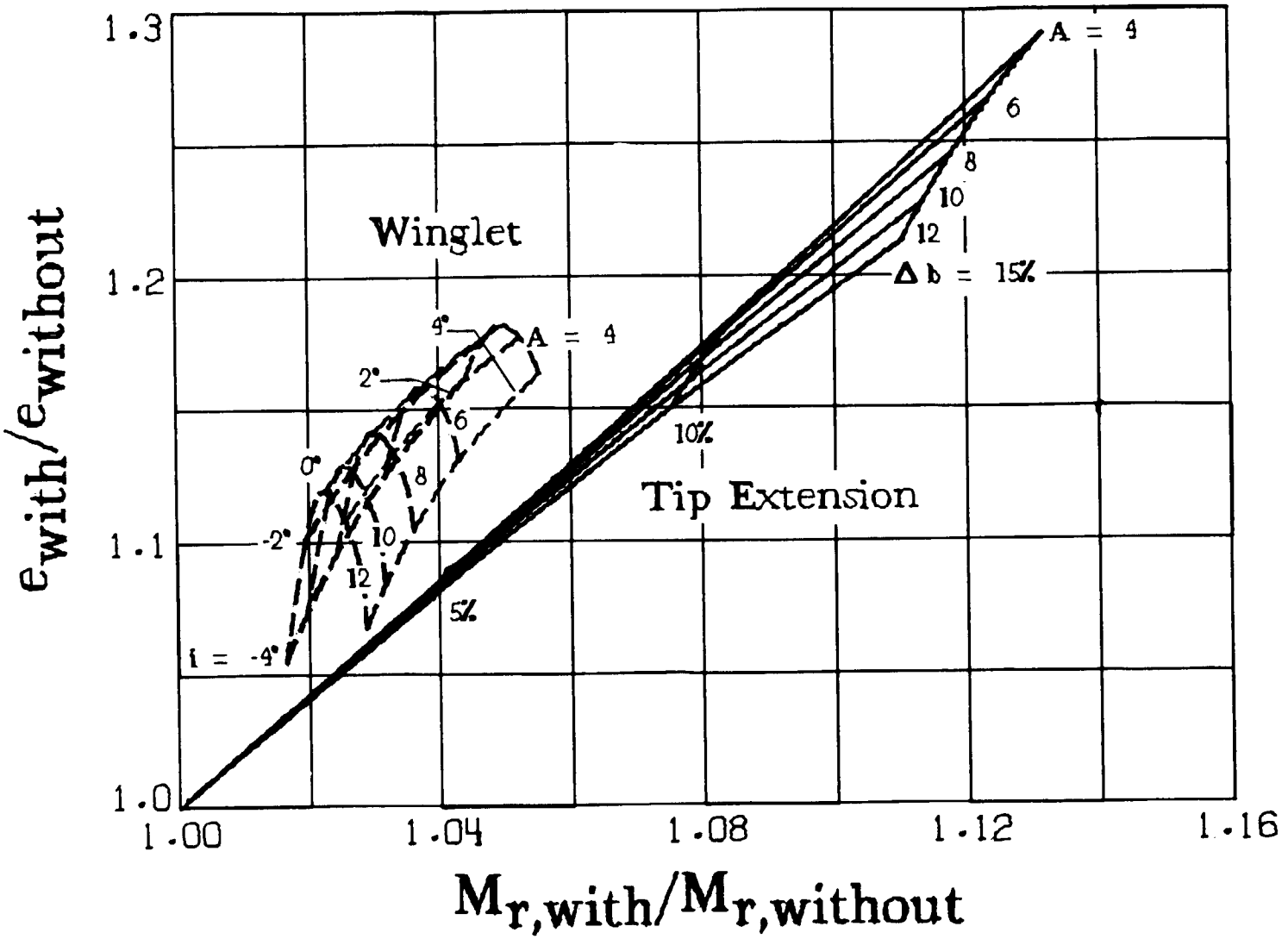

Figure 29.- Comparison of tip extension and winglet when added to a wing with 5^{o} washout. $\lambda = 0.5$. Efficiency factor ratios are calculated for $C_L = 0.4$; moment ratios are calculated for $C_L = 1.0$.

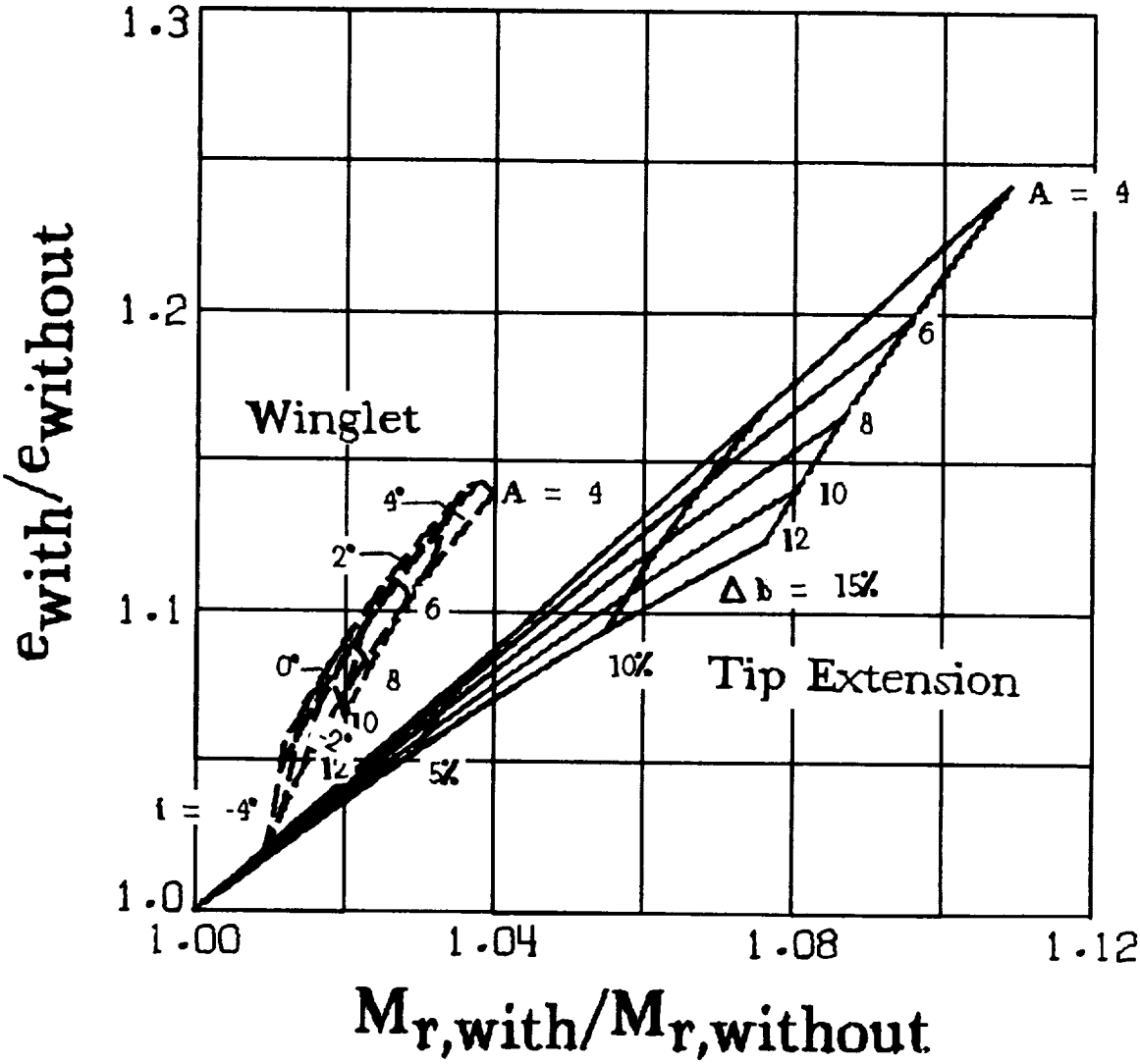

Figure 30.- Comparison of tip extension and winglet when added to a wing with 5^{o} washout. $\lambda = 0.25$. Efficiency factor ratios are calculated for $C_L = 0.4$; moment ratios are calculated for $C_L = 1.0$.

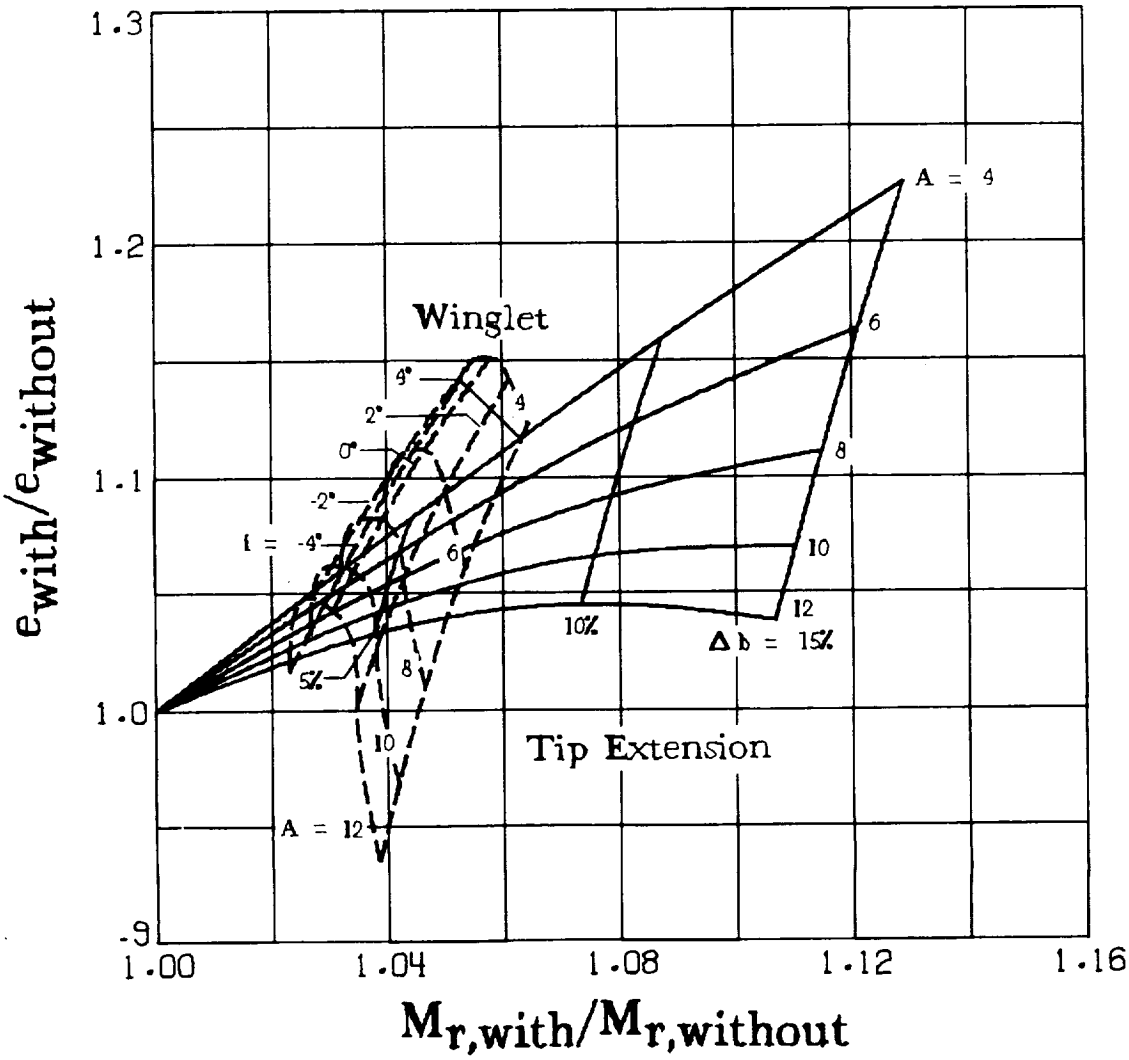

Figure 31.- Comparison of tip extension and winglet when added to a wing with 10^{o} washout. $\lambda = 1.0$. Efficiency factor ratios are calculated for $C_L = 0.4$; moment ratios are calculated for $C_L = 1.0$.

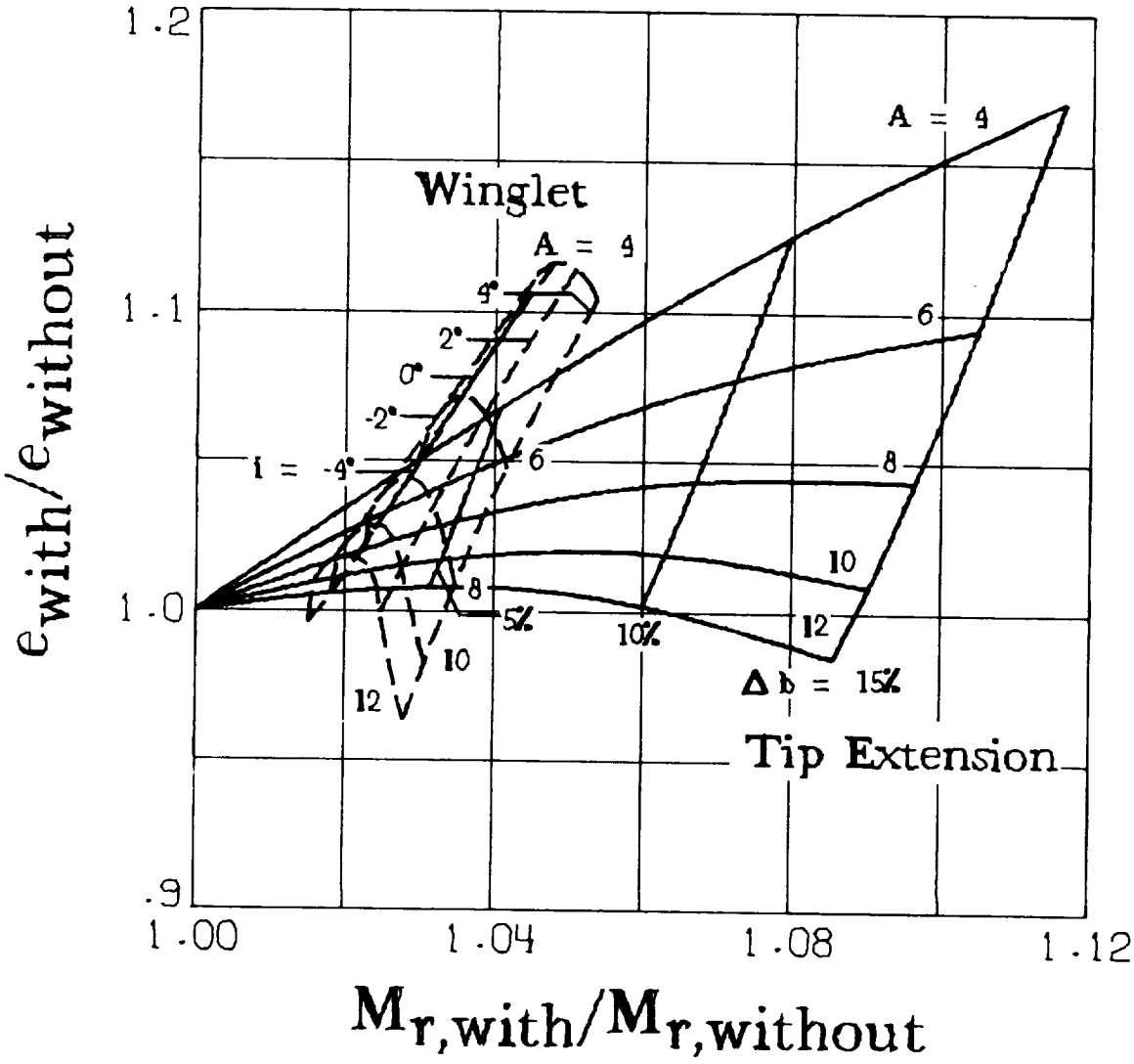

Figure 32.- Comparison of tip extension and winglet when added to a wing with 10^{o} washout. $\lambda = 0.5$. Efficiency factor ratios are calculated for $C_L = 0.4$; moment ratios are calculated for $C_L = 1.0$.

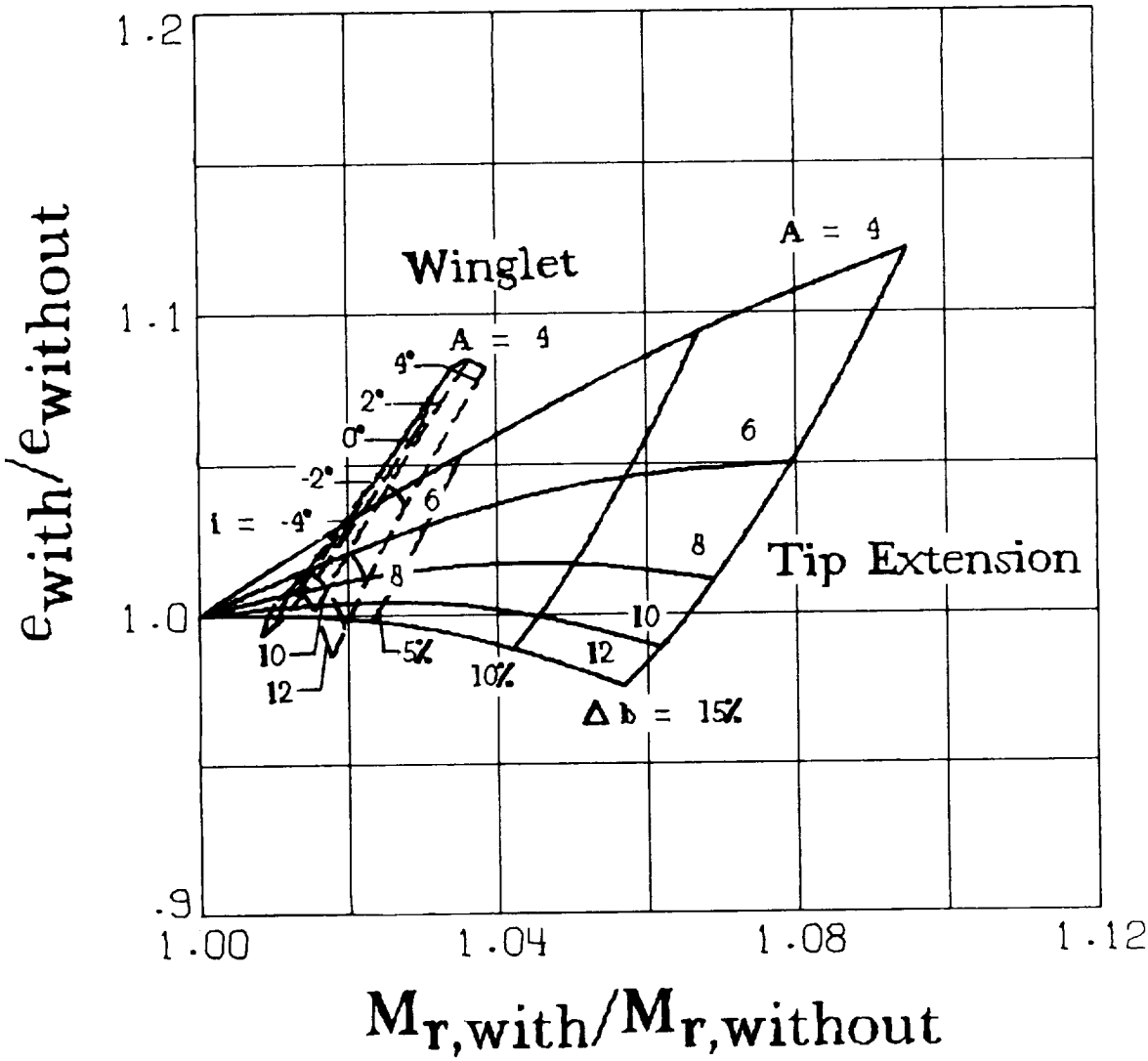

Figure 33.- Comparison of tip extension and winglet when added to a wing with 10^{o} washout. $\lambda = 0.25$. Efficiency factor ratios are calculated for $C_L = 0.4$; moment ratios are calculated for $C_L = 1.0$.

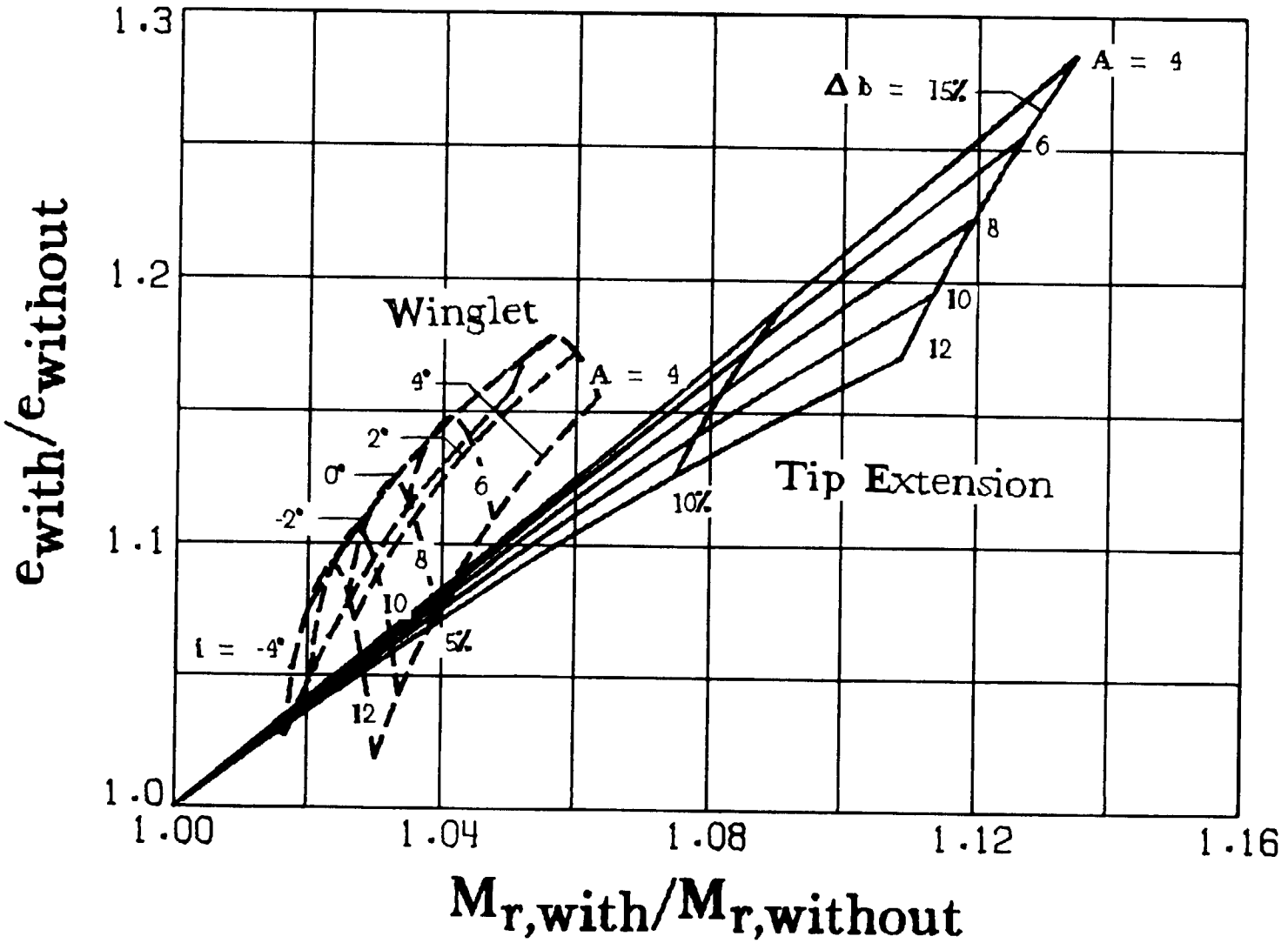

Figure 34.- Comparison of tip extension and winglet at a Mach number of 0.8. Compare with figure 29 for a Mach number of 0. $\lambda = 0.5$; 5^{O} washout. Efficiency factor ratios are calculated for $C_L = 0.4$; moment ratios are calculated for $C_L = 1.0$.

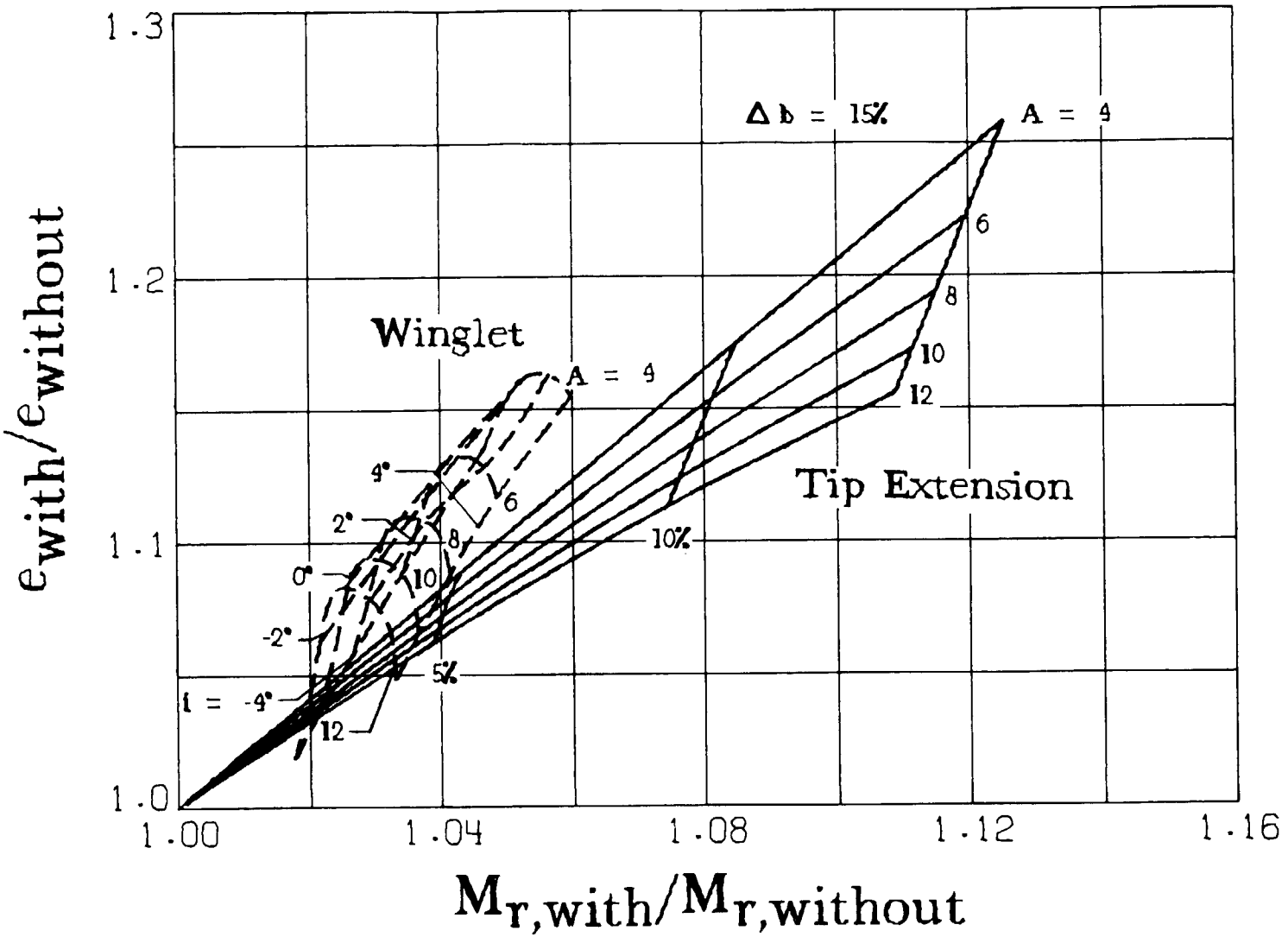

Figure 35.- Comparison of tip extension and winglet when added to a wing with $\Lambda = 0^{o}$. Compare with figure 29 for $\Lambda = 30^{o}$. $\lambda = 0.5$; 5^{o} washout. Efficiency factor ratios are calculated for $C_L = 0.4$; moment ratios are calculated for $C_L = 1.0$.

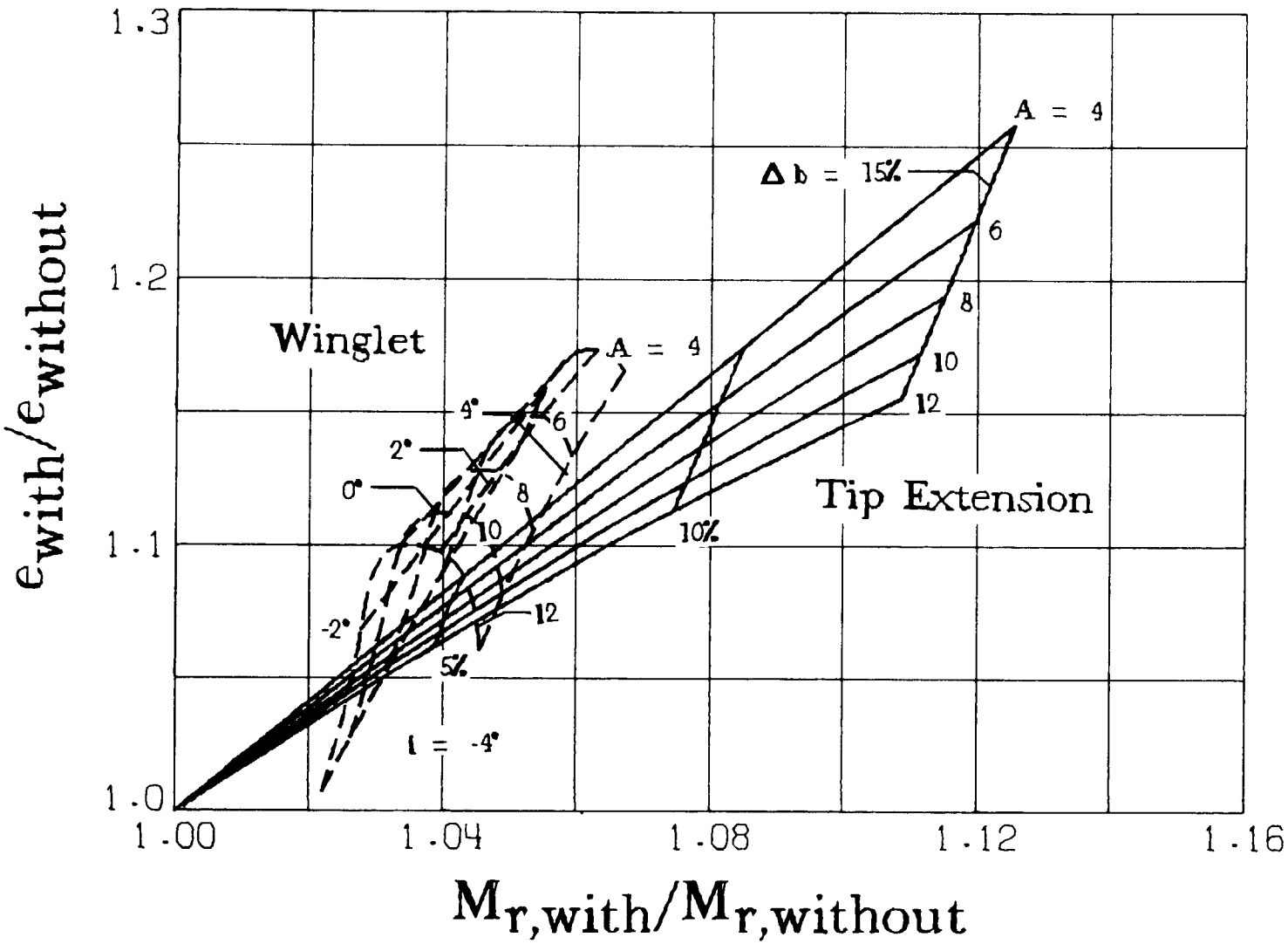

Figure 36.- Comparison of tip extension and unswept winglet ($\Lambda_W = 0^o$) when added to a wing with $\Lambda = 0^o$. Compare with figure 29 ($\Lambda = 30^o$, $\Lambda_W = 45^o$) and figure 35 ($\Lambda = 0^o$, $\Lambda_W = 45^o$). $\lambda = 0.5$; 5^o washout. Efficiency factor ratios are calculated for $C_L = 0.4$; moment ratios are calculated for $C_L = 1.0$.

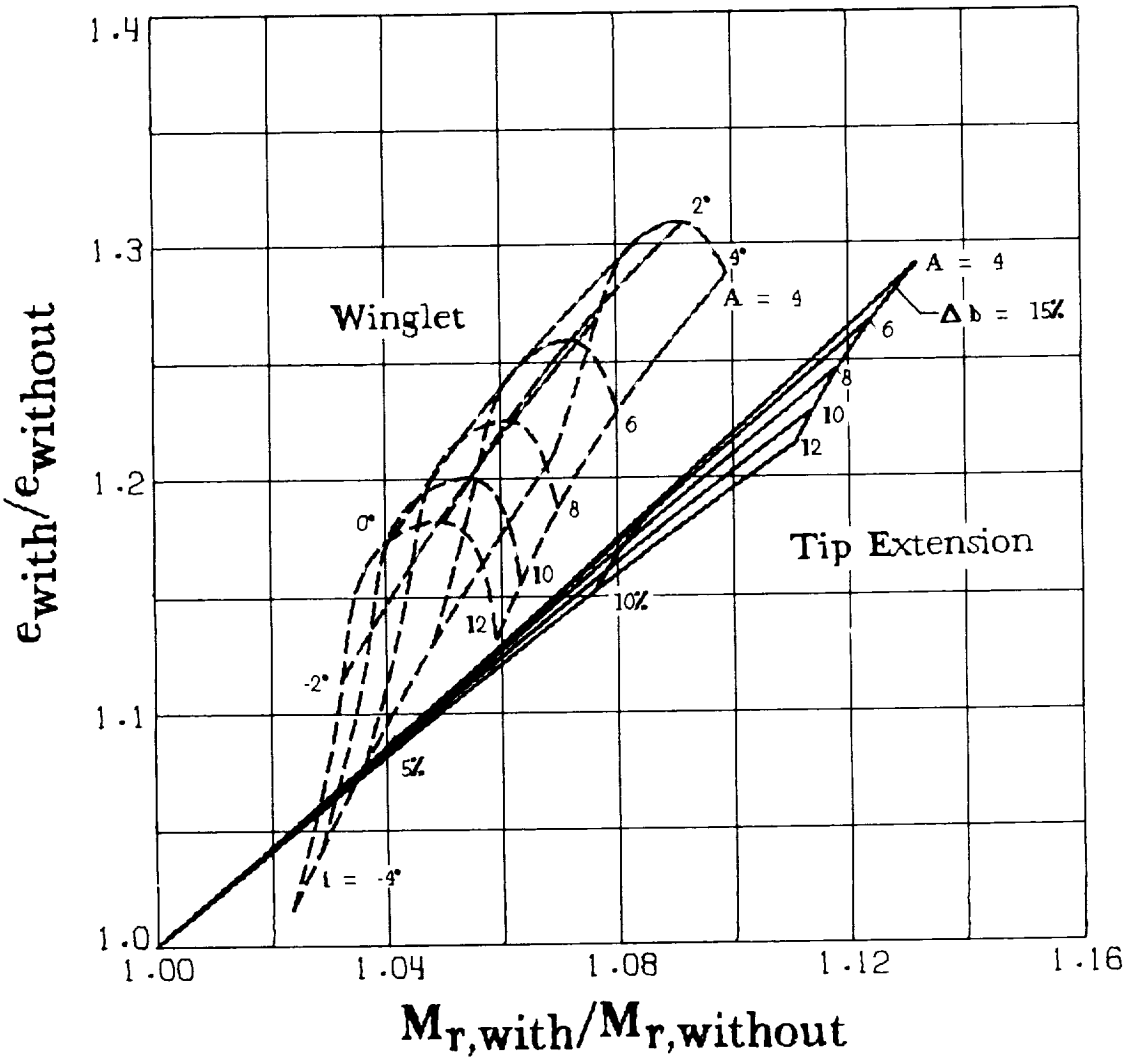

Figure 37.- Comparison of tip extension and winglet with a length of 0.30b/2. Compare with figure 29 for a winglet length of 0.15b/2. $\lambda = 0.5$; 5^{o} washout. Efficiency factor ratios are calculated for $C_L = 0.4$; moment ratios are calculated for $C_L = 1.0$.

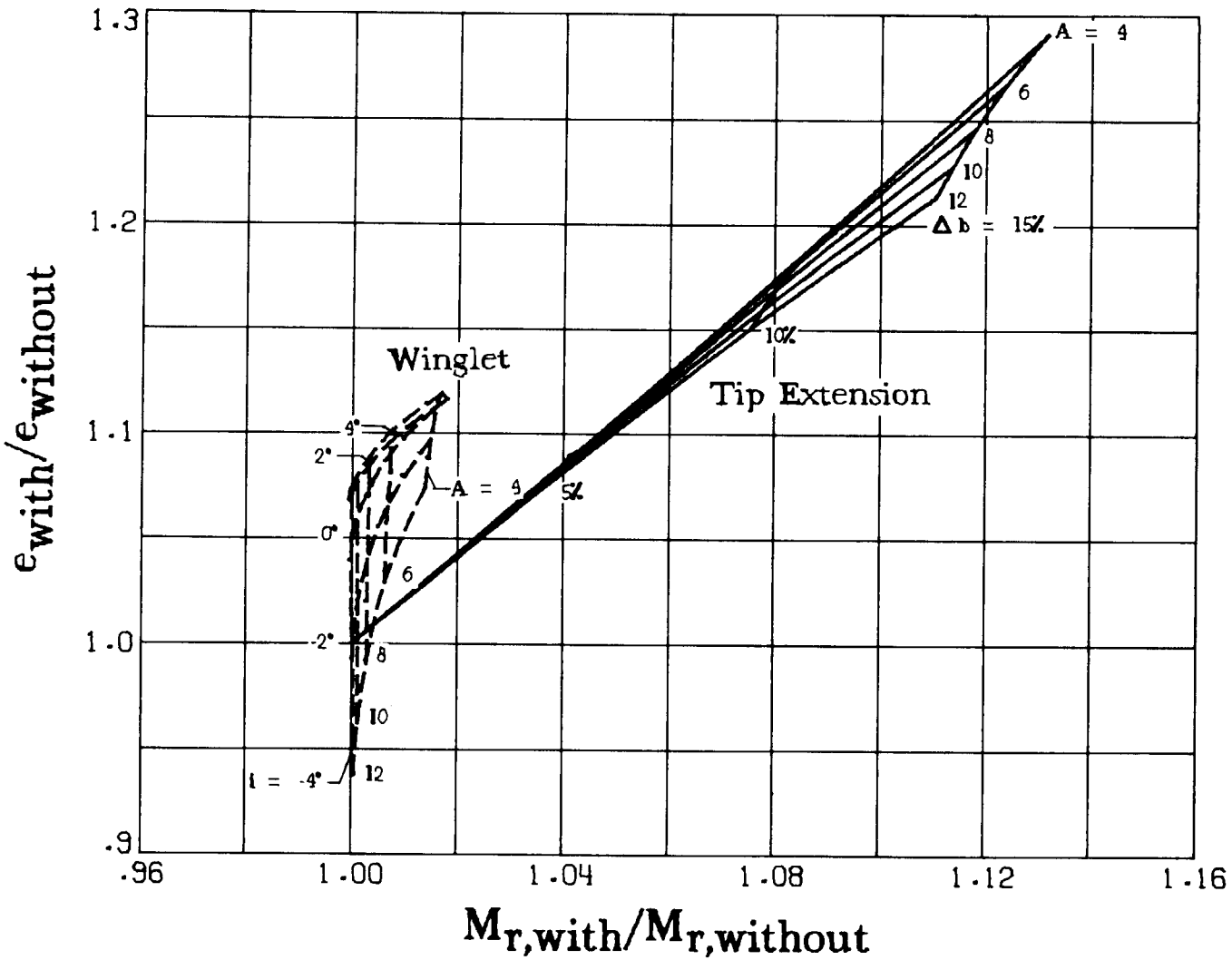

(a) $\gamma = -15^{o}$.

Figure 38.- Comparison of tip extension and a winglet of varying cant angle. Compare with figure 29 or 38(c) for a cant angle of 15^{o}. $\lambda = 0.5$; 5^{o} washout. Efficiency factor ratios are calculated for $C_L = 0.4$; moment ratios are calculated for $C_L = 1.0$.

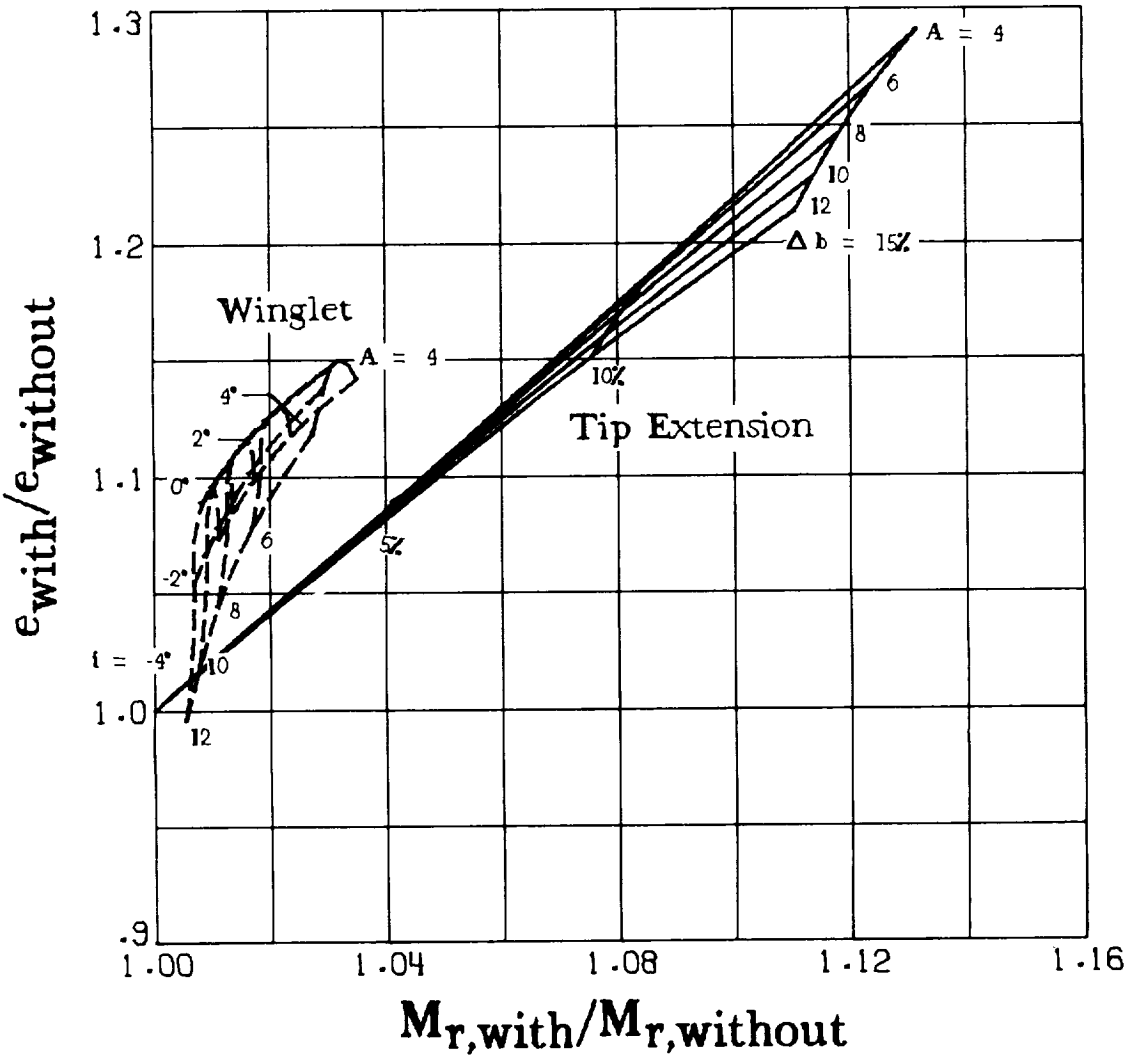

(b) $\gamma = 0^{o}$.

Figure 38.- Continued.

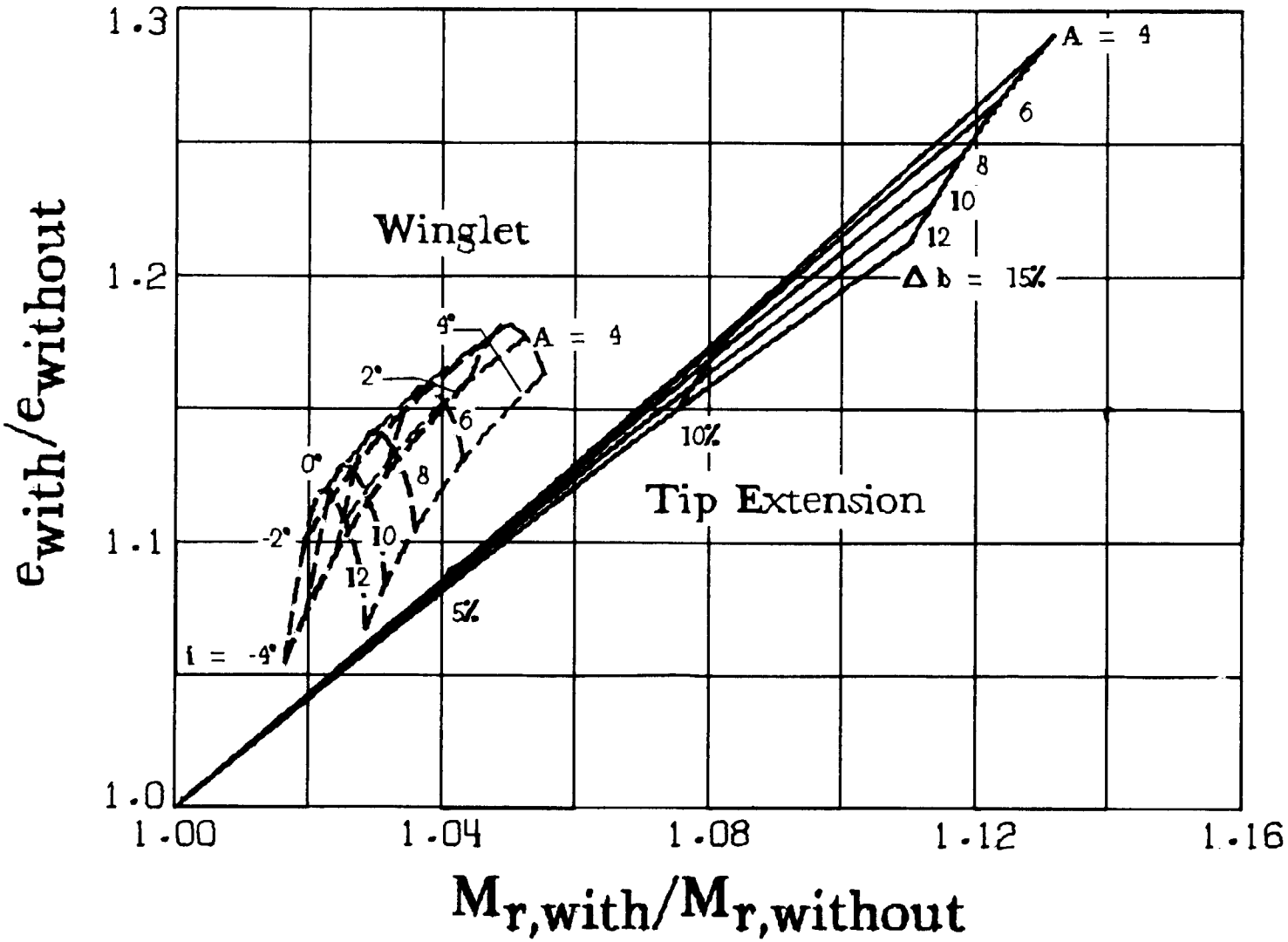

(c) $\gamma = 15^{o}$.

Figure 38.- Continued.

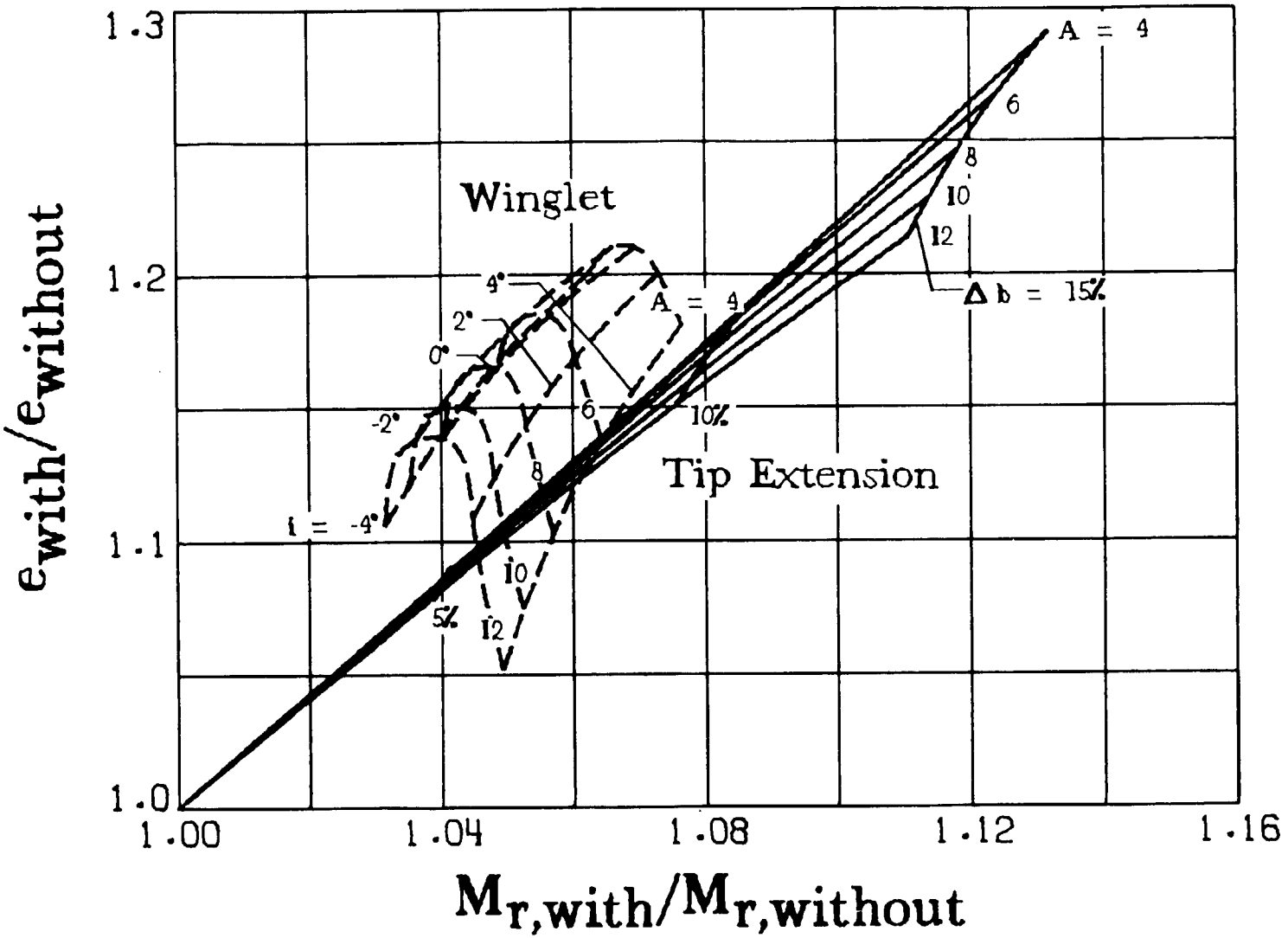

(d) $\gamma = 30^{o}$.

Figure 38.- Continued.

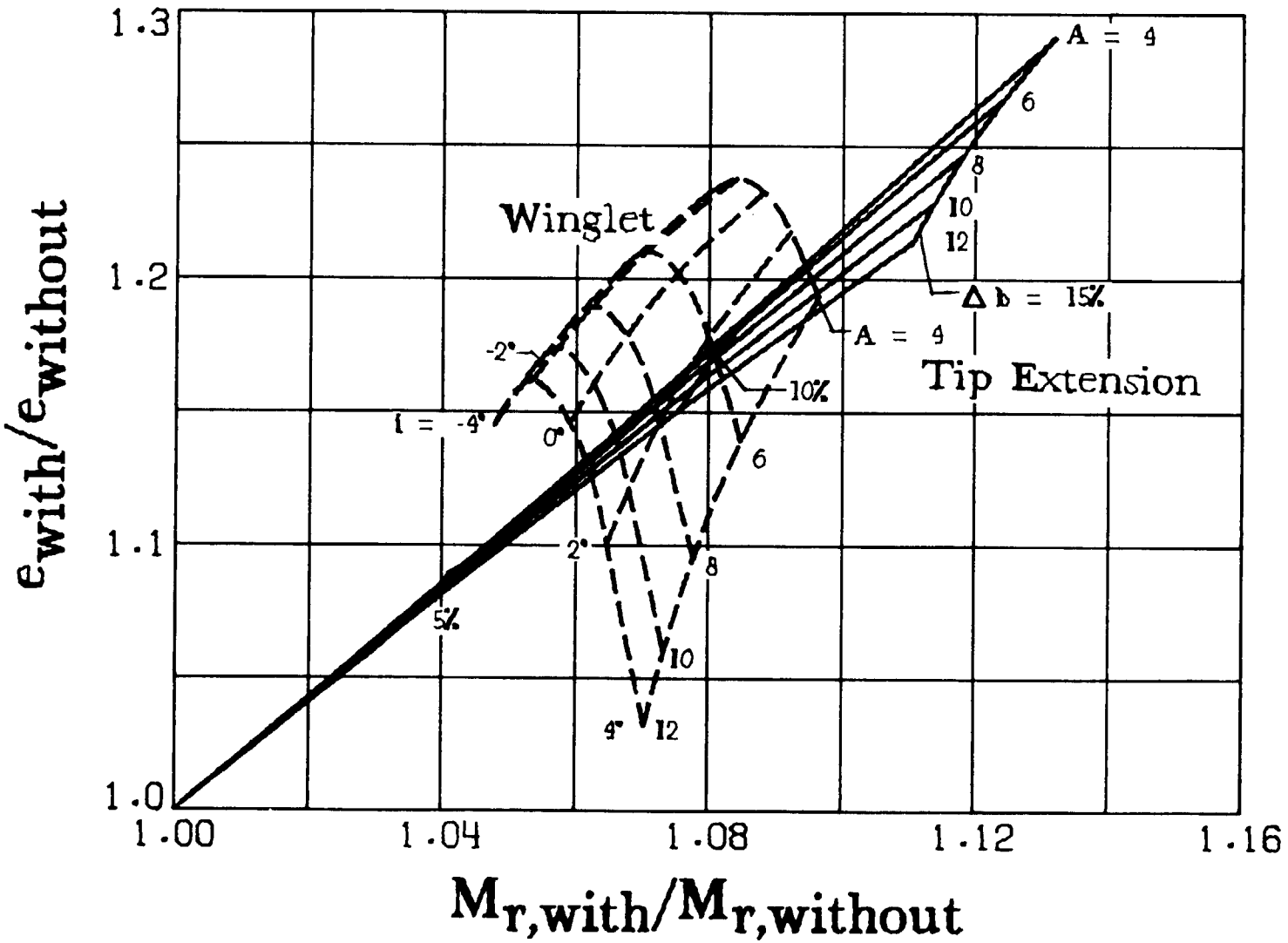

(e) $\gamma = 45^{o}$.

Figure 38.- Continued.

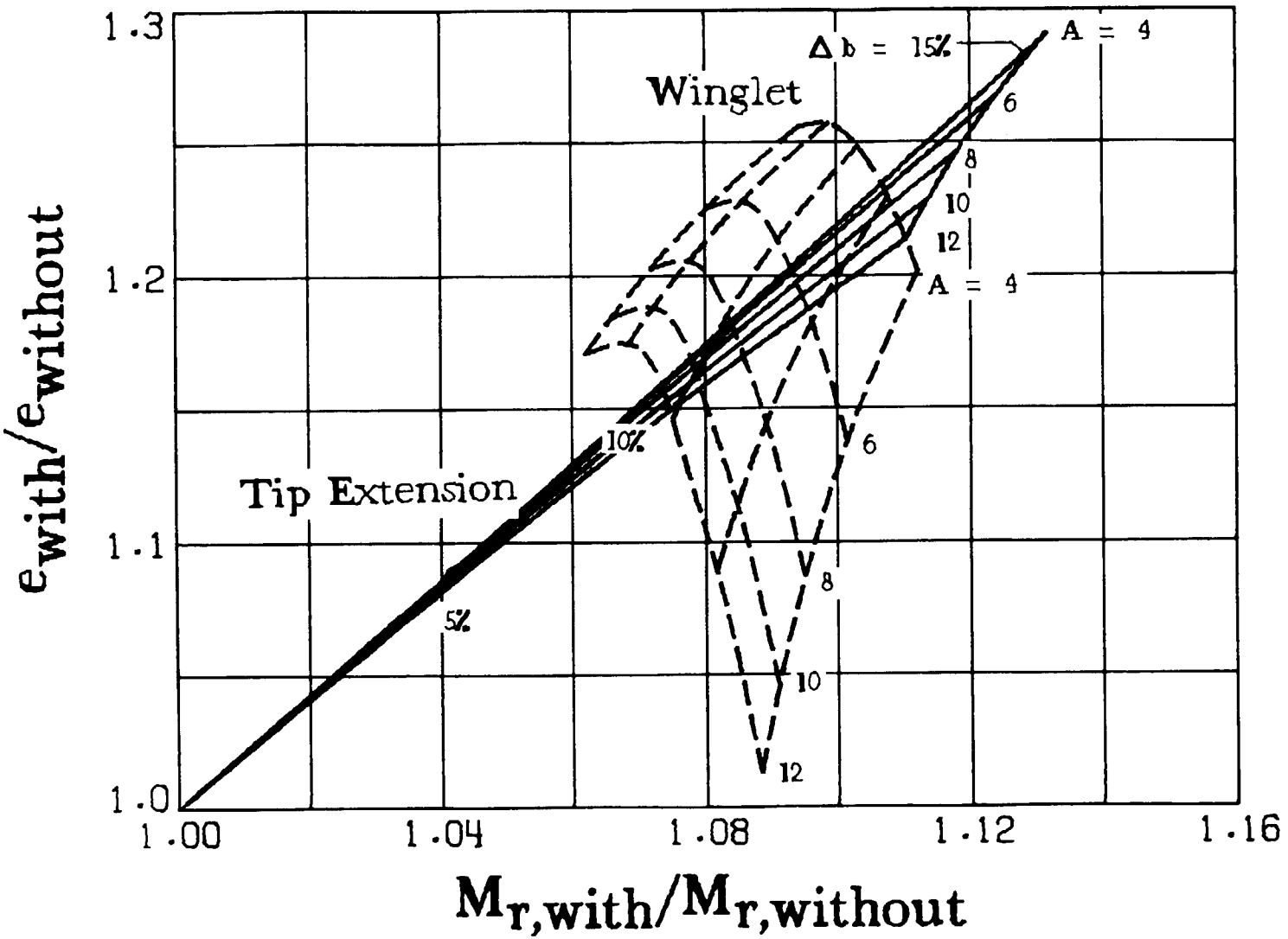

(f) $\gamma = 60^{o}$.

Figure 38.- Continued.

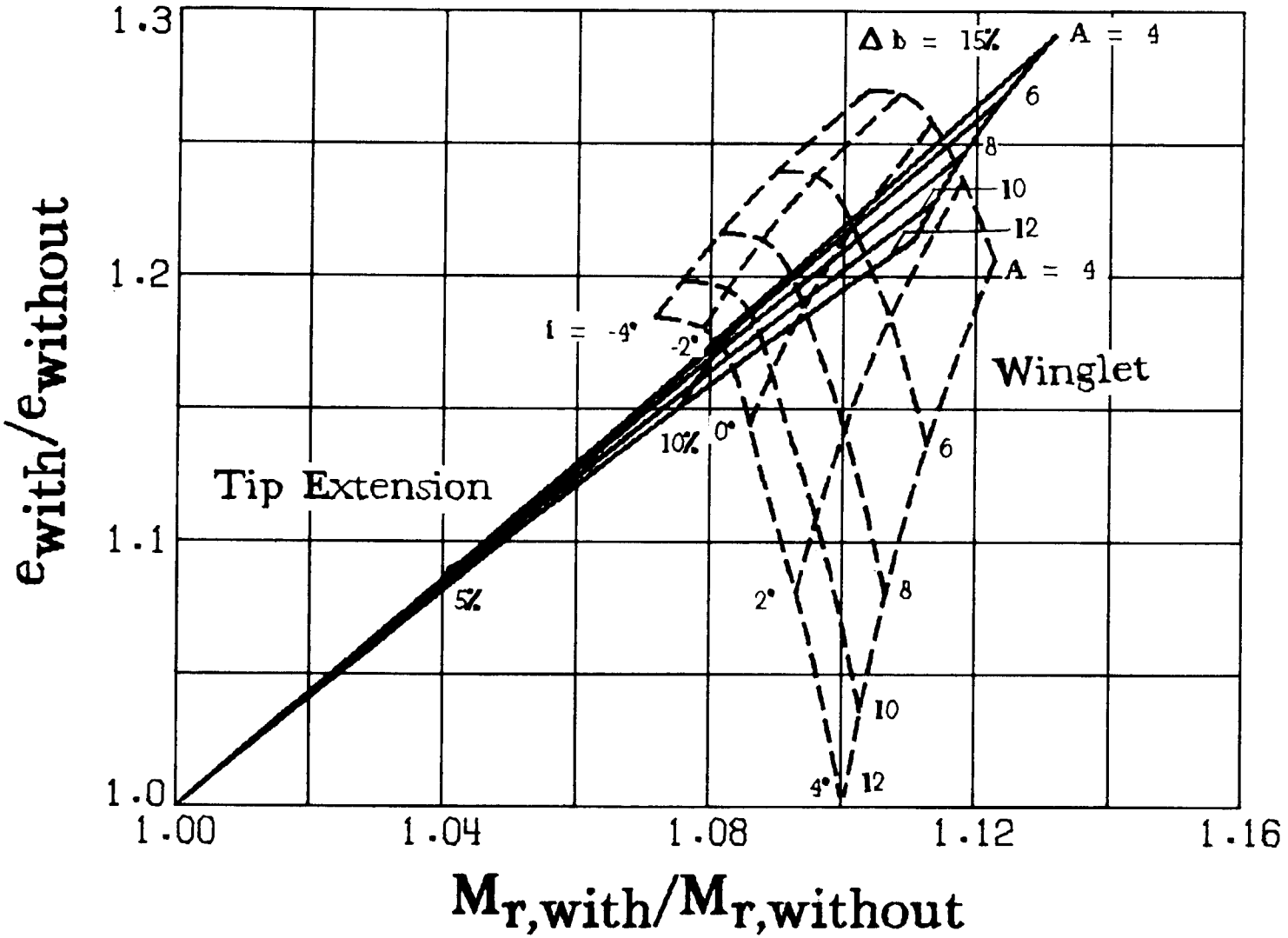

(g) $\gamma = 75^{o}$.

Figure 38.- Continued.

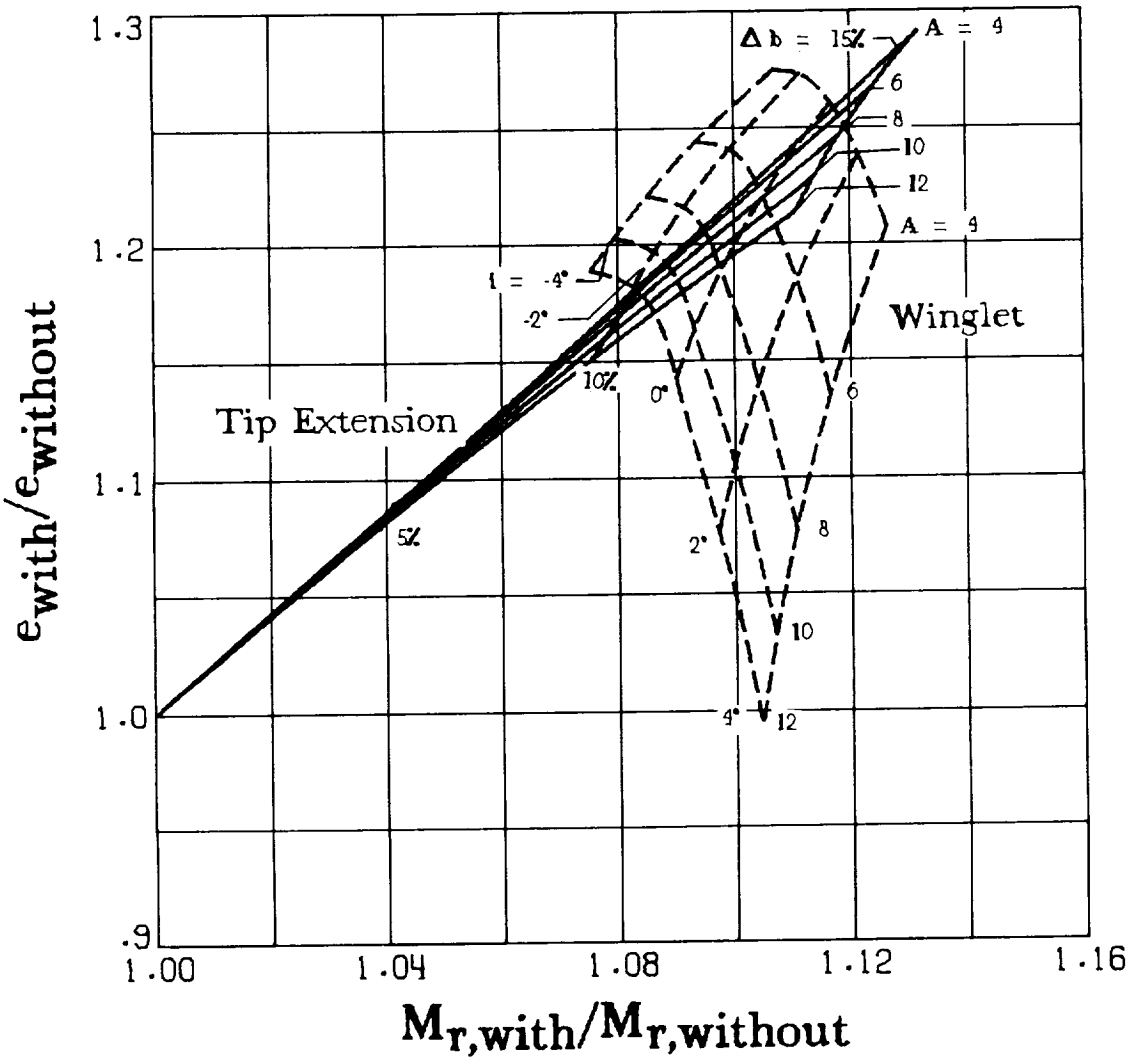

(h) $\gamma = 90^{o}$.

Figure 38.- Concluded.

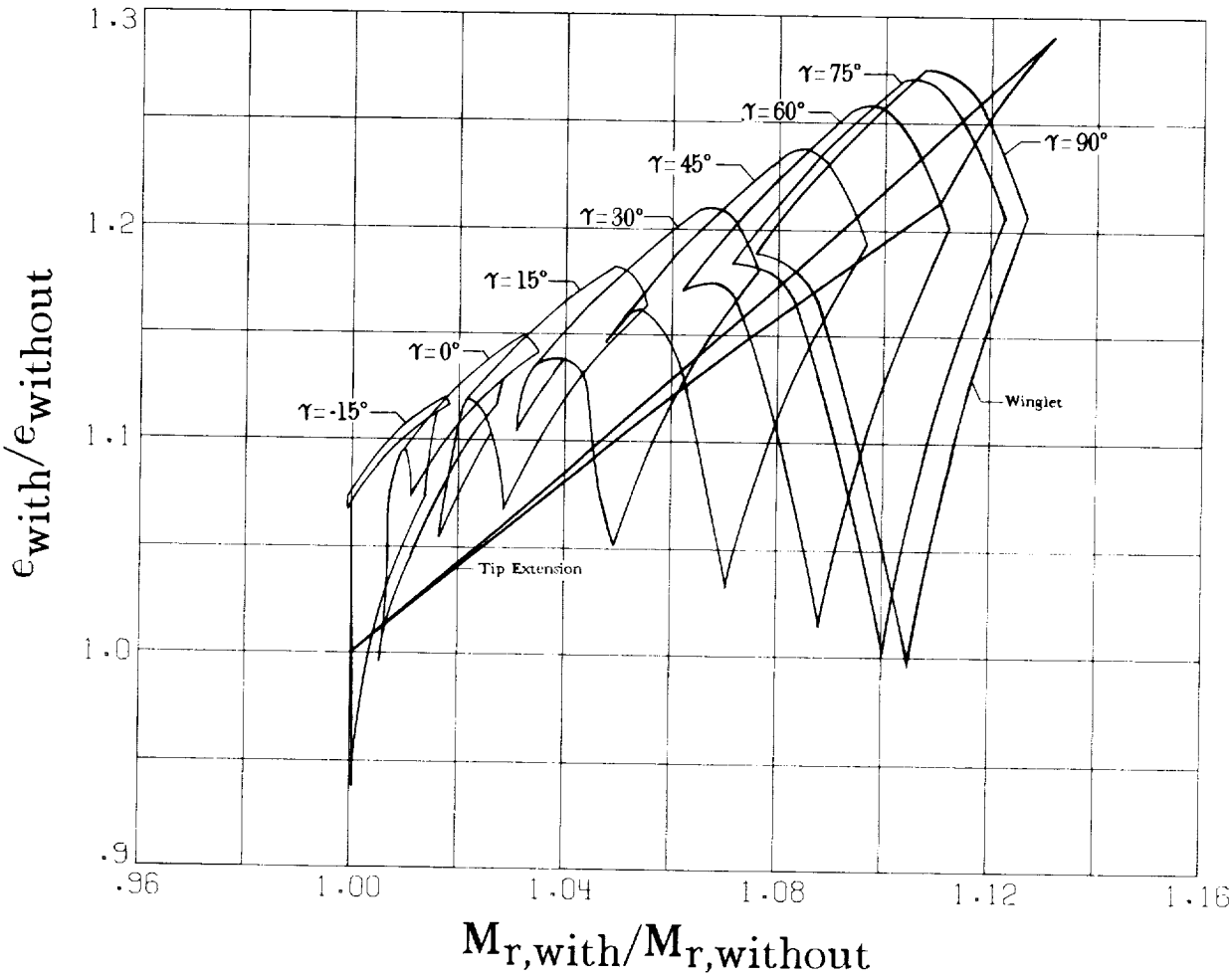

Figure 39.- Summary of effect of winglet cant angle on the comparison of tip extension and winglet. Only the envelopes of the curves of figure 38 are shown. $\lambda = 0.5^{o}$; 5^{o} washout. Efficiency factor ratios are calculated for $C_L = 0.4$; moment ratios are calculated for $C_L = 1.0$.

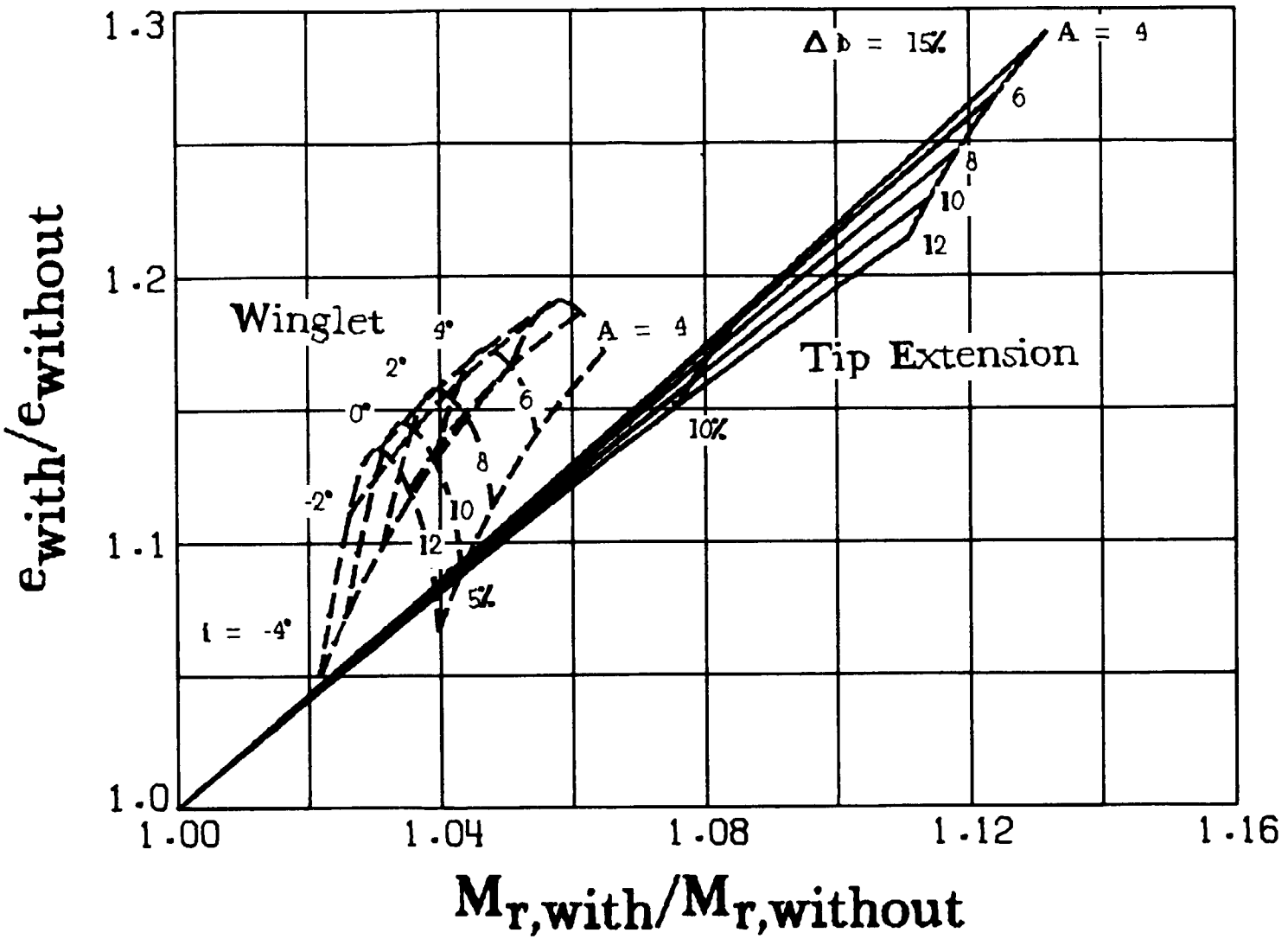

(a) $\Lambda_W = 0^o$.

Figure 40.- Effect of winglet leading-edge sweep on the comparison of tip extension and winglet. Compare with figure 29 for $\Lambda_W = 45^o$. $\lambda = 0.5$; 5^o washout. Efficiency factor ratios are calculated for $C_L = 0.4$; moment ratios are calculated for $C_L = 1.0$.

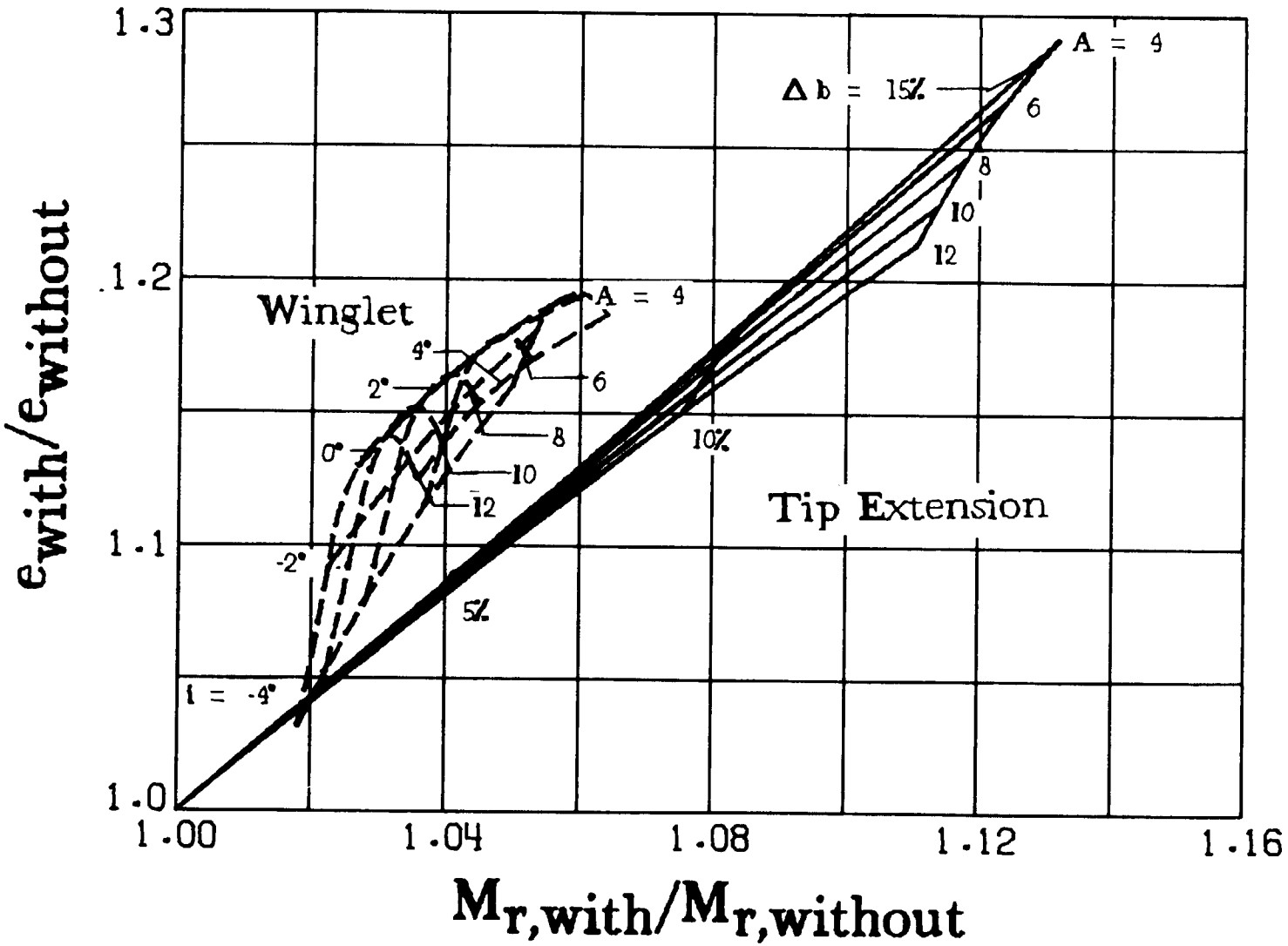

(b) $\Lambda_W = -45^o$.

Figure 40.- Concluded.

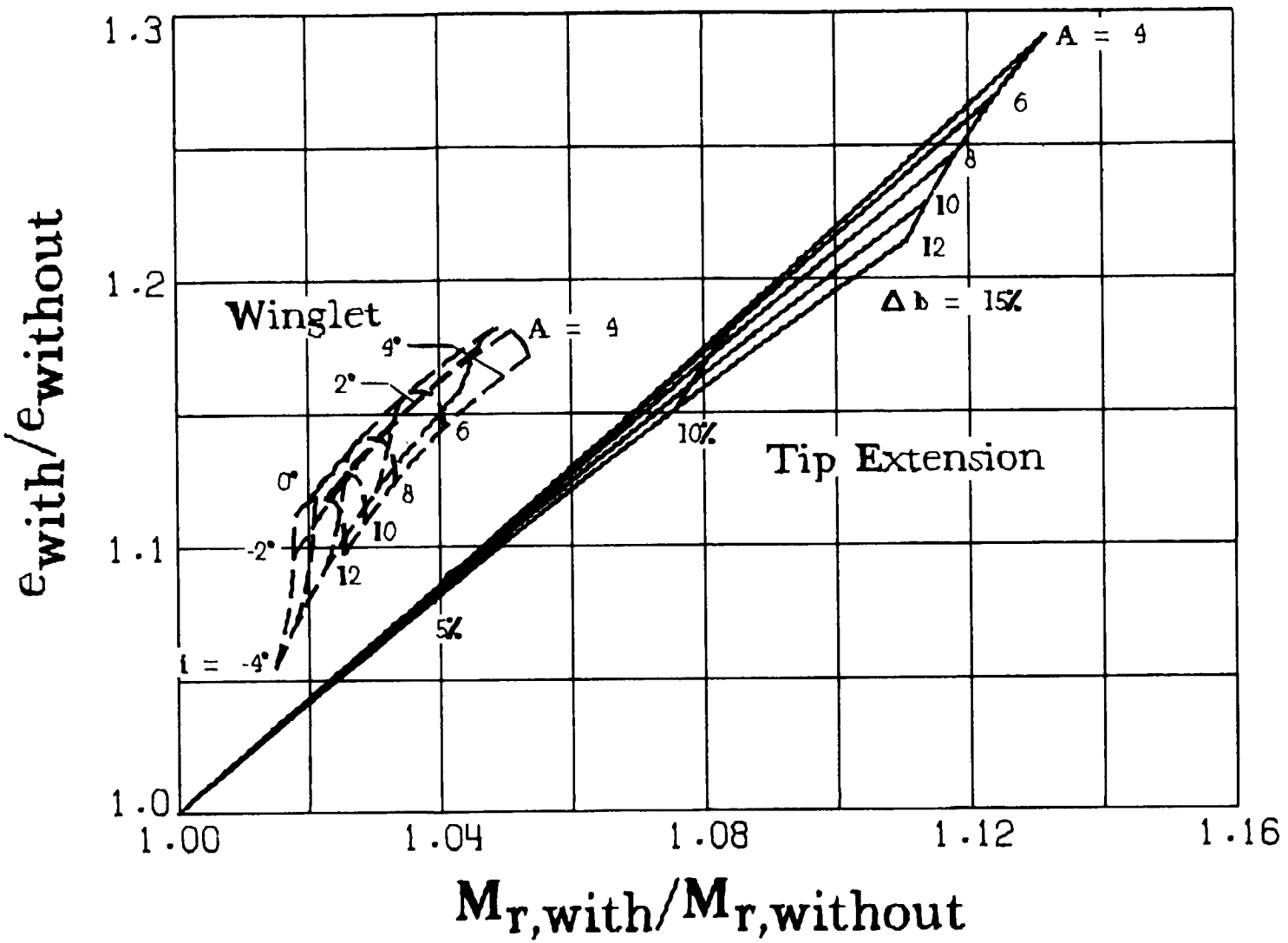

Figure 41.- Comparison of tip extension and winglet ($\lambda_W = 0.5$). Compare with figure 29 for $\lambda_W = 1.0$. $\lambda = 0.5$; 5^o washout. Efficiency factor ratios are calculated for $C_L = 0.4$; moment ratios are calculated for $C_L = 1.0$.

1. Report No. NASA TP-1020	2. Government Accession No.	3. Recipient's Catalog No.
4. Title and Subtitle THEORETICAL PARAMETRIC STUDY OF THE RELATIVE ADVANTAGES OF WINGLETS AND WING-TIP EXTENSIONS		5. Report Date September 1977 6. Performing Organization Code
7. Author(s) Harry H. Heyson, Gregory D. Riebe, and Cynthia L. Fulton		8. Performing Organization Report No. L-11679
9. Performing Organization Name and Address NASA Langley Research Center Hampton, VA. 23665		10. Work Unit No. 791-40-08-01 11. Contract or Grant No.
12. Sponsoring Agency Name and Address National Aeronautics and Space Administration Washington, DC 20546		13. Type of Report and Period Covered Technical Paper 14. Sponsoring Agency Code
15. Supplementary Notes Supersedes NASA TM X-74003.		

16. Abstract

This study provides confirmation, for a wide range of wings, of the recommendations of Richard T. Whitcomb in NASA Technical Note D-8260. For identical increases in bending moment, a winglet provides a greater gain in induced efficiency than a tip extension. Winglet toe-in angle allows design trades between efficiency and root moment. A winglet shows the greatest benefit when the wing loads are heavy near the tip. Washout diminishes the benefit of either tip modification, and the gain in induced efficiency becomes a function of lift coefficient; thus, heavy wing loadings obtain the greatest benefit from a winglet, and low-speed performance is enhanced even more than cruise performance. Both induced efficiency and bending moment increase with winglet length and outward cant. The benefit of a winglet relative to a tip extension is greatest for a nearly vertical winglet. Root bending moment is proportional to the minimum weight of bending material required in the wing; thus, it is a valid index of the impact of tip modifications on a new wing design.

17. Key Words (Suggested by Author(s))	18. Distribution Statement
Aerodynamics Induced efficiency Root bending moment Winglet Tip extension	Unclassified – Unlimited Subject Category 02

19. Security Classif. (of this report)	20. Security Classif. (of this page)	21. No. of Pages	22. Price*
Unclassified	Unclassified	73	$4.50

*For sale by the National Technical Information Service, Springfield, Virginia 22161

NASA-Langley, 1977